

Dynamic Systems Part 2

The mathematics behind the "Simulator" computer program

The computer program "Simulator", the use of which is described in a separate manual, enables the simulation of simple dynamic systems and experimentation with them. The code is publicly accessible on GitHub, written in VB.NET, provided with detailed comments and can be extended as required. This requires the free community version of Microsoft Visual Studio, at least version 17.9, which is based on Microsoft Framework 8.0.

This document describes the mathematical principles for the "Simulator". Part 1 deals with the systems listed in the corresponding table of contents. Further systems follow in Part 2. The technical documentation for the "Simulator" can be found in the document "Technical Documentation".

Version 8.0 – 2025/06/01

Contents

Contents	1
Introduction.....	2
1. The N-body problem.....	4
1.1 The Two-Body Problem.....	4
1.2 Kepler's laws	14
1.3 Some data about our solar system	15
1.4 The N-body Problem	16
1.5 Numerical approximation of the N-body Problem	18
1.6 Choice of Coordinate System.....	19
1.7 Representation of the Universe in the "simulator"	21
1.8 Representation of the orbit sketch when placing a star.....	22
1.9 The collision problem.....	23
1.10 Conservation laws and phase diagram	24
1.11 The Newtonian Universe.....	24
1.12 Alternative Universes.....	25
1.13 Periodically stable tracks.....	27
1.14 Exercise examples	28
a. Changing the star mass	29
2. 3D Attractors	30
2.1 Linear mappings $\mathbb{R}^3 \rightarrow \mathbb{R}^3$	30
2.2 Continuously differentiable mappings $\mathbb{R}^3 \rightarrow \mathbb{R}^3$	39
2.3 The Lorenz system	42
2.4 Elementary properties of the Lorenz system.....	45

2.5	Pitchfork and Hopf bifurcation	49
2.6	Projection of the Lorenz attractor	56
2.7	Strange attractors	58
2.8	Numerical solution with the Runge Kutta method	60
2.9	Exercise examples	61
3.	Fractal Sets.....	62
3.1	Lindenmayer Systems	62
3.2	Historical Excursus: From descriptive to abstract thinking.....	64
3.3	The Koch curve (or snowflake curve).....	65
3.4	The Dragon curve.....	68
3.5	The Hilbert and Peano curves.....	73
3.6	Tree structures.....	79
3.7	Self-similarity	82
3.8	Fractal Dimension	83
3.9	Exercise examples	89
	Further reading.....	91

Introduction

There are many programs on the Internet that enable the simulation of simple dynamic systems. However, their code is hardly public, and the underlying mathematics is also poorly documented. The "Simulator" enables the iteration of simple real functions, the simulation of mathematical billiards, the investigation of numerical methods for solving ordinary differential equations, the simulation of various coupled pendulums or Newton's universe. The code of the program is written in VB.NET and is publicly available on Github in the repository "HermannBiner/Simulator". To work with it, the community version 2022 of Microsoft Visual Studio is sufficient, which can be downloaded free of charge and easily installed. The installation of Microsoft Framework 8.0 is also a prerequisite for the "Simulator".

The GitHub link is as follows:

<https://github.com/HermannBiner/Simulator>

The mathematics on which the "Simulator" is based is dealt with at an elementary level in this document. Examples of exercises or suggestions for extending the "Simulator" are intended to encourage students to do their own work. Mathematics at grammar school is more than full of material. Nevertheless, interested pupils may be offered further topics as part of an optional subject or a seminar. The "Simulator" and this document are intended to contribute to this.

The following systems are implemented in version 8 of the program:

- Growth models and iteration of quadratic functions such as logistic growth, tent mapping, iteration on the parabola including related topics such as the Feigenbaum diagram.

- Mathematical billiards with various billiard table shapes: elliptical billiards, stadium billiards, oval billiards. The analogue to the Feigenbaum diagram is the C-diagram.
- The investigation of numerical methods for solving ordinary differential equations. Some simple methods are compared here using the example of the spring pendulum.
- The simulation of coupled pendulums: Double pendulum, oscillating spring pendulum and horizontal shaking pendulum.
- Iterations in the complex plane: Newton iteration and basins of roots of unity. Zeros of third degree polynomials.
- Generation of Mandelbrot- and Julia-sets for the quadratic function and the n-th power function
- Simulation of Newton's universe including our planetary system
- Strange attractors like the Lorenz System
- Fractal sets

The use of the "Simulator" is documented in detail in a manual in German and a manual in English. In addition, technical documentation explains the architecture of the "Simulator". The language in the user interface and in all documentation can be selected between German and English. The code contains detailed comments in English.

The only prerequisite is mathematics, which is either covered at grammar school or which can be made accessible to a secondary school student with little effort. Topics from geometry (conic sections and plane vector geometry), analysis (continuity, differential calculus and ordinary differential equations) and physics (Lagrange formalism, gravitation) are covered.

The individual subject areas are largely independent, so that a selection is possible depending on interest and the time available.

Special thanks go to Prof. em. Dr. Urs Kirchgraber of ETH Zurich, who drew my attention to chaos theory in the nineties. I would also like to thank Prof. Dr. Norbert Hungerbühler of ETH Zurich, who has supported me in many ways and to whom I owe valuable advice.

1. The N-body problem

The N-body problem deals with N bodies that are positioned in three-dimensional space and whose movement is only influenced by the gravitational forces between them. It occurs, for example, when astronomers want to calculate the orbits of stars or planets. Johannes Kepler (1571 - 1630) formulated laws in the years 1599 - 1619 that correctly describe the two-body problem. Isaac Newton (1642 - 1726) derived these laws from his law of gravitation in 1687.

The case $N > 2$ has later occupied many mathematicians and physicists, without being able to find a closed analytical solution that describes the trajectories of the motion of the N bodies in the general case. Although Quidong Wang found a solution for the general case in 1991 with the help of Taylor series, but these converge so slowly that they are useless in practice. The general case has chaotic properties. Henri Poincaré (1854 - 1912) already discovered this in 1890 when investigating special cases of the three-body problem.

In the following, we will extend the "simulator" with a simulation of the N-body problem. We will only consider the simplified case where all bodies lie in the same plane. You must be aware that the simulation is only a numerical artifact and does not reflect the actual movement of the N-bodies.

An in-depth presentation of the mathematical theory can be found in "Orbital Motion" [1] and "Celestial Mechanics" [2]. Both books report in detail on the N-body problem, but also on general celestial mechanics, while remaining at a largely elementary mathematical level.

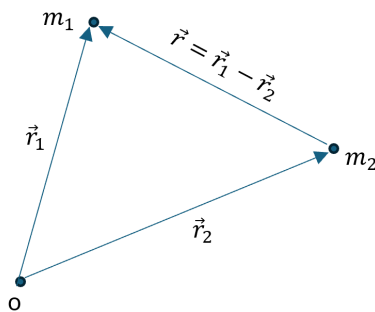
1.1 The Two-Body Problem

Newton's equations

Although the numerical simulation of the two-body problem does not differ significantly from that of the N-body problem, we will treat the two-body problem mathematically here.

We consider two masses m_1, m_2 which are located at the positions $\vec{r}_1(t), \vec{r}_2(t)$ at time t . This should be $\vec{r}_1(0) \neq \vec{r}_2(0)$

The force $\vec{F} = G \frac{m_1 m_2}{|\vec{r}|^2}$ acts between the masses in the direction of the other mass according to *Newton's law of gravitation*, where $\vec{r} = \vec{r}_2 - \vec{r}_1 \neq \vec{0}$ is the difference vector of the positions. $G \approx 6.6743 \cdot 10^{-11} \frac{m^3}{kg \cdot s^2}$ is the gravitational constant.



According to *Newton's laws* and his *law of gravitation*, we have the equations of motion:

$$\begin{cases} m_1 \ddot{\vec{r}}_1 = -G \frac{m_1 m_2}{|\vec{r}|^2} \cdot \frac{\vec{r}}{|\vec{r}|} \\ m_2 \ddot{\vec{r}}_2 = G \frac{m_1 m_2}{|\vec{r}|^2} \cdot \frac{\vec{r}}{|\vec{r}|} \end{cases}$$

Or:

$$(1) \begin{cases} \ddot{\vec{r}}_1 = -G \frac{m_2}{|\vec{r}|^2} \cdot \frac{\vec{r}}{|\vec{r}|} \\ \ddot{\vec{r}}_2 = G \frac{m_1}{|\vec{r}|^2} \cdot \frac{\vec{r}}{|\vec{r}|} \end{cases}$$

The conservation laws

The classical conservation laws follow from these equations. We will first check this for the *law of momentum*. If we add the above equations, we obtain:

$$m_1 \ddot{\vec{r}}_1 + m_2 \ddot{\vec{r}}_2 = \vec{0}$$

And by integrating according to t , the total momentum of the system is obtained:

$$m_1 \dot{\vec{r}}_1 + m_2 \dot{\vec{r}}_2 = \vec{p}$$

Whereby \vec{p} is constant.

If \vec{R} is the coordinate of the center of gravity and $M := m_1 + m_2$, then the total momentum is also

$$M \dot{\vec{R}} = m_1 \dot{\vec{r}}_1 + m_2 \dot{\vec{r}}_2$$

By integrating to t and determining the integration constants using special cases such as $m_1 = 0$, you obtain the position vector for the center of gravity:

$$\vec{R} = \frac{m_1 \vec{r}_1 + m_2 \vec{r}_2}{M}$$

It also follows from $M \dot{\vec{R}} = \vec{p} = \text{constant}$ that the center of gravity of the system moves at a constant speed.

Now we will examine the *angular momentum theorem*. The following applies to the total angular momentum \vec{L} of the system:

$$\begin{aligned} \frac{d}{dt} \vec{L} &= \frac{d}{dt} (\vec{r}_1 \times m_1 \dot{\vec{r}}_1 + \vec{r}_2 \times m_2 \dot{\vec{r}}_2) = \vec{r}_1 \times m_1 \ddot{\vec{r}}_1 + \vec{r}_2 \times m_2 \ddot{\vec{r}}_2 \\ &= -\vec{r}_1 \times G \frac{m_1 m_2}{|\vec{r}|^2} \cdot \frac{\vec{r}}{|\vec{r}|} + \vec{r}_2 \times G \frac{m_1 m_2}{|\vec{r}|^2} \cdot \frac{\vec{r}}{|\vec{r}|} = \vec{r} \times G \frac{m_1 m_2}{|\vec{r}|^2} \cdot \frac{\vec{r}}{|\vec{r}|} = \vec{0} \end{aligned}$$

The angular momentum \vec{L} of the system is therefore constant.

We also check that the *total energy* of the system is constant. The potential energy is at the distance $|\vec{a}|$ from the center of gravity (if the zero point is defined at infinity):

$$E_{pot} = - \int_{|\vec{a}|}^{\infty} G \frac{m_1 m_2}{|\vec{r}|^2} \cdot \frac{\vec{r}}{|\vec{r}|} d\vec{r} = -G \frac{m_1 m_2}{|\vec{a}|}$$

Therefore

$$E = \frac{1}{2}m_1|\dot{\vec{r}}_1|^2 + \frac{1}{2}m_2|\dot{\vec{r}}_2|^2 - G\frac{m_1m_2}{|\vec{r}|}$$

$$\frac{d}{dt}E = m_1\dot{\vec{r}}_1 \cdot \ddot{\vec{r}}_1 + m_2\dot{\vec{r}}_2 \cdot \ddot{\vec{r}}_2 + G\frac{m_1m_2}{|\vec{r}|^3}\vec{r} \cdot \dot{\vec{r}}$$

We set $\gamma = G\frac{m_1m_2}{|\vec{r}|^3}$. Then after (1): $m_1\ddot{\vec{r}}_1 = -\gamma\vec{r}$ and $m_2\ddot{\vec{r}}_2 = \gamma\vec{r}$ and you have:

$$\frac{d}{dt}E = -\dot{\vec{r}}_1 \cdot \gamma\vec{r} + \dot{\vec{r}}_2 \cdot \gamma\vec{r} + \gamma\vec{r} \cdot \dot{\vec{r}} = -\dot{\vec{r}} \cdot \gamma\vec{r} + \gamma\vec{r} \cdot \dot{\vec{r}} = 0$$

□

Choice of reference system

In the following, we will now try to determine the orbits of the masses m_1, m_2 . To do this, we first select a suitable coordinate system as a reference system.

It is easy to see that Newton's equations (1) are *independent of the choice of zero point*. If you replace $\vec{r}_{1,2} = \vec{r}_{1,2}' + \vec{c}$, whereby the old zero point is pushed into the new one by the translation \vec{c} , then $\vec{r}_{1,2}'$ fulfill the same equations. Now we choose the centre of gravity of the system, which moves at a constant speed, as the zero point. This gives us an inertial system. Relative to this, the total momentum of the system is zero. Therefore, the following applies:

$$m_1\vec{r}_1 + m_2\vec{r}_2 = 0$$

If equations (1) are subtracted from each other, it follows:

$$\ddot{\vec{r}} = \ddot{\vec{r}}_1 - \ddot{\vec{r}}_2 = -GM\frac{\vec{r}}{|\vec{r}|^3}$$

Where $M = m_1 + m_2$ is the total mass. It also follows from the first equation (1) and since the total momentum is zero:

$$\ddot{\vec{r}}_1 = -G\frac{m_2\vec{r}}{|\vec{r}|^3} = -G\frac{m_2\vec{r}_1 - m_2\vec{r}_2}{|\vec{r}|^3} = -G\frac{m_2\vec{r}_1 + m_1\vec{r}_1}{|\vec{r}|^3} = -GM\frac{\vec{r}_1}{|\vec{r}|^3}$$

An analogous calculation is carried out for \vec{r}_2 and finally the (symmetrical) system of equations relative to the centre of gravity is obtained:

$$(2) \begin{cases} \ddot{\vec{r}}_1 = -GM\frac{\vec{r}_1}{|\vec{r}|^3} \\ \ddot{\vec{r}}_2 = -GM\frac{\vec{r}_2}{|\vec{r}|^3} \\ \ddot{\vec{r}} = -GM\frac{\vec{r}}{|\vec{r}|^3} \end{cases}$$

If we form the cross product with \vec{r} , we have:

$$0 = \vec{r} \times \left(\ddot{\vec{r}} + GM\frac{\vec{r}}{|\vec{r}|^3} \right) = \vec{r} \times \ddot{\vec{r}} = \frac{d}{dt}(\vec{r} \times \dot{\vec{r}})$$

And integration according to t delivers:

$$\vec{r} \times \dot{\vec{r}} = \vec{h}$$

Where \vec{h} is constant and generally $\neq \vec{0}$. It is $\vec{r} \neq \vec{0}$ by assumption and in general $\dot{\vec{r}} \neq \vec{0}$, since the bodies are in each other's gravitational field. If the bodies do not fly towards each other and collide, \vec{r} is also not parallel to $\dot{\vec{r}}$. The path then runs in a plane perpendicular to $\vec{r}, \dot{\vec{r}}$ regardless of t . We place this plane through the centre of gravity.

Can we place the x- and y-axis of the coordinate system in this plane? To do this, we would have to rotate the coordinate system so that the x- and y-axes fall into the plane and the z-axis is perpendicular to this plane. We refer to this rotation as D . This is bijective and D^{-1} returns the rotated coordinate system to the original one. Let $\vec{r}_{1,2}'$ be the positions of the masses in the rotated system. Then the following applies: $\vec{r}_{1,2} = D^{-1}\vec{r}_{1,2}'$. D and thus also D^{-1} keep distances invariant, so $|\vec{r}| = |D^{-1}\vec{r}'| = |\vec{r}'|$ applies. Thus, for example, the first equation (1) changes into:

$$D^{-1}\ddot{\vec{r}}_1' = -G \frac{m_2}{|\vec{r}'|^3} \cdot D^{-1}\vec{r}'$$

Since D^{-1} is bijective, it follows:

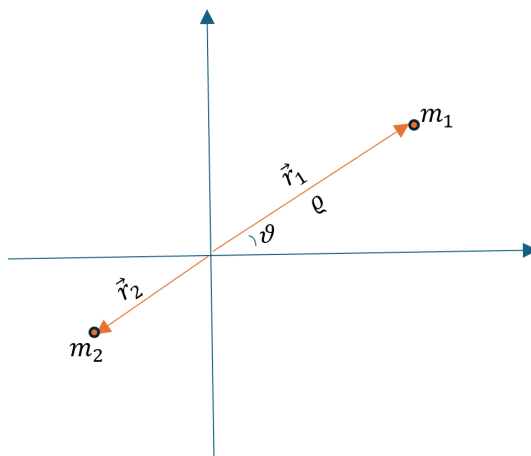
$$\ddot{\vec{r}}_1' = -G \frac{m_2}{|\vec{r}'|^3} \cdot \vec{r}'$$

The same applies to the second equation. This means that the new coordinates fulfil the same equations (*) as the old ones.

The equations of motion are therefore *independent of the rotation of the coordinate system*, and we can place the x and y axes in the plane in which the movement takes place. At the same time, the zero point of the coordinate system lies in the common centre of gravity. We will need this reference point later for the implementation to describe the path of a mass relative to the common centre of gravity.

The path of a mass relative to the common centre of gravity

The following sketch shows the corresponding situation.



Position of the masses relative to the selected coordinate system

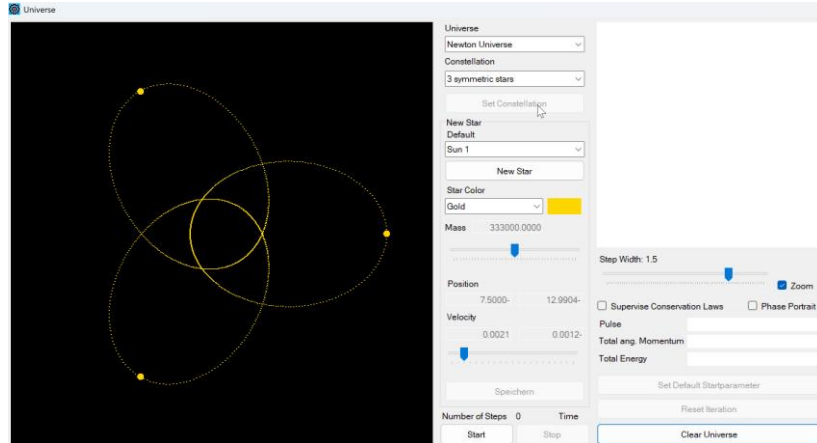
If we look at the first equation (2), we get that the total momentum is zero:

$$\ddot{\vec{r}}_1 = -GM \frac{\vec{r}_1}{|\vec{r}_1|^3} = -GM \frac{\vec{r}_1}{|\vec{r}_1 - \vec{r}_2|^3} = -GM \frac{\vec{r}_1}{\left| \vec{r}_1 + \frac{m_1}{m_2} \vec{r}_1 \right|^3} = -G \frac{Mm_2^3}{M^3} \cdot \frac{\vec{r}_1}{|\vec{r}_1|^3}$$

This gives us an equation in which only the movement of the mass m_1 appears:

$$(3) \ddot{\vec{r}}_1 = -G \frac{m_2^3}{M^2} \cdot \frac{\vec{r}_1}{|\vec{r}_1|^3}$$

These are - broken down into components - three second-order differential equations. When solving them, a total of 6 integration constants must be determined.



Three symmetrical stars in the "simulator"

For the calculation of the displayed orbits, it was assumed that the star orbits around the common centre of gravity. The orbit curve was calculated for each star as a two-body problem with respect to the other masses at the centre of gravity.

Polar coordinates

We now introduce polar coordinates:

$$\begin{aligned}\vec{r}_1 &= \varrho \begin{pmatrix} \cos \vartheta \\ \sin \vartheta \end{pmatrix}, |\vec{r}_1| = \varrho \\ \dot{\vec{r}}_1 &= \dot{\varrho} \begin{pmatrix} \cos \vartheta \\ \sin \vartheta \end{pmatrix} + \varrho \dot{\vartheta} \begin{pmatrix} -\sin \vartheta \\ \cos \vartheta \end{pmatrix} \\ \ddot{\vec{r}}_1 &= \ddot{\varrho} \begin{pmatrix} \cos \vartheta \\ \sin \vartheta \end{pmatrix} + 2\dot{\varrho}\dot{\vartheta} \begin{pmatrix} -\sin \vartheta \\ \cos \vartheta \end{pmatrix} + \varrho \ddot{\vartheta} \begin{pmatrix} -\sin \vartheta \\ \cos \vartheta \end{pmatrix} + \varrho \dot{\vartheta}^2 \begin{pmatrix} -\cos \vartheta \\ -\sin \vartheta \end{pmatrix}\end{aligned}$$

Since we assume that there are two differently positioned (point-like) masses, each mass lies outside the common centre of gravity. **Therefore, it holds $\varrho > 0$!**

The aim is now to find two equations for $\varrho(t)$ and $\vartheta(t)$. Eliminate t from these equations to obtain an equation for $\varrho(\vartheta)$ and thus the orbital equation we are looking for. To do this, we consider the angular momentum and the energy of the mass m_1 . First, we show that this angular momentum is constant

$$\vec{L} := \frac{d}{dt} (\vec{r}_1 \times m_1 \dot{\vec{r}}_1) = \vec{r}_1 \times m_1 \ddot{\vec{r}}_1 = \vec{0}$$

Since according to (3) $\ddot{\vec{r}}_1 \parallel \vec{r}_1$. The angular momentum is always perpendicular to the coordinate plane, and we only consider its magnitude. Then we have in polar coordinates:

$$L := |\vec{L}| = |\vec{r}_1 \times m_1 \dot{\vec{r}}_1| = m_1 \varrho^2 \dot{\vartheta} = \text{constant}$$

This allows us to eliminate the time derivatives.

First we get:

$$\dot{\vartheta} = \frac{L}{m_1} \cdot \frac{1}{\varrho^2}$$

Furthermore:

$$\dot{\varrho} = \frac{d\varrho}{dt} = \frac{d\varrho}{d\vartheta} \cdot \frac{d\vartheta}{dt} = \varrho' \dot{\vartheta} = \frac{L}{m_1} \cdot \frac{\varrho'}{\varrho^2}$$

Now let's look at equation (3) again:

$$m_1 \ddot{\vec{r}}_1 = -G \frac{m_2^3 m_1}{M^2} \cdot \frac{\vec{r}_1}{|\vec{r}_1|^3}$$

The force $-G \frac{m_2^3 m_1}{M^2} \cdot \frac{\vec{r}_1}{|\vec{r}_1|^3}$ acts on m_1 and the associated potential energy is (if the zero point is chosen at infinity):

$$E_{pot} = -G \frac{m_2^3 m_1}{M^2} \cdot \frac{1}{|\vec{r}_1|}$$

This allows the energy of the mass m_1 to be written as:

$$E = \frac{1}{2} m_1 |\dot{\vec{r}}_1|^2 - G \frac{m_2^3 m_1}{M^2} \cdot \frac{1}{|\vec{r}_1|}$$

In polar coordinates we have:

$$E = \frac{m_1}{2} (\dot{\varrho}^2 + \varrho^2 \dot{\vartheta}^2) - G \frac{m_2^3 m_1}{M^2} \cdot \frac{1}{\varrho}$$

Now we eliminate $\dot{\varrho}, \dot{\vartheta}$:

$$E = \frac{m_1}{2} \left[\left(\frac{L}{m_1} \right)^2 \cdot \frac{\varrho'^2}{\varrho^4} + \varrho^2 \left(\frac{L}{m_1} \right)^2 \cdot \frac{1}{\varrho^4} \right] - G \frac{m_2^3 m_1}{M^2} \cdot \frac{1}{\varrho}$$

And preserved:

$$E = \frac{L^2}{2m_1} \cdot \frac{1}{\varrho^2} \left(\frac{\varrho'^2}{\varrho^2} + 1 \right) - G \frac{m_2^3 m_1}{M^2} \cdot \frac{1}{\varrho}$$

If the mass m_1 flies directly towards the centre of gravity and towards the other mass m_2 , $\vec{r}_1 \parallel \dot{\vec{r}}_1$ and thus $L = 0$. Then we simply have a linear motion that ends with the collision of the masses. We exclude this case. **Therefore, $L \neq 0$** and we divide by L :

$$\frac{2m_1 E}{L^2} = \frac{1}{\varrho^2} \left(\frac{\varrho'^2}{\varrho^2} + 1 \right) - 2G \frac{m_2^3 m_1^2}{M^2 L^2} \cdot \frac{1}{\varrho}$$

Solution of the differential equation

We set: $p := \frac{M^2 L^2}{G m_2^3 m_1^2}$ and substitute: $\varrho = \frac{1}{u}$, $\varrho' = -\frac{u'}{u^2}$. This gives us

$$\frac{2m_1 E}{L^2} = u'^2 + u^2 - \frac{2u}{p}$$

Square complement supplies:

$$\frac{2m_1E}{L^2} = u'^2 + \left(u - \frac{1}{p}\right)^2 - \frac{1}{p^2}$$

We take the approach:

$$u(\vartheta) = A\cos(\vartheta - \alpha) + \frac{1}{p}, \quad u'(\vartheta) = -A\sin(\vartheta - \alpha)$$

And obtain by insertion:

$$\frac{2m_1E}{L^2} = A^2 - \frac{1}{p^2}$$

Then we get:

$$A^2 = \frac{2m_1E}{L^2} + \frac{1}{p^2}$$

We first want to check whether this expression is always defined, i.e. whether the right-hand side is always positive.

E is constant. If we look at the energy at perihelion or aphelion, it is $\dot{\varrho} = 0$ and we obtain the kinetic energy at this point:

$$E_{kin} = \frac{m_1}{2} \varrho^2 \dot{\vartheta}^2 = \frac{m_1}{2} \varrho^2 \frac{L^2}{m_1^2 \varrho^4} = \frac{L^2}{2m_1 \varrho^2}$$

And for the total energy:

$$E = \frac{L^2}{2m_1 \varrho^2} - G \frac{m_2^3 m_1}{M^2} \cdot \frac{1}{\varrho} = \frac{L^2}{2m_1} \left(\frac{1}{\varrho^2} - \frac{2}{p} \cdot \frac{1}{\varrho} \right)$$

This delivers:

$$\frac{2m_1E}{L^2} + \frac{1}{p^2} = \frac{1}{\varrho^2} - \frac{2}{p} \cdot \frac{1}{\varrho} + \frac{1}{p^2} = \left(\frac{1}{\varrho} - \frac{1}{p} \right)^2 \geq 0$$

□

Now is:

$$A^2 = \frac{2m_1E}{L^2} + \frac{1}{p^2} = \frac{1}{p^2} \left(\frac{2m_1E}{L^2} \cdot p^2 + 1 \right) = \frac{1}{p^2} \cdot \left(\frac{2EL^2M^4}{G^2m_1^3m_2^6} + 1 \right)$$

We define ε by:

$$\varepsilon^2 := A^2 p^2 = \frac{2EL^2M^4}{G^2m_1^3m_2^6} + 1 \geq 0$$

It is sufficient to consider the case $\varepsilon \geq 0$, because otherwise you can simply add π to $\vartheta - \alpha$.

You have: $A = \varepsilon/p$ and

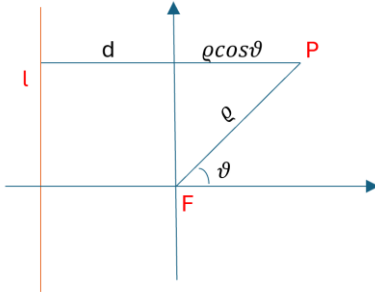
$$u(\vartheta) = \frac{\varepsilon \cos(\vartheta - \alpha) + 1}{p}$$

And thus:

$$(4) \quad \rho(\vartheta) = \frac{p}{1 + \varepsilon \cos(\vartheta - \alpha)}$$

Discussion of the solution

(4) is the equation of a conic section. If we define this as the location of the points which have a constant distance ratio ε from a fixed point (the focal point F) and a fixed straight line (the guiding line l), we obtain:



The point P and its distance from F or l

$$\frac{\rho}{d + \rho \cos \vartheta} = \varepsilon$$

$$\rho = \frac{p}{1 - \varepsilon \cos \vartheta}$$

$p = \varepsilon d = \rho(\frac{\pi}{2})$ is half the cone section at the focal point. For $\alpha = \pi$, equation (4) corresponds to the above equation.

The minimum distance of a planet from the sun or from the focal point is the *perihelion*. If you look at equation (4) again:

$$(4) \quad \rho(\vartheta) = \frac{p}{1 + \varepsilon \cos(\vartheta - \alpha)}$$

You can then see that the minimum is assumed for $\cos(\vartheta - \alpha) = 1$ or $\vartheta = \alpha$

α is just *the argument of the perihelion*, or the angle between the direction of the perihelion and the x-axis. In our solar system, the x-axis is defined by the intersection of the ecliptic and the Earth's equatorial plane at the vernal equinox

Depending on the value of the numerical eccentricity ε , different types of conic section are obtained:

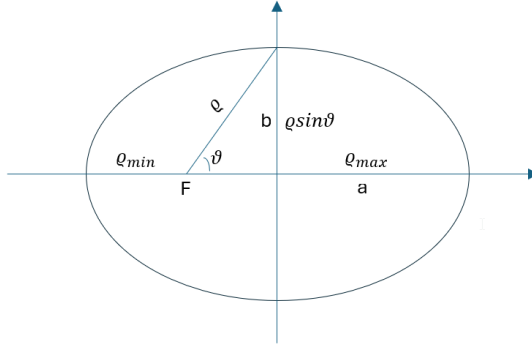
$\varepsilon = 0$: $\rho = p = \text{constant}$. The conic section is a circle.

$0 < \varepsilon < 1$: $\frac{p}{1-\varepsilon} < \rho < \frac{p}{1+\varepsilon}$. The conic section is an ellipse.

$\varepsilon = 1$: $\rho \rightarrow \infty$ for $\vartheta \rightarrow 0$. Otherwise is $\rho > 0$ and defined for all $\vartheta \in]0, 2\pi[$. You have a parabola.

$\varepsilon > 1$: $\rho > 0$ only for $\cos \vartheta < \frac{1}{\varepsilon}$. $\rho \rightarrow \infty$ for $\vartheta \rightarrow \arccos \frac{1}{\varepsilon}$. One has a hyperbole.

In the case of the ellipse, it is useful to calculate the semi-axes. Let a be the major semi-axis and b the minor semi-axis of the ellipse.



Major and minor semi-axis of the ellipse

The following applies:

$$a = \frac{1}{2}(\varrho_{min} + \varrho_{max}) = \frac{1}{2}\left(\varrho\left(\frac{\pi}{2}\right) + \varrho(0)\right) = \frac{1}{2}\left(\frac{p}{1+\varepsilon} + \frac{p}{1-\varepsilon}\right) = \frac{p}{1-\varepsilon^2}$$

To determine b we are looking for the maximum of $\varrho \sin \vartheta$. It is:

$$(\varrho \sin \vartheta)' = \frac{p \cos \vartheta (1 - \varepsilon \cos \vartheta) - p \sin \vartheta \cdot \varepsilon \sin \vartheta}{(1 - \varepsilon \cos \vartheta)^2} = \frac{p \cos \vartheta - \varepsilon p}{(1 - \varepsilon \cos \vartheta)^2} = 0$$

For $\cos \vartheta = \varepsilon$. This gives us:

$$b = \varrho \sin \vartheta = \frac{p \sqrt{1 - \varepsilon^2}}{1 - \varepsilon^2} = \frac{p}{\sqrt{1 - \varepsilon^2}} = a \sqrt{1 - \varepsilon^2}$$

Remark:

We have carried out our calculation with the centre of gravity as the zero point. In the literature, the location of the mass m_2 is sometimes set as the zero point and the movement of m_1 is calculated relative to m_2 . This results in slightly different values for the parameters p, ε in the orbit equation.

Finally, we want to make some considerations about the units of the parameters that occurred in the orbit equation in the case of the two-body problem. This was:

$$\varrho(\vartheta) = \frac{p}{1 + \varepsilon \cos(\vartheta - \alpha)}$$

In it was: $p := \frac{M^2 L^2}{G m_1^2 m_2^3}$. We write the unit of a size in square brackets, and we use the kilogram - meter - second system. Then $[L] = \frac{\text{kg} \cdot \text{m}^2}{\text{s}}$. This becomes:

$$[p] = [M]^2 [L]^2 \cdot [G m_1^2 m_2^3]^{-1} = \text{kg}^2 \cdot \frac{\text{kg}^2 \cdot \text{m}^4}{\text{s}^2} \cdot \frac{\text{kg} \cdot \text{s}^2}{\text{m}^3} \cdot \frac{1}{\text{kg}^5} = \text{m}$$

Therefore, p has the dimension of a length.

Furthermore was:

$$\varepsilon^2 := \frac{2 E L^2 M^4}{G^2 m_1^3 m_2^6} + 1$$

It is:

$$\left[\frac{EL^2M^4}{G^2m_1^3m_2^6} \right] = [EL^2M^4] \cdot [G^2m_1^3m_2^6]^{-1} = \frac{kg \cdot m^2}{s^2} \cdot \frac{kg^2 \cdot m^4}{s^2} \cdot kg^4 \cdot \frac{kg^2 \cdot s^4}{m^6} \cdot \frac{1}{kg^9} = 1$$

ε is dimensionless.

Another problem arises during implementation. The speed at which the centrifugal force and gravitational force are balanced in the gravitational field of a mass M is:

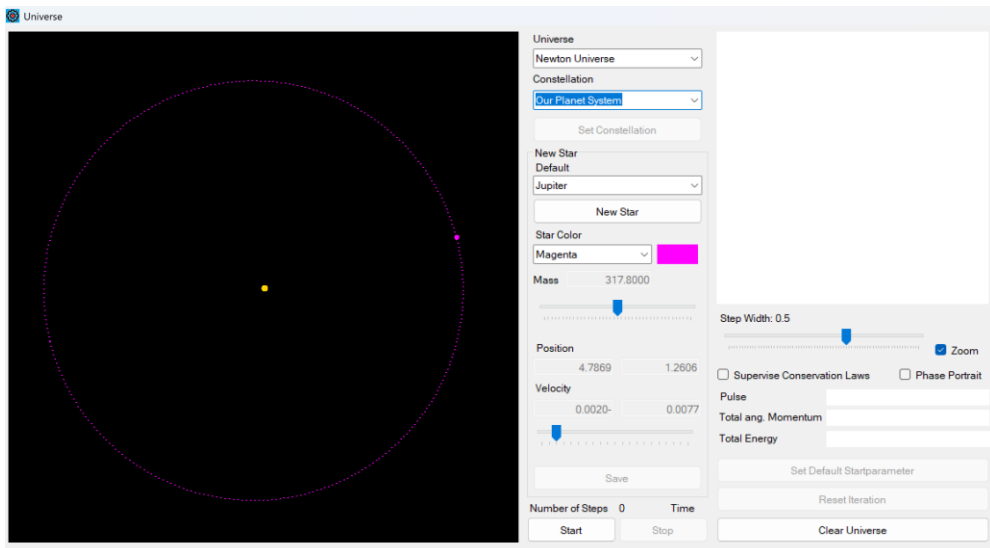
$$v_0 = \sqrt{\frac{GM}{r}}$$

If the moving mass has the distance r to M . In the implementation, when specifying the speed v , we assume that this is the speed at perihelion. However, this is only the case if $v > v_0$. Otherwise, the moving mass will approach the mass M , which means that the starting point of the orbit is actually the aphelion of the orbit. We take this into account in the implementation in that the orbit curve is determined as follows:

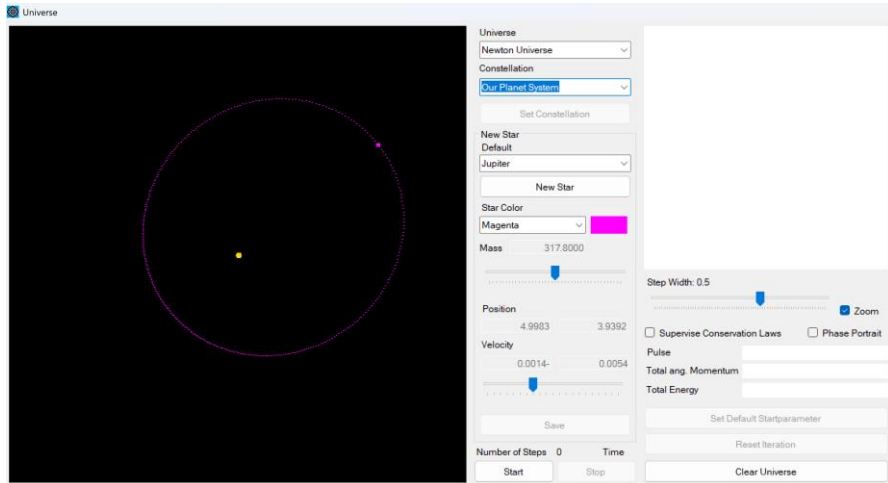
$$\varrho(\vartheta) = \frac{p}{1 + \varepsilon \cos(\vartheta - \alpha)}, \text{ if } v \geq v_0$$

$$\varrho(\vartheta) = \frac{p}{1 - \varepsilon \cos(\vartheta - \alpha)} \cdot \frac{1 - \varepsilon}{1 + \varepsilon}, \text{ if } v < v_0$$

It is easy to see that the starting point for $\vartheta = \alpha$ is identical in both cases. However, the second equation provides an elliptical orbit with the starting point at aphelion.



Jupiter, starting from the actual position at perihelion and the actual speed



Here, the user has changed the starting position and speed

1.2 Kepler's laws

Here we can look at Kepler's laws. The orbital curve of the mass m_1 , calculated in the previous section, immediately provides Kepler's first law: *the planets move on ellipses with the sun at their focal point.*

An infinitesimal surface element, which is swept by the position vector, is in polar coordinates:

$$dF = \frac{1}{2} \varrho^2 \dot{\vartheta} dt = \frac{1}{2} \frac{L}{m_1} dt$$

since the angular momentum L is constant. This means that the area covered during a fixed time Δt is always of the same size. This leads to Kepler's second law: *the line connecting the planet and the sun sweeps over the same area at the same time.*

If T is the orbital period of the mass m_1 , then the elliptical surface $F = \pi ab$ is swept during this time. The following therefore applies:

$$\pi ab = \int_0^T \frac{1}{2} \varrho^2 \dot{\vartheta} dt = \frac{1}{2} \int_0^T \frac{L}{m_1} dt = \frac{1}{2} T \frac{L}{m_1}$$

So it is:

$$T = 2\pi ab \frac{m_1}{L}$$

The definition of p was: $p := \frac{M^2 L^2}{G m_2^3 m_1^2}$. Furthermore, $p = a(1 - \varepsilon^2)$ and thus

$$L = \sqrt{G m_2} \cdot \frac{m_1 m_2}{M} \sqrt{a(1 - \varepsilon^2)}$$

Furthermore, $b = a\sqrt{1 - \varepsilon^2}$. If we use this in the above formula for T , we get

$$T = 2\pi a^2 \sqrt{1 - \varepsilon^2} \cdot m_1 \frac{M}{\sqrt{G m_2 m_1 m_2 \sqrt{a(1 - \varepsilon^2)}}} = 2\pi \sqrt{a^3} \frac{M}{\sqrt{G m_2^3}}$$

Thus:

$$\frac{T^2}{a^3} = 4\pi^2 \frac{M^2}{Gm_2^3} = \text{constant}$$

In the special case of the sun and a planet, we have $m_2 = M_{\text{Sonne}}$ and $M = m_1 + m_2 \approx M_{\text{Sonne}}$

Then it becomes:

$$\frac{T^2}{a^3} = 4\pi^2 \frac{1}{GM_{\text{Sonne}}}$$

In particular, Kepler's third law follows from this: *the squares of the orbital periods are in the same ratio as the cubes of the large semi-major axes.*

1.3 Some data about our solar system

Later, we will check certain calculations for the simulation using our solar system as an example. Individual exercises also refer to this system. Therefore, the necessary data is listed in the following table.

Once again, the gravitational constant: $G \approx 6.6743 \cdot 10^{-11} \frac{\text{m}^3}{\text{kg} \cdot \text{s}^2}$

	Sun	Mercury	Venus	Earth	Mars
Mass in kg	1.9884E+30	3.3010E+23	4.8673E+24	5.9722E+24	6.4200E+23
Mass relative to the earth's mass	332'943	0.055	0.815	1.000	0.107
Mass relative to the mass of the sun	1	1.660E-07	2.448E-06	3.004E-06	3.229E-07
Diameter in km	1'392'000	4'879	12'103	12'735	6'772
Gravitational constant in m/s ²	274.00	3.70	8.87	9.80	3.73
Orbital period around the sun in days	-	87.969	224.701	365.256	686.980
Major semi-axis in million km	-	57.909	108.200	149.600	227.990
Large half-axis in AU	-	0.3871	0.7233	1.000	1.524
Eccentricity of the elliptical path	-	0.2056	0.0068	0.0167	0.0934
Speed relative sun in km/h	-	172'332	126'072	107'208	86'868
Speed relative sun in AU/day	-	0.0276	0.0202	0.0172	0.0139
... and in AU/year	-	10.0700	7.3669	6.2646	5.0760
Escape velocity in km/s *)	617.4	4.3	10.4	11.2	5.0
Argument of the perihelion **)	-	1.3519	2.2956	1.7967	5.8650
Perihelion in AU	-	0.3075	0.7184	0.9833	1.3814
Perihelion Speed in km/h	-	212'328	126'936	109'044	95'400
Perihelion velocity in AU/day	-	0.034063	0.020364	0.017494	0.015305
Aphelion in AU	-	0.467	0.728	1.017	1.666

	Jupiter	Saturn	Uranus	Neptune	
Mass in kg	1.8980E+27	5.6830E+26	8.6800E+25	1.0024E+26	
Mass relative to the earth's mass	317.8	95.2	14.5	16.8	
Mass relative to the mass of the sun	9.545E-04	2.858E-04	4.365E-05	5.041E-05	
Diameter in km	138'346	114'632	50'532	49'105	
Gravitational constant in m/s ²	24.79	10.44	8.87	11.15	
Orbital period around the sun in days	4'329	10'751	30'664	60'148	

Major semi-axis in million km	778.51	1'433.40	2'872.40	4'514.60
Large half-axis in AU	5.204	9.582	19.201	30.178
Eccentricity of the elliptical path	0.0489	0.0542	0.0472	0.0097
Speed relative sun in km/h	47'052	34'884	24'516	19'548
Speed relative sun in AU/day	0.0075	0.0056	0.0039	0.0031
... and in AU/year	2.7393	2.0453	1.4244	1.1322
Escape velocity in km/s *)	60.2	36.1	21.4	23.6
Argument of the perihelion **)	0.2575	1.6132	2.9839	0.7849
Perihelion in AU	4.9501	9.0481	18.3755	29.7667
Perihelion Speed in km/h	49'392	36'648	25'596	19'800
Perihelion velocity in AU/day	0.007924	0.005879	0.004106	0.003176
Aphelion	5.455	10.12	20.11	30.069

*) at the equator

**) Relative to the zero direction, which is defined by the intersection of the ecliptic with the Earth's equatorial plane. The argument is in radian.

The information on the perihelion changes over time. The above data are from the year 2000 and are used as the starting position of a planet when implementing our planetary system. As the numerical approximation becomes imprecise very soon anyway, we refrain from striving for greater accuracy here. Moreover, this would quickly become very time-consuming

1.4 The N-body Problem

The three-body problem is already significantly more complex than the two-body problem. It was already formulated by Newton. There is no closed analytical solution to this problem. Over the last three hundred years, great mathematicians have worked on this problem. Important contributions were made by Pierre Simon Laplace (1749 - 1827) and Henri Poincaré (1854 - 1912). A more recent result from the years 1953 - 1963, which among other things relates to the stability of our planetary system, is the so-called KAM theorem by Andrei Kolmogorov (1903 - 1987), Jürgen Moser (1928 - 1999) and Vladimir Arnold (1937 - 2010).

For n bodies with mass $m_j, j = 1..n$, which are located at the positions $\vec{r}_j, j = 1..n$, Newton's equations of motion are given by

$$m_j \ddot{\vec{r}}_j = \sum_{i \neq j} G \frac{m_j m_i}{|\vec{r}_i - \vec{r}_j|^3} \cdot (\vec{r}_i - \vec{r}_j)$$

We will use these equations when simulating the movement of these bodies for the numerical methods. These equations are invariant under displacement of the zero point, i.e. when replacing $\vec{r}_j = \vec{r}'_j + \vec{c}$, where \vec{c} is a constant vector. We will choose the common centre of gravity of the masses as the zero point. The coordinate \vec{R} of the center of gravity for any coordinate system is given by

$$M\vec{R} = \sum_{j=1}^n m_j \vec{r}_j$$

$$M = \sum_{j=1}^n m_j$$

The sum of all forces cancels out, because for all pairs of bodies the force between these bodies is zero in total. It is therefore:

$$\sum_{j=1}^n m_j \ddot{\vec{r}}_j = 0$$

The momentum theorem follows from this by integration:

$$\sum_{j=1}^n m_j \dot{\vec{r}}_j = \vec{p}$$

Whereby \vec{p} is constant.

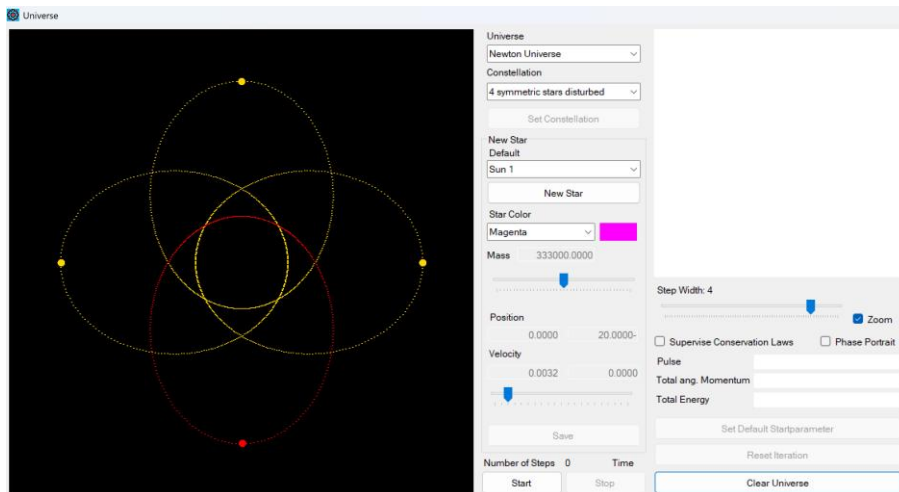
The following applies to the angular momentum \vec{L} :

$$\frac{d}{dt} \vec{L} = \frac{d}{dt} \sum_{j=1}^n \vec{r}_j \times m_j \dot{\vec{r}}_j = \sum_{j=1}^n \vec{r}_j \times m_j \ddot{\vec{r}}_j = \sum_{j=1}^n \vec{r}_j \times \left\{ \sum_{i \neq j} G \frac{m_i m_i}{|\vec{r}_i - \vec{r}_j|^3} \cdot (\vec{r}_i - \vec{r}_j) \right\}$$

In this somewhat complex sum, the summands always occur in pairs, e.g.

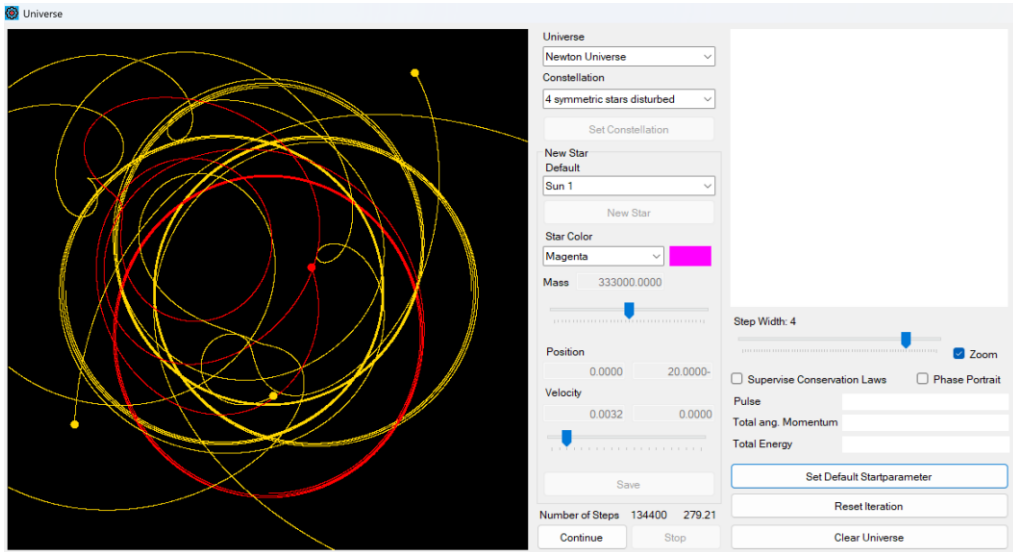
$\vec{r}_1 \times G \frac{m_1 m_2}{|\vec{r}_2 - \vec{r}_1|^3} \cdot (\vec{r}_2 - \vec{r}_1)$ and $\vec{r}_2 \times G \frac{m_1 m_2}{|\vec{r}_1 - \vec{r}_2|^3} \cdot (\vec{r}_1 - \vec{r}_2)$. The sum of such a pair is zero, so in total $\frac{d}{dt} \vec{L} = 0$ and therefore, the angular momentum is constant. For the motion of the N-bodies, the plane perpendicular to \vec{L} is invariant and we can place it in the centre of gravity of the system. It is called the *invariant plane of Laplace*. In the simulation of the N-body problem, we will restrict ourselves to the case where all bodies lie in this plane.

With a similar, but somewhat more complex calculation, it can be shown that the total energy of the system is constant.



4 (almost) symmetrical stars in starting position

The orbits shown were calculated for each star like a two-body problem. The distance of the red star from the centre of gravity is smaller by $5 \cdot 10^{-7} \%$. The system reacts very sensitively to this disturbance and after four orbits it runs "out of control".



The "disturbed" system of the four stars gets out of control after four orbits

1.5 Numerical approximation of the N-body Problem

In the "Simulator", we only consider flat systems, i.e. we calculate with two components.

The acceleration that the body number j experiences is:

$$\ddot{\vec{r}}_j = \sum_{i \neq j} G \frac{m_i}{|\vec{r}_i - \vec{r}_j|^3} \cdot (\vec{r}_i - \vec{r}_j)$$

We write for the position vector of the body:

$$\vec{r}_j = \begin{pmatrix} x_j \\ y_j \end{pmatrix}$$

We set:

$$R_{ji} := \sqrt{(x_i - x_j)^2 + (y_i - y_j)^2}$$

And then, we receive e.g. for the first component of: $\dot{\vec{r}}_j$

$$\dot{x}_j = G \sum_{i \neq j} \frac{m_i}{R_{ji}^3} \cdot (x_i - x_j)$$

For n bodies, this provides a system of $2n$ second-order differential equations. With the substitution: $u_{1j} = x_j, v_{1j} = \dot{x}_j$ or $u_{2j} = y_j, v_{2j} = \dot{y}_j$, a system of first-order differential equations is obtained for the acceleration of body number j :

$$\begin{cases} \dot{u}_{1j} = v_{1j} =: f_1(t, u_1, v_1, u_2, v_2) \\ \dot{v}_{1j} = G \sum_{i \neq j} \frac{m_i}{R_{ji}^3} \cdot (u_{1i} - u_{1j}) =: g_1(t, u_1, v_1, u_2, v_2) \\ \dot{u}_{2j} = v_{2j} =: f_2(t, u_1, v_1, u_2, v_2) \\ \dot{v}_{2j} = G \sum_{i \neq j} \frac{m_i}{R_{ji}^3} \cdot (u_{2i} - u_{2j}) =: g_2(t, u_1, v_1, u_2, v_2) \end{cases}$$

With

$$R_{ji} := \sqrt{(u_{1i} - u_{1j})^2 + (u_{2i} - u_{2j})^2}$$

As in the section on the double pendulum, we now apply the four-order Runge-Kutta method for a simulation of this system. The result will only be a numerical artifact of a real system. However, in the implementation we will monitor the total momentum, the total angular momentum and the total energy of the system and check that these are (reasonably) constant.

To document the implementation in the "simulator", we prepare it in the following algorithm. In it, $u_{1n}, v_{1n}, u_{2n}, v_{2n}$ are the values of the parameters after the n^{th} iteration step. The (constant) step size is d , which must be chosen sufficiently small. Now we try to keep the representation somewhat compact. We carry out the following steps one after the other:

$$\begin{aligned} \vec{z}_{1n} &:= (u_{1n}, v_{1n}, u_{2n}, v_{2n}) \\ \begin{cases} k_{i1} := f_i(t_n, \vec{z}_{1n}) \\ h_{i1} := g_i(t_n, \vec{z}_{1n}) \end{cases}, i \in \{1,2\} \\ \vec{z}_{2n} &:= (u_{1n} + \frac{d}{2}k_{11}, v_{1n} + \frac{d}{2}h_{11}, u_{2n} + \frac{d}{2}k_{21}, v_{2n} + \frac{d}{2}h_{21}) \\ \begin{cases} k_{i2} := f_i(t_n + \frac{d}{2}, \vec{z}_{2n}) \\ h_{i2} := g_i(t_n + \frac{d}{2}, \vec{z}_{2n}) \end{cases}, i \in \{1,2\} \\ \vec{z}_{3n} &:= (u_{1n} + \frac{d}{2}k_{12}, v_{1n} + \frac{d}{2}h_{12}, u_{2n} + \frac{d}{2}k_{22}, v_{2n} + \frac{d}{2}h_{22}) \\ \begin{cases} k_{i3} := f_i(t_n + \frac{d}{2}, \vec{z}_{3n}) \\ h_{i3} := g_i(t_n + \frac{d}{2}, \vec{z}_{3n}) \end{cases}, i \in \{1,2\} \\ \vec{z}_{4n} &:= (u_{1n} + k_{13}, v_{1n} + h_{13}, u_{2n} + k_{23}, v_{2n} + h_{23}) \\ \begin{cases} k_{i4} := f_i(t_n + d, \vec{z}_{4n}) \\ h_{i4} := g_i(t_n + d, \vec{z}_{4n}) \end{cases}, i \in \{1,2\} \\ \begin{cases} t_{n+1} = t_n + d \\ u_{i(n+1)} = u_{in} + \frac{d(k_{i1} + 2k_{i2} + 2k_{i3} + k_{i4})}{6} \\ v_{i(n+1)} = v_{in} + \frac{d(h_{i1} + 2h_{i2} + 2h_{i3} + h_{i4})}{6} \end{cases}, i \in \{1,2\} \end{aligned}$$

These are the equations that are used in the implementation. As the Runge-Kutta method is structurally the same for all universes, it is implemented in the abstract universe class. In contrast, the functions $f_{1,2}, g_{1,2}$ depend on the power law of the universe and are implemented in the specific universe.

After implementation, it was found that the Runge-Kutta method unfortunately delivers very imprecise trajectories, which are only reasonably plausible for very small increments.

There are certain effects in the "simulator", that have not yet been sufficiently clarified, especially when stars collide or come very close to each other.

1.6 Choice of Coordinate System

The zero point of the coordinate system should coincide with the common centre of gravity of all masses. The common centre of gravity is recalculated when a new body is placed. When this placement is complete, all bodies are repositioned so that the centre of gravity coincides with the zero point(0,0) again. If n masses are placed, then the centre of gravity is relative to their centre of gravity:

$$\sum_{i=1}^n m_i \vec{r}_i = \vec{0}$$

Now the mass n+1 is added. The common centre of gravity then shifts by a vector \vec{c} . The following then applies to the new centre of gravity:

$$\sum_{i=1}^{n+1} m_i (\vec{r}_i + \vec{c}) = \vec{0}$$

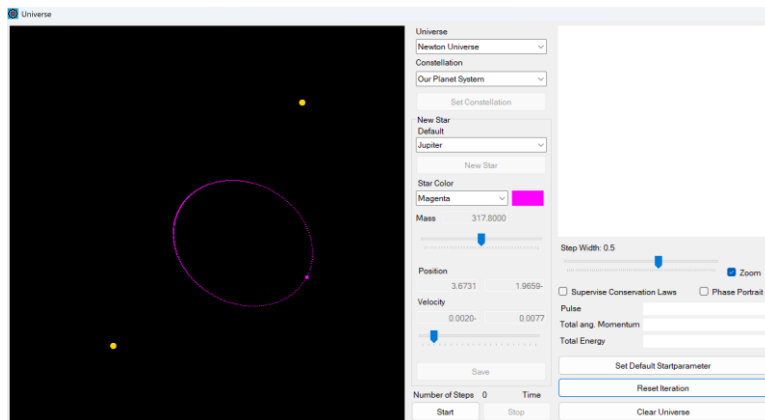
So it is:

$$\vec{c} = -\frac{m_{n+1} \vec{r}_{n+1}}{\sum_{i=1}^{n+1} m_i}$$

In reality, the direction of the x-axis is determined by the intersection of the ecliptic with the Earth's equatorial plane at the vernal equinox. In the simulator, the zero point of the coordinate system is the centre of the display diagram and the x-axis points to the right as usual.

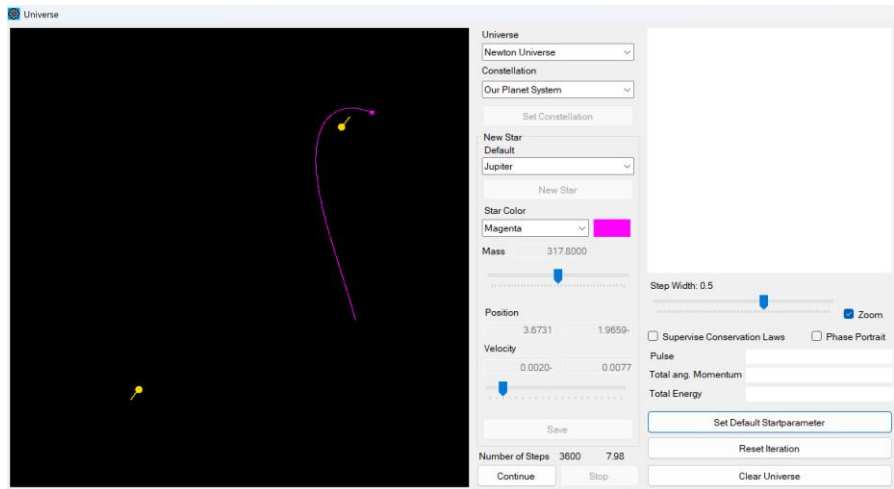
This choice of coordinate system is valid for all universes, as they differ only in the law of force.

In the "Simulator", this causes the entire image to be shifted after a new star has been placed so that the common centre of gravity is at the origin. The coordinates of all previous stars then refer to this new centre of gravity. When a new star is added, its standard coordinates are converted to the new coordinate system during placement.



Two suns and a Jupiter were placed here

In the image above, the coordinates of the suns and Jupiter shown refer to the common centre of gravity. As the suns are at rest, no expected orbit relative to the common shear point is calculated for them. However, this is the case for Jupiter.



The orbits after the start of the iteration

1.7 Representation of the Universe in the "simulator"

An universe in the "simulator" is defined by the law of motion, for example by Newton's law of gravity. Alternative universes are dealt with in a separate section. A universe contains n bodies, which are generally referred to as "stars" in the "simulator", even if they are planets. However, when it comes to the real planets, this term is also used.

By default, certain stars are set as the default, in particular the components of our planetary system. This is the sun including the associated planets. Such a system, for example consisting of the sun plus a selection of planets, is a *constellation*. Different constellations are available for each universe in the "Simulator". In the example of Newton's universe, this includes our planetary system or the system of inner planets. There are also variants with "disturbances", for example when Jupiter is repositioned so that it comes close to the inner planets. Once you have selected a constellation, you can also place the planets or the sun individually and then move them with the mouse or change their mass and speed.

In the "simulator", the area in which the bodies are placed is a square with a side length that is defined for each universe. The zero point of the coordinate system lies at the centre of this square and is the common centre of gravity of the bodies in the universe.

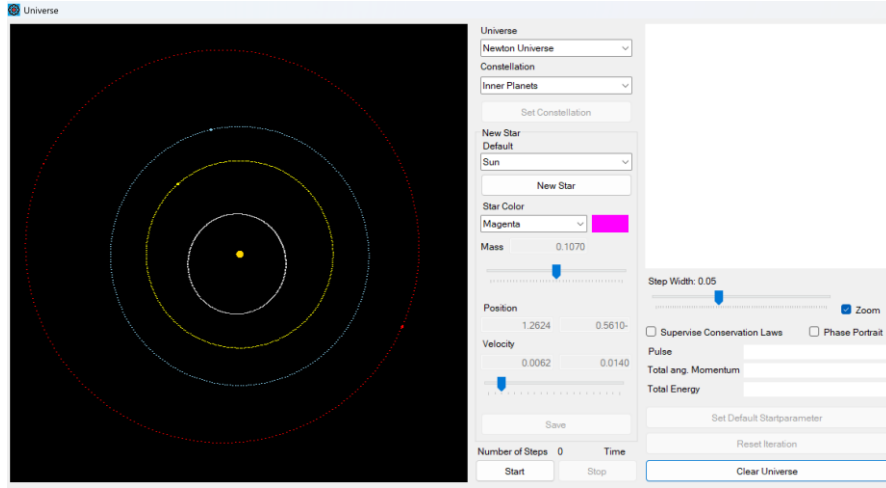
Zoom: If "Zoom" is activated, when new planets or stars are displayed, their position coordinates are converted into mathematical coordinates so that they fit perfectly into the square.

Example

If only the inner planets are considered, then Mars is the outermost planet with a distance of $\sim 1.524 \text{ AU}$ from the Sun. However, its aphelion is 1.666 AU . The scaling (in the implementation of the "zoom") is then selected so that 1.666 AU just corresponds to the number 30. All planetary orbits are then clearly visible. For example, the perihelion of Mercury is 0.3075 AU . This corresponds to the number 5,353 or about 53 pixels.

If the outer planets are also to be shown, then the aphelion of Neptune is 30.069 AU . The scaling is selected so that this value corresponds to the number 29 in mathematical coordinates. The perihelion of Mercury is then still 0.297 in mathematical coordinates, which corresponds to about 3 pixels. It is then no longer visible because the mass of the sun is represented by 8 pixels.

After placing a star, the new common centre of gravity is determined and then all stars are placed relative to this centre of gravity. This means that the current start position then refers to this centre of gravity. When placing a new star, its original starting position, which is saved as the star's default, must also be converted to the new coordinate system.



Representation of the inner planets

The movement of the stars in the "simulator" is usually counterclockwise. In the case of planetary motion, it should be noted that the angular momentum vector of a planetary orbit is parallel to the angular momentum vector of the Earth's rotation. If you look at the Earth "from above", i.e. from the North Pole, then the Earth rotates in an anticlockwise direction. This is the usual positive direction of rotation in mathematical angle measurement. The planets in the simulator therefore also rotate in an anticlockwise direction. This direction of rotation is maintained for alternative universes.

1.8 Representation of the orbit sketch when placing a star

As a placement aid for new planets, their orbit is sketched dynamically in the diagram, as if it were a two-body system with the common mass of all existing bodies in the common centre of gravity. The prerequisite for this is that the newly placed planet or star has a velocity of $v > 0$. It is assumed in the calculation that this is the speed at perihelion.

Here we carry out the necessary calculations that the "simulator" must perform. The following is:

M is the sum of all existing masses. m is the mass of the newly added body.

The following applies to the speed v at perihelion ϱ :

$$v = \varrho \dot{\vartheta}$$

This means that the angular momentum of the newly added mass

$$L = m\varrho^2 \dot{\vartheta} = m\varrho v$$

For their energy you have:

$$E = \frac{1}{2}mv^2 - G \frac{M^3m}{(M+m)^2} \cdot \frac{1}{\varrho} \approx \frac{1}{2}mv^2 - G \frac{Mm}{\varrho}$$

\approx applies if $M \gg m$

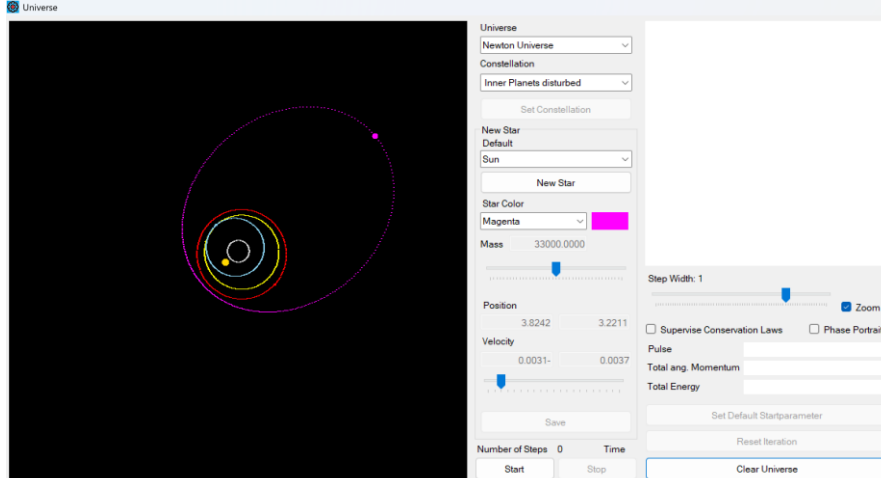
The path parameters are now:

$$p = \frac{(M+m)^2 \varrho^2 v^2}{GM^3} \approx \frac{\varrho^2 v^2}{GM}$$

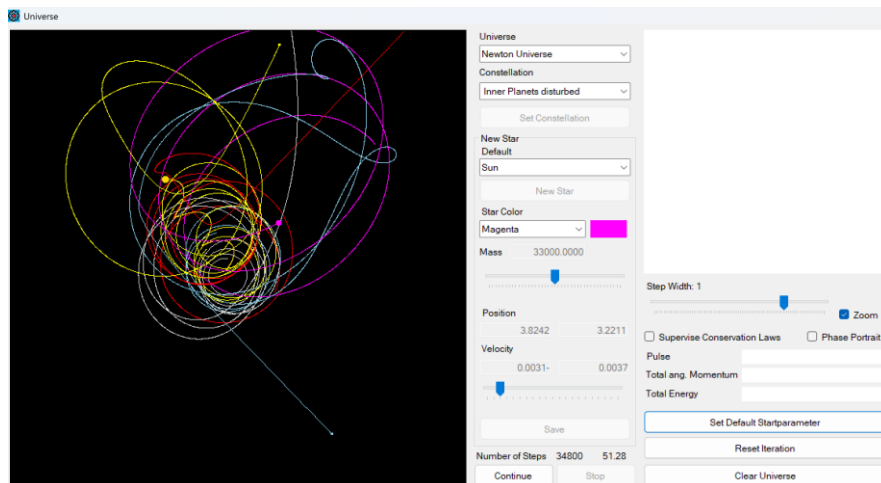
$$\varepsilon^2 - 1 = \frac{2EL^2(M+m)^4}{G^2 m^3 M^6} = \frac{2Em^2 \varrho^2 v^2 (M+m)^4}{G^2 m^3 M^6} \approx \frac{2E\varrho^2 v^2}{G^2 m M^2}$$

The path can then be drawn considering the argument of the perihelion. This will not be the actual path but serves as a guide.

For alternative universes, orbit calculation is not possible if the two-body problem cannot be solved analytically.



The inner planets together with a disturbed Jupiter. The zero point is the common centre of gravity and not the sun



The disturbed Jupiter has just sent Mars into the afterlife and disturbed the Earth's orbit

1.9 The collision problem

If two bodies come closer to each other than two pixels, which is 0.1 in mathematical units or, depending on the scaling and zoom, a correspondingly large value in astronomical units, then this could be regarded as a plastic collision in the simulation.

This was implemented in a version of the "Simulator": The simulation is not stopped, but we replace the two colliding bodies with a body with the sum of both masses. The velocity vector of the new body is then set so that the momentum remains constant. This does not correspond to a physical

reality, but only serves the continuation of the simulation. If $m_{1,2}, \vec{v}_{1,2}$ are the parameters of the bodies before the impact and m, v are the parameters of the new body after the impact, the following applies:

$$m = m_1 + m_2$$

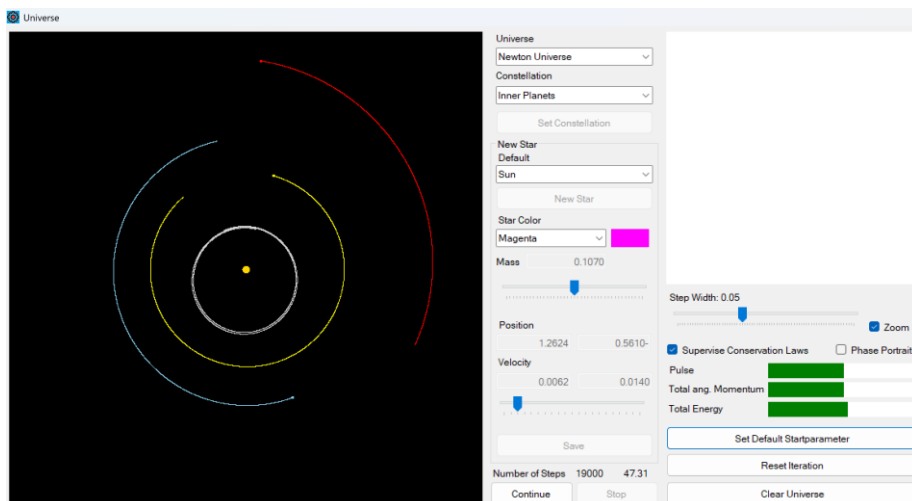
$$\vec{v} = \frac{m_1 \vec{v}_1 + m_2 \vec{v}_2}{m}$$

As you can easily calculate, the angular momentum of the system remains the same, but not the total energy.

However, after experiments with collisions did not have a satisfactory effect, this implementation was removed again. Now it is ensured that bodies "narrowly miss" each other if they come too close.

1.10 Conservation laws and phase diagram

During the simulation, the total momentum, the total angular momentum and the total energy of the system are continuously calculated and compared with the corresponding values at the start of the simulation. A condition for alternative universes is that these conservation laws also apply there. In the user window, these values are displayed in bars to the right below the phase portrait.



Movement of the inner planets around the sun and monitoring the laws of conservation

However, due to the imprecision of the Runge Kutta-method, deviations can always occur here.

You can also activate the representation of the movement in a phase diagram. In this case, the distance of the star from the common centre of gravity is entered for each star in the horizontal direction and the amount of its velocity relative to this in the vertical direction.

1.11 The Newtonian Universe

The aim is to be able to calculate internally in the "Simulator" with the variable type "decimal". For the Newtonian universe, this means that the spatial distances are managed internally in astronomical units AU . The mass is specified for the user in kg , but is managed internally in the number of earth masses ME . The speed of bodies is specified for the user in km/h . Internally, we keep it in AU/day . The gravitational constant must be adjusted accordingly when calculating the force. The following applies:

$$G = 6.6743 \cdot 10^{-11} \frac{m^3}{kg \cdot s^2}$$

And the simulator uses:

$$G_s = 6.6743 \cdot 10^{-11} \cdot \frac{5.9722 \cdot 10^{24} \cdot (3600 \cdot 24)^2}{149.6^3 \cdot 10^{27}} = 8.88736 \cdot 10^{-10} \frac{AU^3}{ME \cdot day^2}$$

As an example, we can perform a small check by calculating the speed of the earth around the sun from the equilibrium condition centrifugal force = gravitational force, first in the m.kg.s system and then in the AU.ME.day system. The equilibrium condition is

$$m \frac{v^2}{r} = G \frac{Mm}{r^2}$$

Or

$$v^2 = \frac{GM}{r}$$

Where M is the mass of the sun and r is the distance between the earth and the sun.

In the m.kg.s system the equation is:

$$v^2 = 6.6743 \cdot 10^{-11} \frac{1.9884 \cdot 10^{30}}{1.496 \cdot 10^{11}} = 8.8711 \cdot 10^8$$

$$v = 2.9784 \cdot 10^4 \text{ m/s}$$

If we convert this into AU/day , the result is

$$v = 2.9784 \cdot 10^4 \cdot \frac{86400}{1.496 \cdot 10^{11}} = 0.0172 \text{ AU/day}$$

If we calculate in the AU.ME.day system right from the start, we have:

$$v^2 = 8.88736 \cdot 10^{-10} \cdot \frac{332942.6}{1} = 2.959 \cdot 10^{-4}$$

$$v = 0.0172 \text{ AU/day}$$

If the unit of velocity is chosen too high, e.g. AU/year, then the step size of the Runge Kutta method must be chosen very low so that the method leads to a reasonably plausible-looking orbit. This makes the movement of the planets very slow. If, on the other hand, $v \ll |\vec{r}|$, e.g. as here, then the Runge Kutta method is reasonably plausible even with larger step sizes and at the same time the speed of the planets is acceptable. We have not investigated this effect further here. However, the implementation includes a factor τ , which can be used as a factor for changing the unit of velocity. If the speed is adjusted by changing the unit of time: $v' = \tau v$, the gravitational constant in the law of motion must be corrected accordingly: $G' = \tau^2 G$, since time appears in the gravitational constant squared. This factor can be adjusted individually for each universe. Based on experiments, the Newtonian universe, $\tau = 1$

1.12 Alternative Universes

An alternative universe should only differ from Newton's universe in terms of the law of force. Essential properties of Newton's universe should be retained. These include the conservation laws and the independence of the law of motion from the choice of coordinate system.

To this end, we assume that a force law of form also applies in alternative universes between two masses m_1, m_2 and the positions \vec{r}_1, \vec{r}_2 :

$$\begin{cases} m_1 \ddot{\vec{r}}_1 = F(|\vec{r}|) \cdot \frac{\vec{r}}{|\vec{r}|} \\ m_2 \ddot{\vec{r}}_2 = -F(|\vec{r}|) \cdot \frac{\vec{r}}{|\vec{r}|} \end{cases}$$

$$\vec{r} = \vec{r}_2 - \vec{r}_1.$$

Newton's three laws therefore apply:

- a) If no force acts on a body, it moves at a constant speed
- b) *Force = mass x acceleration*
- c) Force = - counterforce

The *momentum theorem* follows from this.

Furthermore, the magnitude of the force depends only on the distance between the masses. This means that the equations of motion are *independent of the choice of zero point*.

As the direction of the force vector is parallel to \vec{r} , the *angular momentum theorem* follows and therefore the movement of the masses runs *in a plane*. It also follows that the equations of motion are *invariant to rotations of the coordinate system*.

We also assume that the force can be derived from a potential function. This means that there is a function $\Phi: \mathbb{R}^3 \rightarrow \mathbb{R}, \vec{r} \mapsto \Phi(\vec{r})$ such

$$\vec{F} = -\nabla \Phi := \begin{pmatrix} -\frac{\partial \Phi(\vec{r})}{\partial x} \\ -\frac{\partial \Phi(\vec{r})}{\partial y} \\ -\frac{\partial \Phi(\vec{r})}{\partial z} \end{pmatrix}, \vec{r} = (x, y, z)$$

The *energy theorem* follows from the last condition.

We leave the proof of these statements as an exercise.

The *normalized universe* is implemented in the simulator. Here, the law of force is identical to Newton's universe, but the units are normalized more conveniently. The following applies to the implementation:

The masses are in the range $m_i \in [0.5, 2], \forall i$ and their positions in the range $|\vec{r}_i| \leq 2$. The gravitational constant is $G = 1$ and the velocities are in the range $|\dot{\vec{r}}_i| \leq 1$

The parameters for calculating the orbit are the same as in Newton's universe, with the only difference that the gravitational constant is $G = 1$. For N bodies, we sketch the orbit of a mass as a two-body problem, namely as the movement of the mass relative to the common centre of gravity, with all other masses united at one point. The derivation is therefore the same as for the two-body problem in Newton's universe:

$$L = m_1 |\vec{r}_1| |\dot{\vec{r}}_1|$$

$$E = \frac{1}{2}m_1|\vec{r}_1|^2 - \frac{M^3 m_1}{(m_1 + M)^2} \cdot \frac{1}{|\vec{r}_1|}$$

If M = mass of all other stars.

This reintroduces the parameters:

$$p := \frac{(m_1 + M)^2 L^2}{m_1^2 M^3}$$

$$\varepsilon^2 := \frac{2EL^2(m_1 + M)^4}{m_1^3 M^6} + 1$$

And obtain the equation for the trajectory in polar coordinates as in the section on the two-body problem:

$$\varrho(\vartheta) = \frac{p}{1 + \varepsilon \cos(\vartheta - \alpha)}$$

For universes that do not obey Newton's law of gravity, the trajectory cannot generally be calculated.

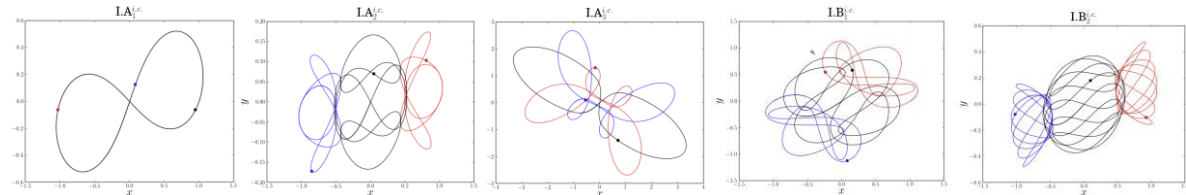
1.13 Periodically stable tracks

An exciting topic in the (normalized) universe is the question of periodically stable orbits, especially in the three-body problem. The first families of such periodic orbits were found by Leonhard Euler (1707 - 1783) and later by Joseph Louis Lagrange (1736 - 1813).

Examples can be found on the Internet under the links:

<https://numericaltank.sjtu.edu.cn/three-body/three-body.htm>

<https://numericaltank.sjtu.edu.cn/three-body/three-body-movies.htm>



Examples of periodic stable orbits on the Internet

Further explanations can also be found in the links above. Some of these scenarios are saved as constellations in the "Simulator". In particular, the case of three stars with the same mass $m_1 = m_2 = m_3 = 1$ and the initial positions $\vec{r}_1 = (-1, 0), \vec{r}_2 = (1, 0), \vec{r}_3 = (0, 0)$

The initial velocities are: $\vec{v}_1 = (c_1, c_2) = \vec{v}_2, \vec{v}_3 = (-2c_1, -2c_2)$ where the values of $c_{1,2}$ can be found in the following table. Note that the total momentum is zero at the start.

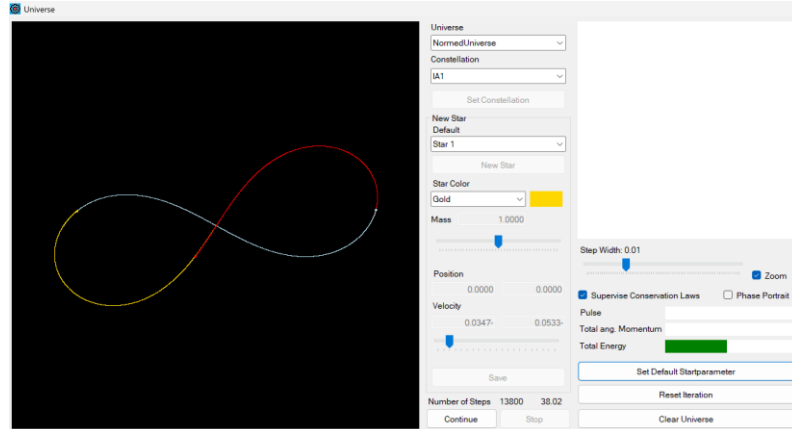
Several examples with a low period are implemented, whereby the Runge Kutta method clearly reaches its limits:

Constellation	C_1	C_2
IA1	0.3471168881	0.5327249454
IA2	0.3068934205	0.1255065670
IA3	0.6150407229	0.5226158545
IB1	0.4644451728	0.3960600146

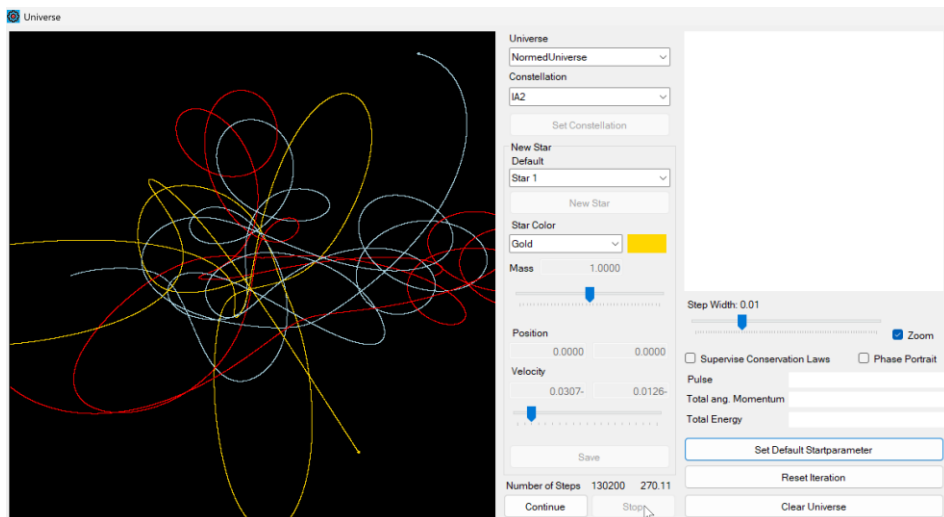
IB2	0.4059155671	0.2301631260
IIC1	0.2827020949	0.3272089716

Hundreds of thousands of such orbits have been found in recent decades, even with stars of different masses.

In the normalized universe, the factor for the unit of time is set as $\tau = 0.1$



The periodically stable path IA1



The Runge Kutta method is not precise enough for the representation of path IA2

1.14 Exercise examples

1. Two-body problem: Calculate the path of the mass m_1 relative to the position of the mass m_2 and compare the result with the calculation of the path relative to the centre of gravity.
2. Two body problem: Calculate the path of the mass m_2 relative to the center of mass.
3. From the polar form of the conic section equation, determine its equation in Cartesian coordinates.
4. The gravitational constant is known. The most important data from this system are also given in the chapter "Information on our solar system".

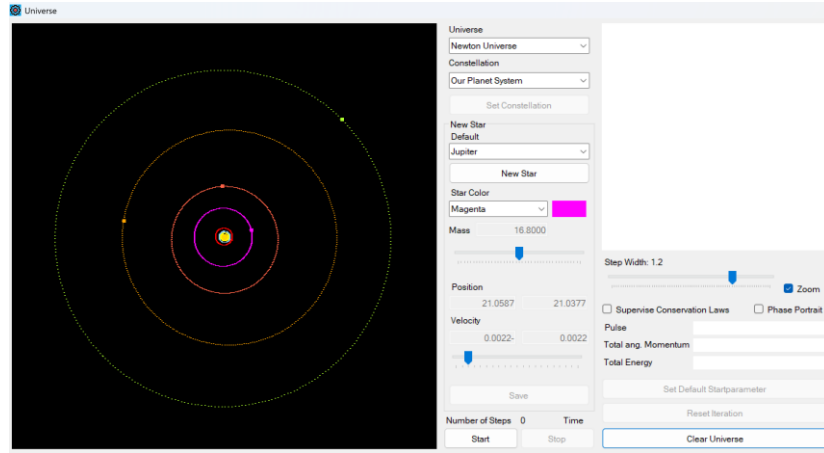
- a) Calculate the orbital period T of the earth around the sun from this information.
 - b) Calculate the angular momentum of the Earth-Sun system.
 - c) Calculate the explicit polar equation of the Earth's orbit around the Sun.
 - d) The orbital period of Mars around the sun is 687 Earth days. Use this information to determine the major semi-axis of Mars' orbit.
5. Determine the total energy for a system with N bodies. Show that the derivative of the energy with respect to time is zero because the summands belonging to two bodies cancel to zero in pairs.
6. Investigate symmetrical starting positions in the "simulator". This means that the bodies under consideration all have the same mass and their starting position and starting speed are rotationally symmetrical to the zero point.
7. Determine the equation of Jupiter's orbit around the sun in astronomical units.
8. A body lies on an ellipse with a major axis $a = 2$ and minor axis $b = 1$. At the start, the body is in the position $\vec{r}_0 = \begin{pmatrix} 0.5176 \\ 1.9318 \end{pmatrix}$ and $\vartheta_0 = 1.309$. Determine the path equation of the ellipse.
9. Determine the orbital equation of Jupiter in AU. Use it to calculate Jupiter's aphelion and perihelion. Compare the result with data from the internet. Note that the result is only an approximation.
10. If the earth were moving in a circular path around the sun, gravitational force and centrifugal force would just balance each other out. What would then be the speed of the Earth in km/h? Compare the result with the speed given in the table about the solar system.
11. Prove the statements in the section on alternative universes.
12. Search for further examples of stable periodic orbits on the Internet and implement them as corresponding constellations in the normalized universe.

a. Changing the star mass

When placing a new body, its mass can also be adjusted. This can vary between $3.3010 \cdot 10^{23}$ or 0.055 Earth masses (Mercury) and $1.9884 \cdot 10^{30}$ or 332942.6 Earth masses (Sun). The mass can be entered manually or via a shift register. The shift register only adjusts the mass relative to the initial mass by a factor that varies between 1 and 100. This means that Mercury can no longer be reduced in size, but all orders of magnitude between Mercury and 100 times the size of the sun can be represented. It is assumed that a body of the desired minimum size is already selected by default. Changing a mass results in the recalculation of the common centre of gravity.

The size of the mass is indicated in the diagram by the diameter. The number of pixels for the representation is at least 1 and otherwise the exponent of the mass minus 22. 1 pixel stands for the magnitude 10^{23} (Mercury, Mars). For the magnitude 10^{24} (Earth, Venus) 2 pixels. Jupiter with the magnitude 10^{27} is then represented by 5 pixels and the sun by 8 pixels.

The permissible definition range of mass depends on the universe and is defined individually for each universe.



Representation of our planetary system. The inner planets are barely visible.

2. 3D Attractors

2.1 Linear mappings $\mathbb{R}^3 \rightarrow \mathbb{R}^3$

Introduction

In the first chapter of the mathematical documentation for the "Simulator", we looked at (continuously differentiable) mappings $f: \mathbb{R} \rightarrow \mathbb{R}$. We saw that a fixed point $f(\xi) = \xi$ is attractive if and only if $|f'(\xi)| < 1$ applies. Now we want to transfer this to higher dimensions. If you are familiar with the Jacobian matrix and the concepts of eigenvalues and eigenvectors from linear algebra, you can skip this section. However, a basic knowledge of complex numbers and knowledge of plane or spatial vector geometry is required for the following.

We consider a continuously differentiable mapping $f: \mathbb{R}^3 \rightarrow \mathbb{R}^3$ given by one equation for each component:

$$f(\vec{r}) = \begin{cases} f_1(\vec{r}) \\ f_2(\vec{r}) \\ f_3(\vec{r}) \end{cases}, \vec{r} = (x, y, z) \in \mathbb{R}^3$$

This function is *vector-valued*, but we do not use the notation \vec{f} .

If you want to view mappings of $\mathbb{R}^2 \rightarrow \mathbb{R}^2$ instead of \mathbb{R}^3 , simply omit the third component.

Example

$$f(x, y, z) = \begin{cases} x - 2y + xz \\ 2x + y + yz \\ xy - z \end{cases}$$

You can see that this mapping is defined at \mathbb{R}^3 and assigns to each point an image point in \mathbb{R}^3 . It is also continuously differentiable in every variable.

In general, the "effect" of such a mapping is not easy to discuss. We start with the simplest such functions, namely the linear ones.

The mapping matrix

Linear mappings $\mathbb{R}^3 \rightarrow \mathbb{R}^3$ are given by a mapping of the form

$$f(x, y, z) = \begin{cases} a_1x + b_1y + c_1z \\ a_2x + b_2y + c_2z \\ a_3x + b_3y + c_3z \end{cases}$$

Where all coefficients $a_i, b_i, c_i \in \mathbb{R}, i = 1, 2, 3$.

We introduce the matrix notation for these mappings. The mapping matrix A is given by

$$A = \begin{bmatrix} a_1 & b_1 & c_1 \\ a_2 & b_2 & c_2 \\ a_3 & b_3 & c_3 \end{bmatrix}$$

The image of a vector $\vec{r} = \begin{pmatrix} x \\ y \\ z \end{pmatrix}$ is then defined as:

$$A\vec{r} = \begin{bmatrix} a_1 & b_1 & c_1 \\ a_2 & b_2 & c_2 \\ a_3 & b_3 & c_3 \end{bmatrix} \begin{pmatrix} x \\ y \\ z \end{pmatrix} := \begin{pmatrix} a_1x + b_1y + c_1z \\ a_2x + b_2y + c_2z \\ a_3x + b_3y + c_3z \end{pmatrix}$$

Each row of the image vector is the scalar product of the corresponding matrix row with the vector \vec{r} .

The mapping matrix A is often identified with the corresponding linear mapping $\mathbb{R}^3 \rightarrow \mathbb{R}^3$: We then speak of the linear mapping A . Since the dimension "3" does not play a significant role here, because many statements apply to vector spaces of any dimension, we often omit " $\mathbb{R}^3 \rightarrow \mathbb{R}^3$ " and speak only of the linear mapping A . As you can easily see, the following applies to a linear mapping:

Theorem

Let $A: \mathbb{R}^3 \rightarrow \mathbb{R}^3$ be a linear mapping. Then the following applies for any vectors $\vec{r}, \vec{s} \in \mathbb{R}^3$ and $\lambda \in \mathbb{R}$:

$$A(\lambda\vec{r} + \vec{s}) = \lambda A\vec{r} + A\vec{s}$$

The proof follows by direct calculation.

Note: The inverse is also true for this theorem: A mapping f (somehow defined, not by a mapping matrix) is linear if the following applies for any vectors $\vec{r}, \vec{s} \in \mathbb{R}^3$ and $\lambda \in \mathbb{R}$:

$$f(\lambda\vec{r} + \vec{s}) = \lambda f(\vec{r}) + f(\vec{s})$$

The linearity of A has a first important consequence: We can work with the basis vectors. If $\{\vec{e}_1, \vec{e}_2, \vec{e}_3\}$ are basis vectors of \mathbb{R}^3 (usually given by unit vectors in the direction of the three coordinate axes), then each vector can be written as a linear combination of these basis vectors:

$$\vec{r} = \begin{pmatrix} x \\ y \\ z \end{pmatrix} = x\vec{e}_1 + y\vec{e}_2 + z\vec{e}_3$$

Due to the linearity of A , the following applies:

$$A\vec{r} = xA\vec{e}_1 + yA\vec{e}_2 + zA\vec{e}_3$$

If we now consider the first base vector $\vec{e}_1 = \begin{pmatrix} 1 \\ 0 \\ 0 \end{pmatrix}$, for example, the following applies, as you can easily calculate:

$$A\vec{e}_1 = \begin{pmatrix} a_1 \\ a_2 \\ a_3 \end{pmatrix}$$

The same applies to the other two basis vectors and you have the

Theorem

Let f be a linear mapping. Then the corresponding mapping matrix is given by the images of the basis vectors in their columns.

Example

We consider a rotation D of 120° (clockwise) around the axis in space, which is generated by the vector $\begin{pmatrix} 1 \\ 1 \\ 1 \end{pmatrix}$. This mapping is linear because it does not matter whether I first rotate vectors and then combine them linearly, or first combine them linearly and then rotate them: $D(\lambda\vec{r} + \vec{s}) = \lambda D\vec{r} + D\vec{s}$. D swaps the basis vectors cyclically: $D\vec{e}_1 = \vec{e}_3, D\vec{e}_3 = \vec{e}_2, D\vec{e}_2 = \vec{e}_1$. Thus, the mapping matrix of D is given by:

$$D = \begin{bmatrix} 0 & 1 & 0 \\ 0 & 0 & 1 \\ 1 & 0 & 0 \end{bmatrix}$$

This example also shows that the axis of rotation remains "stationary" or is invariant:

$$D \begin{pmatrix} 1 \\ 1 \\ 1 \end{pmatrix} = \begin{pmatrix} 1 \\ 1 \\ 1 \end{pmatrix}$$

To define a linear mapping, it is therefore sufficient to know the images of the basis vectors!

Kernel and determinant

The question of which vectors are transferred in a linear mapping to $\vec{0}$ will prove to be very helpful. The set of these vectors is called *the kernel* of the linear mapping A .

Definition

Let A be a linear mapping. Then is: $\text{Kern } A := \{\vec{x}: A\vec{x} = \vec{0}\}$

Example

Let A be a linear mapping and $\vec{x}, \vec{y} \in \text{Kern } A$. Then for $\lambda, \mu \in \mathbb{R}$ is also $\lambda\vec{x} + \mu\vec{y} \in \text{Kern } A$. You can easily check this: $A(\lambda\vec{x} + \mu\vec{y}) = \lambda A\vec{x} + \mu A\vec{y} = \vec{0}$

Conclusion

Let $A: \mathbb{R}^3 \rightarrow \mathbb{R}^3$ be a linear mapping. Then the kernel is either the zero point, a straight line through the zero point, a plane through the zero point or the entire space (if A is the zero matrix).

Proof: See exercise.

The kernel is therefore again a vector space that is contained in \mathbb{R}^3 . It is also referred to as a *subspace* of \mathbb{R}^3 .

The question now is how to easily check whether the kernel is different from the zero point. If this is the case, then there is at least one vector $\vec{x} \neq \vec{0}$ with $A\vec{x} = \vec{0}$. If $\vec{x} = x\vec{e}_1 + y\vec{e}_2 + z\vec{e}_3$, then $A\vec{x} =$

$xA\vec{e}_1 + yA\vec{e}_2 + zA\vec{e}_3 = \vec{0}$. The images of the basis vectors or the columns of the mapping matrix are therefore linearly dependent. For example, if $z \neq 0$, the third column vector can be represented as a linear combination of the first two: $A\vec{e}_3 = -\frac{1}{z}(xA\vec{e}_1 + yA\vec{e}_2)$.

The scalar triple product of the column vectors $[A\vec{e}_1, A\vec{e}_2, A\vec{e}_3]$ is equal to the volume of the parallelepiped spanned by the three vectors, as we know from vector geometry. If these three vectors are linearly dependent, i.e. lie in a plane, then this product is zero. This provides the desired criterion. In the case of a linear mapping, we do not speak of the scalar triple product, but of the determinant, as this definition can be generalised to higher dimensions. The following definition is sufficient for us:

Definition

Let $A: \mathbb{R}^3 \rightarrow \mathbb{R}^3$ be a linear mapping. Then the *determinant* of A is defined by :

$$\det A := [A\vec{e}_1, A\vec{e}_2, A\vec{e}_3] = (A\vec{e}_1 \times A\vec{e}_2) \cdot A\vec{e}_3$$

Theorem

$$\text{Kern } A \neq \vec{0} \Leftrightarrow \det A = 0$$

" \Rightarrow " See section above.

" \Leftarrow " The images of the base vectors are linearly dependent, e.g. $A\vec{e}_3 = xA\vec{e}_1 + yA\vec{e}_2$. Then $\vec{z} := x\vec{e}_1 + y\vec{e}_2 - \vec{e}_3 \in \text{Kern } A$ and $\vec{z} \neq \vec{0}$.

Eigenvalues and eigenvectors

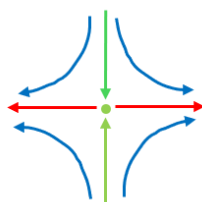
Now we come to the last important instrument for later investigating the behaviour of the mapping in the neighbourhood of fixed points.

In contrast to the one-dimensional case, it can happen in higher dimensions that a fixed point is repulsive in certain directions and attractive in other directions. In two dimensions, for example, the following cases may exist:



On the left an attractive fixed point (sink) and on the right a repulsive fixed point (source)

In contrast to the one-dimensional case, there can be a "mixture" here, namely when the fixed point is attractive in certain directions and repulsive in others. This is referred to as a *homoclinic fixed point*.



Homoclinic fixed point (saddle point)

It can become correspondingly more complicated in three dimensions.

The zero point is always a fixed point of a linear mapping. If there are certain directions in the mapping that are invariant, we can analyse whether the mapping is contracting or expanding in these directions. A direction is invariant if a vector is merely stretched or compressed in this direction. If A is a linear mapping, we look for solutions to the equation:

$$A\vec{x} = \lambda\vec{x}$$

For $\lambda \in \mathbb{R}$ and a vector $\vec{x} \in \mathbb{R}^3$. If the equation has such a solution, then λ is the eigenvalue of A and \vec{x} is the corresponding eigenvector. If $\lambda = 1$, then every point on the line spanned by \vec{x} is a fixed point. For $\lambda > 1$ the mapping is dilating, for $\lambda < 1$ it is contracting at the zero point.

Example

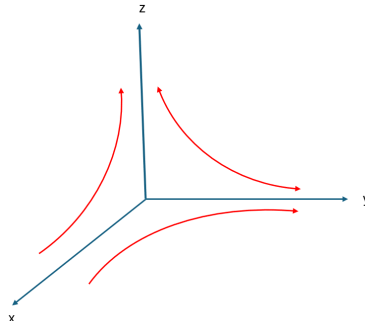
$$A = \begin{bmatrix} 0.5 & 0 & 0 \\ 0 & 1.5 & 0 \\ 0 & 0 & 2 \end{bmatrix}$$

The fixed point of this mapping is the zero point. This mapping is contracting in the direction of the first basis vector and dilating in the direction of the second and third. There are no further fixed

points, because the condition $A\vec{x} = \vec{x}$ leads to $(A - \mathbb{E})\vec{x} = \vec{0}$, if $\mathbb{E} = \begin{bmatrix} 1 & 0 & 0 \\ 0 & 1 & 0 \\ 0 & 0 & 1 \end{bmatrix}$ is the unit matrix. So

$\vec{x} \in \text{Kern}(A - \mathbb{E})$, but $\det(A - \mathbb{E}) = \det \begin{bmatrix} -0.5 & 0 & 0 \\ 0 & 0.5 & 0 \\ 0 & 0 & 1 \end{bmatrix} = -0.25 \neq 0$. Therefore

$$\text{Kern}(A - \mathbb{E}) = \vec{0}$$



The behaviour of the mapping above near the zero point

Now is:

$$A\vec{x} = \lambda\vec{x} \Leftrightarrow (A - \lambda\mathbb{E})\vec{x} = \vec{0}$$

And there is only one solution if

$$\text{Kern}(A - \lambda\mathbb{E}) \neq \vec{0} \Leftrightarrow \det(A - \lambda\mathbb{E}) = 0$$

We are therefore looking for λ in such a way that with the previous designations for A applies:

$$\det \begin{bmatrix} a_1 - \lambda & b_1 & c_1 \\ a_2 & b_2 - \lambda & c_2 \\ a_3 & b_3 & c_3 - \lambda \end{bmatrix} = 0$$

The corresponding polynomial

$$p(\lambda) := \det \begin{bmatrix} a_1 - \lambda & b_1 & c_1 \\ a_2 & b_2 - \lambda & c_2 \\ a_3 & b_3 & c_3 - \lambda \end{bmatrix}$$

This is called *the characteristic polynomial* of A . In our case it has degree 3, from which it follows:

Theorem

A linear mapping $A: \mathbb{R}^3 \rightarrow \mathbb{R}^3$ has either three real eigenvalues or one real eigenvalue and two conjugate complex eigenvalues.

In particular, there is always at least one direction that is invariant in the mapping.

Example

Be

$$A = \begin{bmatrix} 0 & -\frac{1}{2} & -\frac{3}{2} \\ 1 & \frac{3}{2} & \frac{3}{2} \\ -1 & \frac{1}{2} & \frac{1}{2} \end{bmatrix}$$

We investigate the behaviour of the mapping near the zero point. To do this, we look for invariant directions or the eigenvalues and eigenvectors of the mapping. To do this, we calculate the characteristic polynomial and set this to zero:

$$p(\lambda) := \det \begin{bmatrix} -\lambda & -\frac{1}{2} & -\frac{3}{2} \\ 1 & \frac{3}{2} - \lambda & \frac{3}{2} \\ -1 & \frac{1}{2} & \frac{1}{2} - \lambda \end{bmatrix} = -\lambda^3 + 2\lambda^2 + \lambda - 2 = 0$$

This polynomial has the zeros $\lambda_{1,2,3} = 1, 2, -1$. The eigenvector for eigenvalue 1 is in the kernel of

$$(A - 1 \cdot \mathbb{E}) = \begin{bmatrix} -1 & -\frac{1}{2} & -\frac{3}{2} \\ 1 & \frac{1}{2} & \frac{3}{2} \\ -1 & \frac{1}{2} & -\frac{1}{2} \end{bmatrix}$$

If we look at the first and third lines, for example, the eigenvector $\vec{x}_1 = \begin{pmatrix} x_1 \\ y_1 \\ z_1 \end{pmatrix}$ must apply:

$$\begin{cases} -x_1 - \frac{y_1}{2} - \frac{3z_1}{2} = 0 \\ -x_1 + \frac{y_1}{2} - \frac{z_1}{2} = 0 \end{cases}$$

$$\Rightarrow \begin{cases} x_1 = y_1 \\ z_1 = -y_1 \end{cases}$$

Since only the direction of \vec{x}_1 is searched for, you can freely select a parameter, e.g. $\vec{x}_1 = \begin{pmatrix} 1 \\ 1 \\ -1 \end{pmatrix}$

Check: $A\vec{x}_1 = 1 \cdot \vec{x}_1$. The other two eigenvectors are obtained in the same way. For the eigenvalue $\lambda_2 = 2$ you have the eigenvector $\vec{x}_2 = \begin{pmatrix} 1 \\ -1 \\ -1 \end{pmatrix}$ and for the eigenvalue $\lambda_2 = -1$ the eigenvector $\vec{x}_3 = \begin{pmatrix} 1 \\ -1 \\ 1 \end{pmatrix}$. With these eigenvectors as the basis, the matrix has the following form:

$$A = \begin{bmatrix} 1 & 0 & 0 \\ 0 & 2 & 0 \\ 0 & 0 & -1 \end{bmatrix}$$

Every point on the line spanned by \vec{x}_1 is a fixed point. Each point on the line spanned by \vec{x}_3 is cyclic of order two: It is mirrored at the zero point during the mapping. The mapping is dilating in the direction of \vec{x}_2 .

Note that the eigenvectors generally do not form an orthonormal basis.

□

Now we will analyse the case where a mapping has one real eigenvalue and two conjugate complex eigenvalues. Let the eigenvalues be $\lambda_3 \in \mathbb{R}$ and $\lambda_{1,2} = \alpha \pm i\beta \in \mathbb{C}$. Let the eigenvector associated with λ_3 be $\vec{x}_3 \in \mathbb{R}^3$. The eigenvectors belonging to $\lambda_{1,2}$ are conjugate complex. Suppose they have the form: $\vec{x}_{1,2} = \vec{u} \pm i\vec{v}$ with $\vec{u}, \vec{v} \in \mathbb{R}^3$. If we choose $\vec{x}_1, \vec{x}_2, \vec{x}_3$ as the basis, the matrix has diagonal form:

$$A = \begin{bmatrix} \alpha + i\beta & 0 & 0 \\ 0 & \alpha - i\beta & 0 \\ 0 & 0 & \lambda_3 \end{bmatrix}$$

However, we can also choose $\vec{u}, \vec{v}, \vec{x}_3$ as the basis, because $\vec{x}_{1,2}$ can be clearly represented as a (complex) linear combination of \vec{u}, \vec{v} . What form does the matrix A have with respect to this basis?

Since \vec{x}_1 is an eigenvector, the following applies:

$$A\vec{x}_1 = (\alpha + i\beta)\vec{x}_1 = (\alpha + i\beta)(\vec{u} + i\vec{v}) = (\alpha\vec{u} - \beta\vec{v}) + i(\beta\vec{u} + \alpha\vec{v})$$

If you compare the real and imaginary parts, you can see:

$$A\vec{u} = \alpha\vec{u} - \beta\vec{v}, A\vec{v} = \beta\vec{u} + \alpha\vec{v}$$

The image of the first basis vector \vec{u} under the mapping A is therefore $\begin{pmatrix} \alpha \\ -\beta \\ 0 \end{pmatrix}$ and the image of \vec{v} is $\begin{pmatrix} \beta \\ \alpha \\ 0 \end{pmatrix}$. Thus, the matrix with respect to the basis $\vec{u}, \vec{v}, \vec{x}_3$ has the form

$$A = \begin{bmatrix} \alpha & \beta & 0 \\ -\beta & \alpha & 0 \\ 0 & 0 & \lambda_3 \end{bmatrix}$$

The sub-matrix $\tilde{A} = \begin{bmatrix} \alpha & \beta \\ -\beta & \alpha \end{bmatrix}$ is a spiral similarity in the \vec{u}, \vec{v} plane.

Justification:

Each base vector is stretched by the same amount, namely by $\sqrt{\alpha^2 + \beta^2}$. This means that every linear combination of these, i.e. every vector, is also stretched by this amount. The basis vectors are

generally not an orthonormalised system. We want to show that the angle between \vec{u} , \vec{v} and $\tilde{A}\vec{u}$, $\tilde{A}\vec{v}$ is preserved. To do this, we introduce an orthogonal system.

If, for example, \vec{u}, \vec{v} forms a right-hand system, we can normalise \vec{u} to length 1 and select this normalised vector in the direction of \vec{u} as the first basis vector \vec{e}_1 . Then we select the second basis vector perpendicular to \vec{e}_1 , so that it forms a right-hand system with it. In this orthogonal system, \vec{u}, \vec{v} then has the components:

$$\vec{u} = \begin{pmatrix} 1 \\ 0 \end{pmatrix}, \vec{v} = \begin{pmatrix} v \\ 1 \end{pmatrix}$$

For a suitable $v \in \mathbb{R}$.

Then the angle φ between \vec{u} and \vec{v} is given by

$$\cos\varphi = \frac{\vec{u} \cdot \vec{v}}{|\vec{u}| |\vec{v}|} = \frac{v}{\sqrt{1+v^2}}$$

The angle φ' between $\tilde{A}\vec{u}$ and $\tilde{A}\vec{v}$ is given by

$$\cos\varphi' = \frac{\tilde{A}\vec{u} \cdot \tilde{A}\vec{v}}{|\tilde{A}\vec{u}| |\tilde{A}\vec{v}|} = \frac{\begin{pmatrix} \alpha \\ -\beta \end{pmatrix} \cdot \begin{pmatrix} \alpha v + \beta \\ -\beta v + \alpha \end{pmatrix}}{\sqrt{\alpha^2 + \beta^2} \cdot \sqrt{(\alpha^2 + \beta^2)(1+v^2)}} = \frac{v}{\sqrt{1+v^2}}$$

Finally, the cross product is $\begin{pmatrix} \alpha \\ -\beta \end{pmatrix} \times \begin{pmatrix} \beta \\ \alpha \end{pmatrix} = (\alpha^2 + \beta^2) \begin{pmatrix} 0 \\ 0 \end{pmatrix} > 0$, so the direction of rotation is preserved by the mapping. We therefore do not have a dilatation followed by a reflection, but a spiral similarity and $\varphi' = \varphi$.

If $\sqrt{\alpha^2 + \beta^2} < 1$, then the zero point in the \vec{u}, \vec{v} plane is attractive and the rotation causes the orbit of a point in this plane to spiral around the zero point. If $\sqrt{\alpha^2 + \beta^2} > 1$, then such a point moves away from the origin on a spiral.

During implementation, we look at the matrix:

$$A = \begin{bmatrix} \alpha & -\beta & 0 \\ \beta & \delta & 0 \\ 0 & 0 & \lambda \end{bmatrix}$$

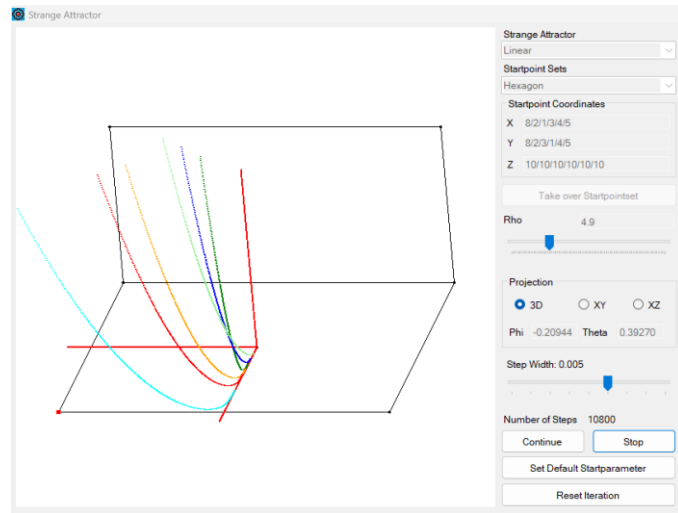
And look at the cases:

- $\beta = 0, \alpha > 0, \delta > 0, \lambda > 0$. So, all eigenvalues are real. Depending on the setting of the parameter $\rho, \alpha, \delta, \lambda$ will be just below 1 or just above. The zero point is then weakly attractive or weakly repulsive, depending on the direction.
- $\lambda > 0, \lambda \sim 1$. $\varphi = StepWidth * \pi / 100$. And $\alpha = a * \cos\varphi, \beta = a * \sin\varphi$ with $a \sim 1, \delta = \alpha$

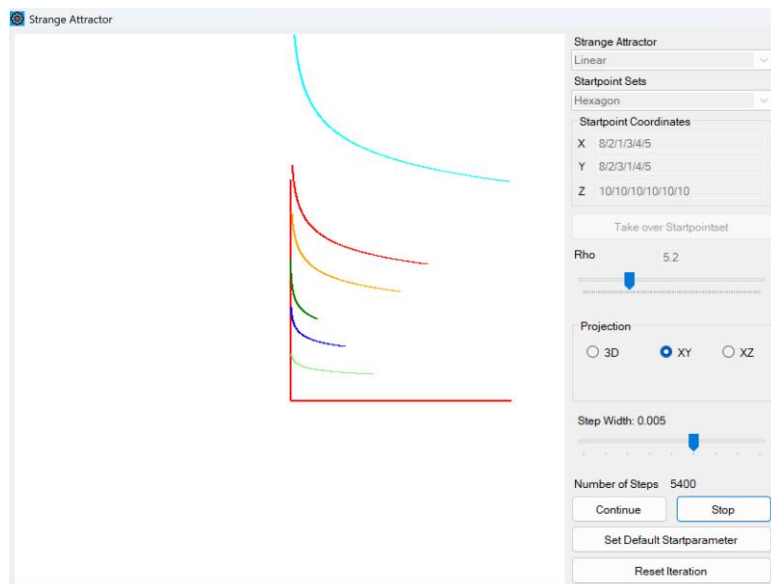
The angle φ is set via the *StepWidth* and the values of α, δ, λ via the parameter ρ as follows:

- The zero point is always attractive in the z-direction, i.e. $\lambda < 1$ for all $\rho \in [0, 20]$
- For $\rho \in [0, 10]$ you have three real eigenvalues.
 - $\alpha < 1$ for $\rho < 7.5$. In this area, the zero point in the x-direction is attractive
 - $\delta < 1$ for $\rho < 5$. In this area, the zero point in the y-direction is attractive.
- For $\rho \in [10, 20]$ you have two conjugate complex eigenvalues and accordingly a spiral similarity in the x-y plane.

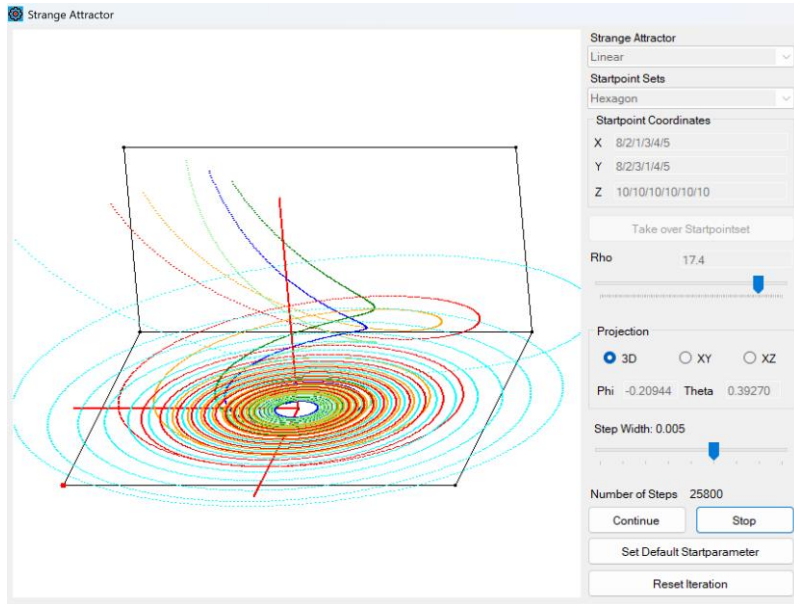
- $\alpha = \delta < 1$ for $\varrho < 17.5$. In this area, the path of a starting point spirals around the zero point and approaches it.



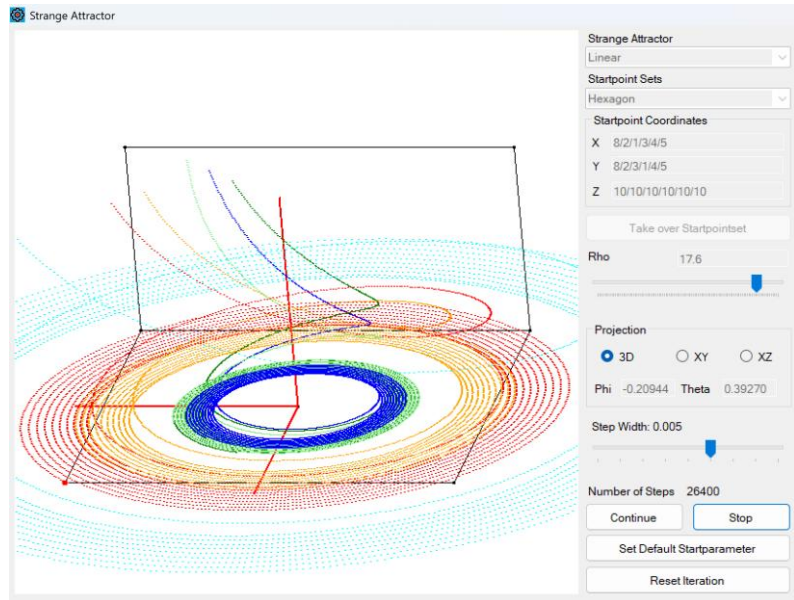
Trajectory curves for $\varrho = 4.9$. The zero point is attractive in all directions.



Path curves for $\varrho = 5.2$ in the x-y projection. The zero point is repulsive in the y-direction.



Trajectory curves for $\rho = 17.4$. The zero point is attractive and the trajectories are spiral-shaped



Path curves for $\rho = 17.6$. The zero point is only attractive in the z-direction and repulsive in the y-x plane

2.2 Continuously differentiable mappings $\mathbb{R}^3 \rightarrow \mathbb{R}^3$

In order to investigate the behaviour of a real and continuously differentiable function f , which is iterated, in the neighbourhood of a fixed point ξ , we have "replaced" this function in the one-dimensional case with a linear function using the derivative of this function:

$$f(\xi + h) \approx f(\xi) + f'(\xi) \cdot h, h \approx 0$$

The result was relatively simple. The fixed point is attractive if and only if $|f'(\xi)| < 1$.

We do the same in the multidimensional case. We consider a function

$$f: \mathbb{R}^3 \rightarrow \mathbb{R}^3, \begin{pmatrix} x \\ y \\ z \end{pmatrix} \mapsto \begin{pmatrix} f_1(x, y, z) \\ f_2(x, y, z) \\ f_3(x, y, z) \end{pmatrix}$$

Which is differentiable in every component and every variable. This is also known as *f being partially differentiable*. Furthermore, the derivatives should be continuous. If f has a fixed point $\vec{\xi} \in \mathbb{R}^3$, i.e. a point with $f(\vec{\xi}) = \vec{\xi}$, then we want to investigate the behaviour of f in the neighbourhood of $\vec{\xi}$. As in the one-dimensional case, we do this by replacing f in the neighbourhood of $\vec{\xi}$ with a linear function.

In preparation for this, we analysed the properties of a linear mapping in the neighbourhood of a fixed point (the zero point) in the previous section.

In order to find the appropriate linear approximation at the fixed point $\vec{\xi}$, we must first estimate how small changes in the variables affect the function value. This leads us to the concept of the *total differential*.

We look at this component by component. We estimate the change in the function $f_1(x, y, z)$ if the variables (x, y, z) change slightly. If (dx, dy, dz) denotes this (arbitrarily small) change in the corresponding variable and df_1 denotes the resulting change in the function value, then we can write:

$$\begin{aligned} df_1 &:= f_1(x + dx, y + dy, z + dz) - f_1(x, y, z) \\ &= f_1(x + dx, y + dy, z + dz) - f_1(x, y + dy, z + dz) \\ &\quad + f_1(x, y + dy, z + dz) - f_1(x, y, z + dy) \\ &\quad + f_1(x, y, z + dz) - f_1(x, y, z) \end{aligned}$$

For the differences, only one variable changes at a time and we can use the approximation for the one-dimensional case: $f_1(x + dx) - f_1(x) = f_1'(x) \cdot dx$. This then results in

$$df_1 = \frac{\partial f_1}{\partial x}(x, y + dy, z + dz) \cdot dx + \frac{\partial f_1}{\partial y}(x, y, z + dz) \cdot dy + \frac{\partial f_1}{\partial z}(x, y, z) \cdot dz$$

Because of the continuity of the derivative is: $\frac{\partial f_1}{\partial x}(x, y + dy, z + dz) = \frac{\partial f_1}{\partial x}(x, y, z)$ and $\frac{\partial f_1}{\partial x}(x, y, z + dz) = \frac{\partial f_1}{\partial x}(x, y, z)$. The result is the so-called *total differential*:

$$df_1 = \frac{\partial f_1}{\partial x}(x, y, z) \cdot dx + \frac{\partial f_1}{\partial y}(x, y, z) \cdot dy + \frac{\partial f_1}{\partial z}(x, y, z) \cdot dz$$

The analogue equation also applies to the other components f_2, f_3 . In the fixed point $\vec{\xi}$ then applies:

$$\begin{cases} df_1 = \frac{\partial f_1}{\partial x}(\vec{\xi})dx + \frac{\partial f_1}{\partial y}(\vec{\xi})dy + \frac{\partial f_1}{\partial z}(\vec{\xi})dz \\ df_2 = \frac{\partial f_2}{\partial x}(\vec{\xi})dx + \frac{\partial f_2}{\partial y}(\vec{\xi})dy + \frac{\partial f_2}{\partial z}(\vec{\xi})dz \\ df_3 = \frac{\partial f_3}{\partial x}(\vec{\xi})dx + \frac{\partial f_3}{\partial y}(\vec{\xi})dy + \frac{\partial f_3}{\partial z}(\vec{\xi})dz \end{cases}$$

We can also write this in matrix form:

$$df = \begin{bmatrix} \frac{\partial f_1}{\partial x}(\vec{\xi}) & \frac{\partial f_1}{\partial y}(\vec{\xi}) & \frac{\partial f_1}{\partial z}(\vec{\xi}) \\ \frac{\partial f_2}{\partial x}(\vec{\xi}) & \frac{\partial f_2}{\partial y}(\vec{\xi}) & \frac{\partial f_2}{\partial z}(\vec{\xi}) \\ \frac{\partial f_3}{\partial x}(\vec{\xi}) & \frac{\partial f_3}{\partial y}(\vec{\xi}) & \frac{\partial f_3}{\partial z}(\vec{\xi}) \end{bmatrix} \begin{pmatrix} dx \\ dy \\ dz \end{pmatrix}$$

We have now found our linear approximation function:

$$df = \mathfrak{J}_f(\vec{\xi}) \begin{pmatrix} dx \\ dy \\ dz \end{pmatrix} = \mathfrak{J}_f(\vec{\xi}) d\vec{x}$$

Whereby

$$\mathfrak{J}_f(\vec{\xi}) = \begin{bmatrix} \frac{\partial f_1}{\partial x}(\vec{\xi}) & \frac{\partial f_1}{\partial y}(\vec{\xi}) & \frac{\partial f_1}{\partial z}(\vec{\xi}) \\ \frac{\partial f_2}{\partial x}(\vec{\xi}) & \frac{\partial f_2}{\partial y}(\vec{\xi}) & \frac{\partial f_2}{\partial z}(\vec{\xi}) \\ \frac{\partial f_3}{\partial x}(\vec{\xi}) & \frac{\partial f_3}{\partial y}(\vec{\xi}) & \frac{\partial f_3}{\partial z}(\vec{\xi}) \end{bmatrix}$$

Is the so-called Jacobi Matrix, named after Carl Gustav Jacobi (1804 - 1851).

If the partial derivatives of f are continuous, the following applies (without us proving it here):

$$\lim_{|d\vec{x}| \rightarrow 0} |df - \mathfrak{J}_f(\vec{\xi}) d\vec{x}| = 0$$

One then also calls f *totally differentiable*.

Example

$$f: \mathbb{R}^3 \rightarrow \mathbb{R}^3, \begin{pmatrix} x \\ y \\ z \end{pmatrix} \mapsto \begin{pmatrix} \frac{1}{3}x^2y + z + \frac{1}{3} \\ xy - yz - 1 \\ x + y^2z - 1 \end{pmatrix}$$

It's easy to see: $\vec{\xi} = \begin{pmatrix} 1 \\ -1 \\ 1 \end{pmatrix}$ is a fixed point of f .

The Jacobi Matrix is:

$$\mathfrak{J}_f(\vec{\xi}) = \begin{bmatrix} \frac{2}{3}xy & \frac{1}{3}x^2 & 1 \\ y & x-z & -y \\ 1 & 2yz & y^2 \end{bmatrix}$$

$$\mathfrak{J}_f(\vec{\xi}) = \begin{bmatrix} -\frac{2}{3} & \frac{1}{3} & 1 \\ -1 & 0 & 1 \\ 1 & -2 & 1 \end{bmatrix}$$

To investigate the behaviour of the mapping in the neighbourhood of the fixed point, we analyse the linear mapping $\mathfrak{J}_f(\vec{\xi})$ and search for its eigenvalues and eigenvectors. The characteristic polynomial is then:

$$p(\lambda) = \text{Det} \begin{bmatrix} -\frac{2}{3} - \lambda & \frac{1}{3} & 1 \\ -1 & -\lambda & 1 \\ 1 & -2 & 1 - \lambda \end{bmatrix} = -\lambda^3 + \frac{1}{3}\lambda^2 - \frac{2}{3}\lambda + \frac{4}{3}$$

And we are looking for its zeros.

Obviously, $\lambda_1 = 1$ is a zero. If we divide $p(\lambda)$ by $\lambda - 1$, the condition for the remaining two zeros remains:

$$\lambda^2 + \frac{2}{3}\lambda - 1 = 0$$

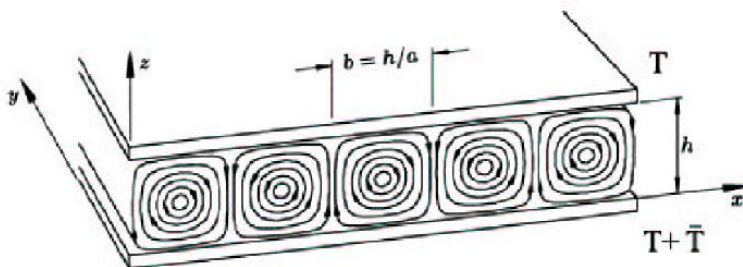
This provides the two further zeros:

$$\lambda_{2,3} = -\frac{1}{3} \pm \frac{2\sqrt{2}}{3}$$

f is therefore indifferent in the direction of the first eigenvector (neither attractive nor repulsive). In the direction of the second eigenvector, f is attractive, as $|\lambda_2| \approx 0.609 < 1$ and in the direction of the third eigenvector it is repulsive, as $|\lambda_3| \approx 1.276 > 1$.

2.3 The Lorenz system

At the beginning of the 20th century, the physicists Henri Bénard (1874 - 1939) and the Nobel Prize-winning Lord Rayleigh (1842 - 1919) investigated convection currents. Their model looked like this:



Model for analysing convection currents (source: [3])

A viscous (i.e. deformable) and incompressible liquid is located between two plates at a distance h . There is a temperature difference between the top and bottom \bar{T} , which leads to the formation of convection rolls above a critical value, as sketched above. Liquid elements heated from below rise due to their lower density and colder liquid volumes sink.

In 1963, the American mathematician and meteorologist Edward Lorenz (1917 - 2008) used this model as the starting point for modelling the Earth's atmosphere with the aim of deriving a long-term weather forecast. He emphasised that his model was highly simplified and only provided realistic results for limited parameter values.

The Lorenz system he developed consists of three differential equations:

$$\begin{cases} \dot{x} = -\sigma x + \sigma y \\ \dot{y} = \rho x - y - xz \\ \dot{z} = -\beta z + xy \end{cases}$$

This contains σ, β, ρ fixed parameters that have the following meaning:

σ is the so-called "Prandtl number", named after the engineer Ludwig Prandtl (1875 - 1953). It describes the properties of the fluid under consideration in terms of viscosity and thermal diffusivity. Lorenz worked with the fixed value $\sigma = 10$ for his analyses of atmospheric flows.

$\beta = \frac{4}{1+a^2}$ is a measure of the cell geometry. Lorenz worked with the fixed value $a = \frac{h}{b} = \sqrt{2}$, i.e. $\beta = \frac{8}{3}$.

ϱ is the so-called Rayleigh number, which sets the buoyant and decelerating forces in relation to each other. This number is positive and the behaviour of the convection flow depends on it. In the "Simulator", this number can be varied in the interval [0, 30]. We will discuss some critical values of ϱ later.

x is proportional to the intensity of the convection flow. y is proportional to the temperature difference between the rising and falling flow. z is proportional to the deviation from the linear temperature profile along the vertical axis.

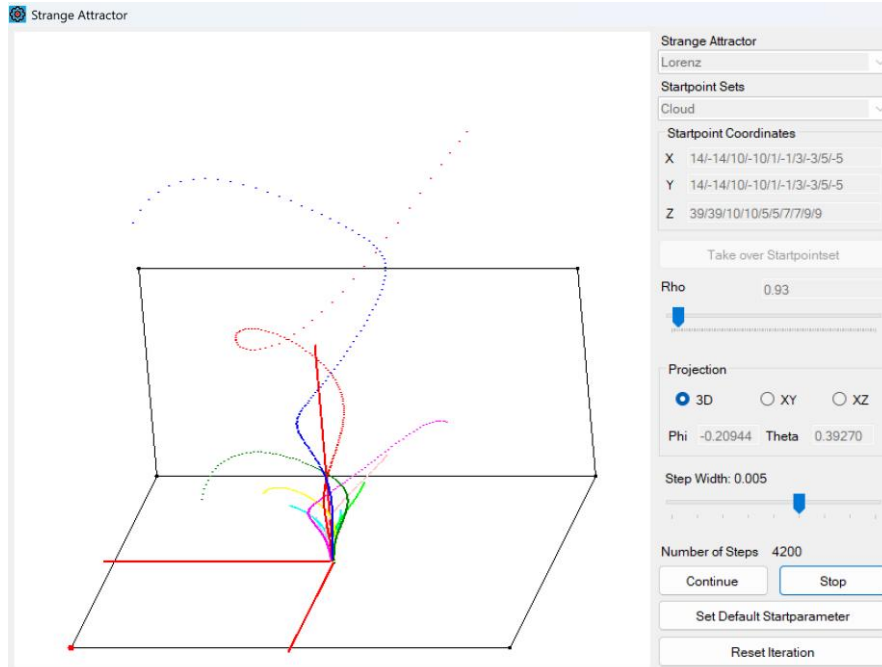
A more detailed description of these parameters is beyond our scope here. The same applies to a mathematical derivation of the Lorenz system. They result from three conservation laws:

- Conservation of mass (the continuity equation and the concept of divergence are used here)
- Conservation of momentum (here you need the Navier-Stokes differential equations)
- Conservation of energy (here you need the heat transport equation)

Furthermore, some simplifying conditions are assumed, for example that the convection rolls develop independently of the geometric y -direction.

A precise derivation can be found in [3]. However, some properties of the system can be analysed elementarily.

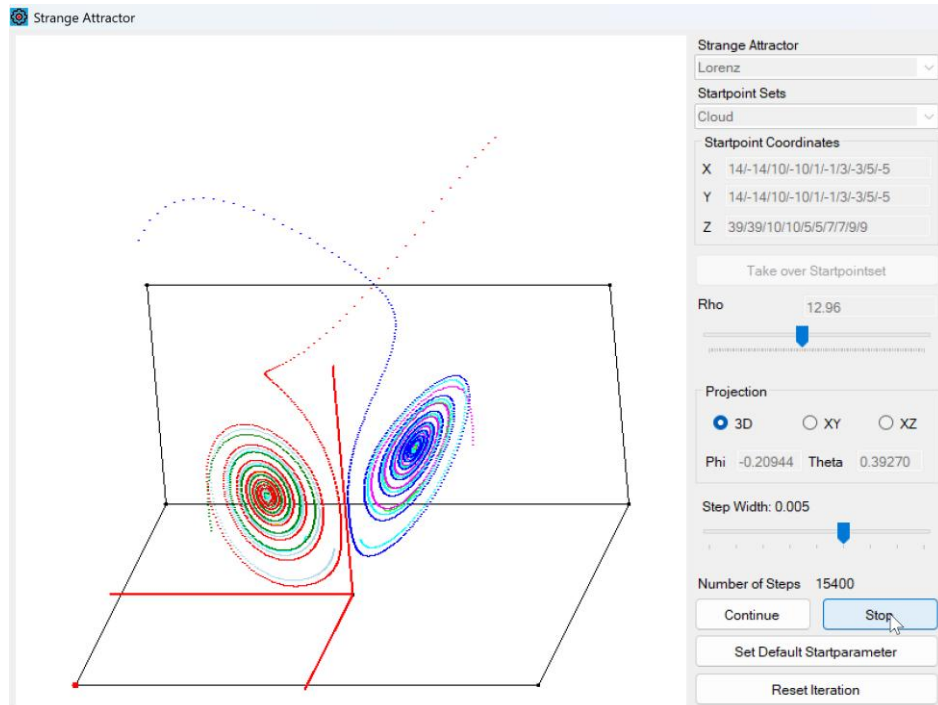
We can state the following: The Lorenz system is a very simplified model for the weather. There is only one static air mass (apart from the convection flow), without the influence of lateral winds, topographical conditions etc. *One could therefore assume that the system can be predicted well.*



Experiment with $\varrho = 0.93$ and a point cloud as a starting set

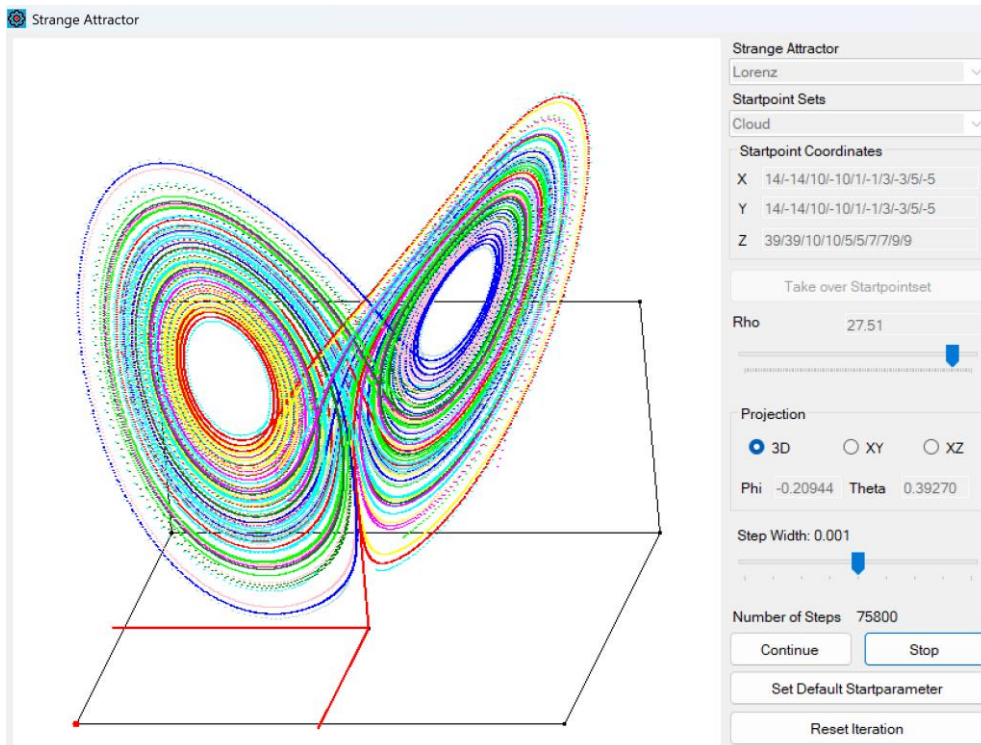
In this first experiment, all points of the point cloud converge towards the zero point.

For $\rho = 12.96$, the individual points of the same point cloud as a starting set obviously strive towards two different points, depending on the starting point.



Experiment with $\rho = 12.96$ and the same point cloud as starting set

If you perform the same experiment with $\rho = 27.51$, the previous fixed points appear to have become repulsive. The point cloud "smears" over a quantity that looks like a butterfly.



The same starting pointset with $\rho = 27.51$

In the latter case, the system does not appear to be predictable. On closer examination, Edward Lorenz came across chaotic properties of the system. At that time, the concept of chaos had not yet been mathematically specified. It came as a surprise to Lorenz that even a very simplified weather model had properties that made a long-term forecast impossible. In particular, the system reacts sensitively to the smallest changes in the initial conditions. Lorenz states in [4]:

"When our results concerning the instability of non-periodic flow are applied to the atmosphere, which is ostensibly non-periodic, they indicate that prediction of the sufficiently distant future is impossible by any method, unless the present conditions are known exactly".

This characteristic is sensitivity and the statement that the flap of a butterfly's wings in Brazil can trigger a tornado in Texas is attributed to Lorenz.

In the following, we will now analyse the properties of the Lorenz system as far as they are elementarily accessible.

2.4 Elementary properties of the Lorenz system

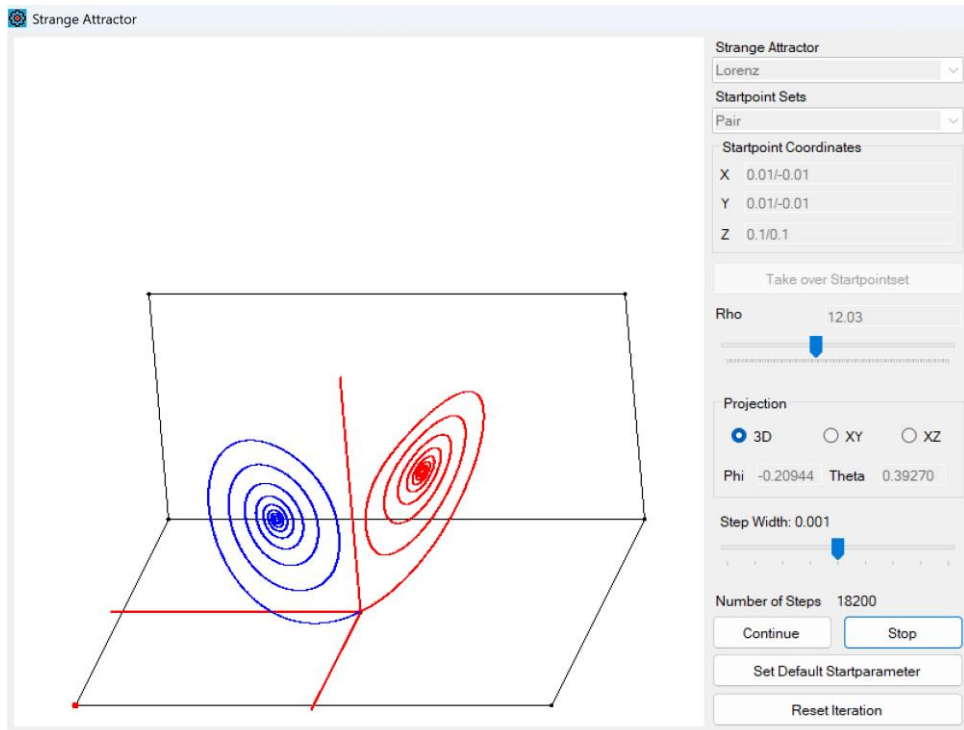
Mirror symmetry relative to the z-axis

If in the system of equations

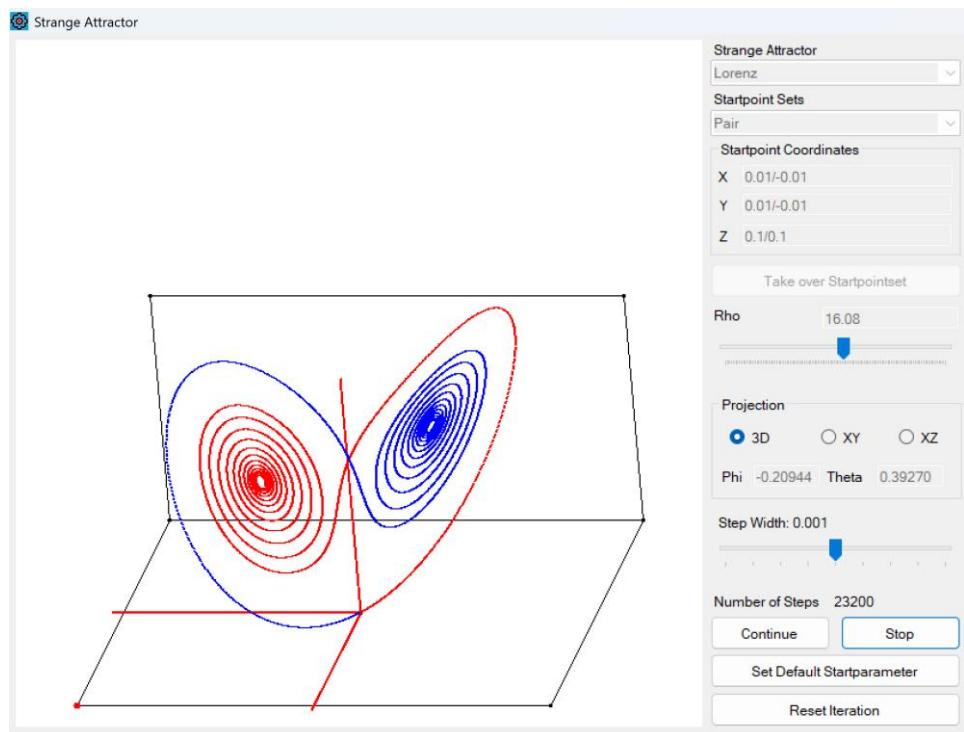
$$\begin{cases} \dot{x} = -\sigma x + \sigma y \\ \dot{y} = \rho x - y - xz \\ \dot{z} = -\beta z + xy \end{cases}$$

x is replaced by $-x$ and y by $-y$, it does not change. This means that starting points that are mirrored on the z-axis also generate a mirror-symmetrical orbit.

We consider two starting points that are very close to each other: $(0.01, 0.01, 0.1)$ (blue) and $(-0.01, -0.01, 0.1)$ (red). These are symmetrical to the z-axis and provide symmetrical orbits. We set $\rho = 12.03$. Due to the symmetry, these starting points provide symmetrical orbits and converge towards different, symmetrical fixed points.



Symmetrical orbits for two starting points close to each other



For $\rho = 16.08$ the orbits of the same starting points are "swapped"

This already indicates that the system reacts sensitively to changes: If the starting point changes minimally, a significantly different orbit can be generated depending on the situation.

Invariance of the z-axis

A starting point on the z-axis $(0, 0, z)$ remains on the z-axis because

$$\begin{cases} \dot{x} = 0 \\ \dot{y} = 0 \\ \dot{z} = -\beta z \end{cases}$$

The z-axis is invariant. Furthermore, if the time is denoted by t : $z = Ce^{-\beta t}, C \in \mathbb{R}$. For $t \rightarrow \infty$, orbits on the z-axis run towards the zero point.

Equilibrium positions

Equilibrium positions are points at which the system no longer changes. They correspond, for example, to the fixed points in the growth models analysed earlier. In this case, this means that all derivatives after the three variables disappear. They are solutions of the system of equations:

$$\begin{cases} 0 = -\sigma x + \sigma y \\ 0 = \varrho x - y - xz \\ 0 = -\beta z + xy \end{cases}$$

Obviously, the zero point $(0, 0, 0)$ is a solution to this system of equations and thus an equilibrium position.

Now we exclude the zero point. The first equation leads to $x = y$. If $x \neq 0$ the second equation leads to $z = \varrho - 1$ and the third equation to $x = \pm\sqrt{\beta(\varrho - 1)}$ for $\varrho > 1$. This gives us two more equilibrium positions (or fixed points):

$$C^\pm = (\pm\sqrt{\beta(\varrho - 1)}, \pm\sqrt{\beta(\varrho - 1)}, \varrho - 1)$$

These two are only defined for $\varrho > 1$. The symmetry with respect to the z-axis can also be seen here.

If a starting point close to a fixed point tends towards it, then this equilibrium position is *stable*. This corresponds to an *attractive fixed point*.

If a starting point near a fixed point leads to an orbit that moves away from the fixed point, then this equilibrium position is *unstable*. This corresponds to a *repulsive fixed point*.

The zero point

Now we use it to investigate the behaviour of the Lorenz system near the zero point, i.e. for the function $f: \mathbb{R}^3 \rightarrow \mathbb{R}^3$ with

$$f(x, y, z) = \begin{cases} -\sigma x + \sigma y \\ \varrho x - y - xz \\ -\beta z + xy \end{cases}$$

And the fixed point $\vec{\xi}_1 = (0, 0, 0)$.

The Jacobi matrix from the previous section is then

$$\mathfrak{J}_f(\vec{x}) = \begin{bmatrix} -\sigma & \sigma & 0 \\ \varrho - z & -1 & -x \\ y & x & -\beta \end{bmatrix}$$

And

$$\mathfrak{J}_f(\vec{\xi}_1) = \begin{bmatrix} -\sigma & \sigma & 0 \\ \varrho & -1 & 0 \\ 0 & 0 & -\beta \end{bmatrix}$$

The following therefore applies near the zero point:

$$\begin{cases} \dot{x} = -\sigma x + \sigma y \\ \dot{y} = \varrho x - y \\ \dot{z} = -\beta z \end{cases}$$

In the third component, we have the equation $\dot{z} = -\beta z$ with the solution $z = Ce^{-\beta t}, C \in \mathbb{R}$. For $t \rightarrow \infty$, orbits on the z-axis run against the zero point

Now we consider the x-y plane and the (linear) mapping $A: \mathbb{R}^2 \rightarrow \mathbb{R}^2$ given by the matrix

$$A = \begin{bmatrix} -\sigma & \sigma \\ \varrho & -1 \end{bmatrix}$$

The corresponding characteristic polynomial is

$$p(\lambda) = \lambda^2 + (1 + \sigma)\lambda - \varrho\sigma$$

With the zeros

$$\lambda_{1,2} = \frac{1 + \sigma}{2} \pm \frac{1}{2}\sqrt{(1 + \sigma)^2 + 4\sigma(\varrho - 1)} = -\frac{1 + \sigma}{2} \pm \frac{1}{2}\sqrt{(\sigma - 1)^2 + 4\sigma\varrho}$$

Since $\varrho > 0$ the expression under the root is always positive. The corresponding eigenvectors are:

$$\vec{e}_{1,2} = \begin{pmatrix} \sigma \\ \frac{\sigma - 1}{2} \pm \frac{1}{2}\sqrt{(\sigma - 1)^2 + 4\sigma\varrho} \end{pmatrix}$$

The question now is for which $\lambda_{1,2}$ the system of equations in the neighbourhood of the zero-point leads to a contraction. In this case, the zero point would be a sink or attractive.

We choose the eigenvectors $\vec{e}_{1,2}$ as the basis for our coordinate system. This is possible because $\vec{e}_1 \neq \vec{e}_2$. Then we move along \vec{e}_1 . We therefore choose a starting point that has the coordinates $\begin{pmatrix} x \\ 0 \end{pmatrix}$ with respect to the new coordinate system. The mapping equation then reads:

$$\begin{pmatrix} \dot{x} \\ 0 \end{pmatrix} = A \begin{pmatrix} x \\ 0 \end{pmatrix} = xA\vec{e}_1 = x\lambda_1\vec{e}_1 = \begin{pmatrix} \lambda_1 x \\ 0 \end{pmatrix}$$

Or $\dot{x} = \lambda_1 x$. This differential equation has the solution $x(t) = C_1 e^{\lambda_1 t}, C_1 \in \mathbb{R}$. Thus, the mapping in this direction is contracting if $\lambda_1 < 0$ and dilating for $\lambda_1 > 0$.

For a point that moves along \vec{e}_2 , i.e. $\begin{pmatrix} x \\ y \end{pmatrix} = \beta \cdot \vec{e}_2$, you also get: $\dot{y} = \lambda_2 y$ with the solution: $y(t) = C_2 e^{\lambda_2 t}, C_2 \in \mathbb{R}$. The mapping is contracting in this direction if $\lambda_2 < 0$ and dilating for $\lambda_2 > 0$.

Now we have:

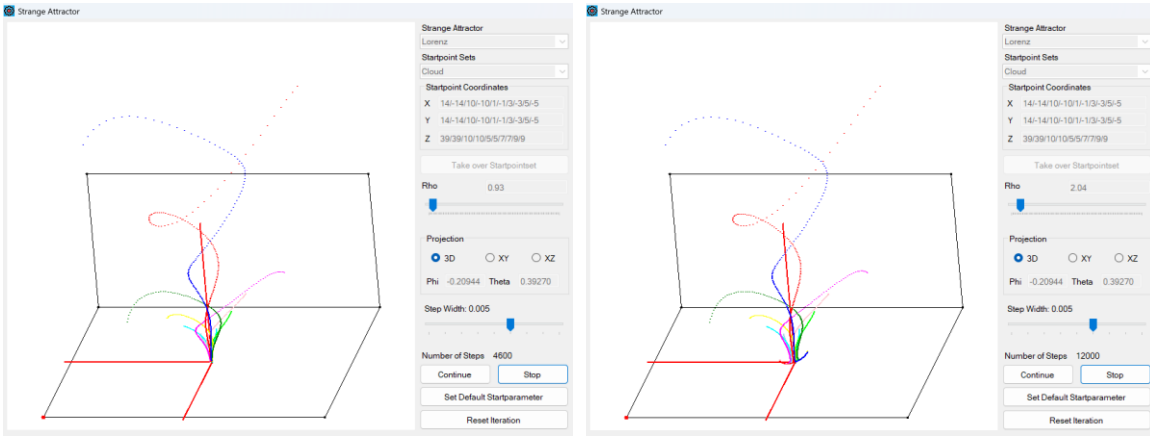
$$\lambda_1 = -\frac{1 + \sigma}{2} + \frac{1}{2}\sqrt{(\sigma - 1)^2 + 4\sigma\varrho} < 0 \Leftrightarrow \varrho < 1$$

$$\lambda_2 = -\frac{1 + \sigma}{2} - \frac{1}{2}\sqrt{(\sigma - 1)^2 + 4\sigma\varrho} < 0, \forall \varrho$$

This gives us the final result:

Theorem

The zero point is a sink for $\varrho < 1$ and a saddle point for $\varrho > 1$.



Orbits of a point cloud for $\varrho = 0.93$ on the left and the corresponding orbits for $\varrho = 2.04$ on the right. They first move towards the zero point, but then away from it. The coordinate system is shown in red and the zero point is visible accordingly.

Further equilibrium positions

In addition to the zero point, $\varrho > 1$ has two other equilibrium positions, as we saw earlier, namely

$$C^\pm = (\pm\sqrt{\beta(\varrho - 1)}, \pm\sqrt{\beta(\varrho - 1)}, \varrho - 1)$$

For $\varrho = 1$ these coincide with the zero point. We want to investigate these equilibrium positions in more detail.

2.5 Pitchfork and Hopf bifurcation

If ϱ is greater than 1, the zero point becomes a saddle point and two new equilibrium positions are created C^\pm . In the following its always $\varrho > 1$.

The original system of equations has the corresponding Jacobi matrix

$$\mathfrak{J}_f = \begin{bmatrix} -\sigma & \sigma & 0 \\ \varrho - z & -1 & -x \\ y & x & -\beta \end{bmatrix}$$

And at $C^\pm = \begin{pmatrix} \pm\sqrt{\beta(\varrho-1)} \\ \pm\sqrt{\beta(\varrho-1)} \\ \varrho-1 \end{pmatrix}$ you will find this:

$$\mathfrak{J}_f(C^\pm) = \begin{bmatrix} -\sigma & \sigma & 0 \\ 1 & -1 & \mp\sqrt{\beta(\varrho-1)} \\ \pm\sqrt{\beta(\varrho-1)} & \pm\sqrt{\beta(\varrho-1)} & -\beta \end{bmatrix}$$

To analyse the effect of the mapping $A := \mathfrak{J}_f(C^\pm) : \mathbb{R}^3 \rightarrow \mathbb{R}^3$, we again look for the eigenvalues and eigenvectors of the matrix A . In an exercise, we show that the corresponding characteristic polynomial for both equilibrium positions C^\pm is:

$$p(\lambda) = \lambda^3 + (\sigma + \beta + 1)\lambda^2 + \beta(\sigma + \varrho)\lambda + 2\sigma\beta(\varrho - 1)$$

The values you are looking for at λ are the zeros of this polynomial.

To investigate the polynomial further, we set

$$\begin{cases} a = \sigma + \beta + 1 = \frac{41}{3} \\ b = \beta(\sigma + \varrho) = \frac{8}{3}(\varrho + 10) \\ c = 2\sigma\beta(\varrho - 1) = \frac{160}{3}(\varrho - 1) \end{cases}$$

And have:

$$p(\lambda) = \lambda^3 + a\lambda^2 + b\lambda + c$$

As the degree of the polynomial is odd, there is at least one real zero. As all coefficients of the polynomial are positive ($\varrho > 1$), this real zero must be negative

If this zero point is λ_1 and the corresponding eigenvector is \vec{e}_1 , then we can write C^+ with position vector \vec{c}^+ for a starting point \vec{x} near an equilibrium position, for example:

$$\vec{x} = \vec{c}^+ + h \vec{e}_1$$

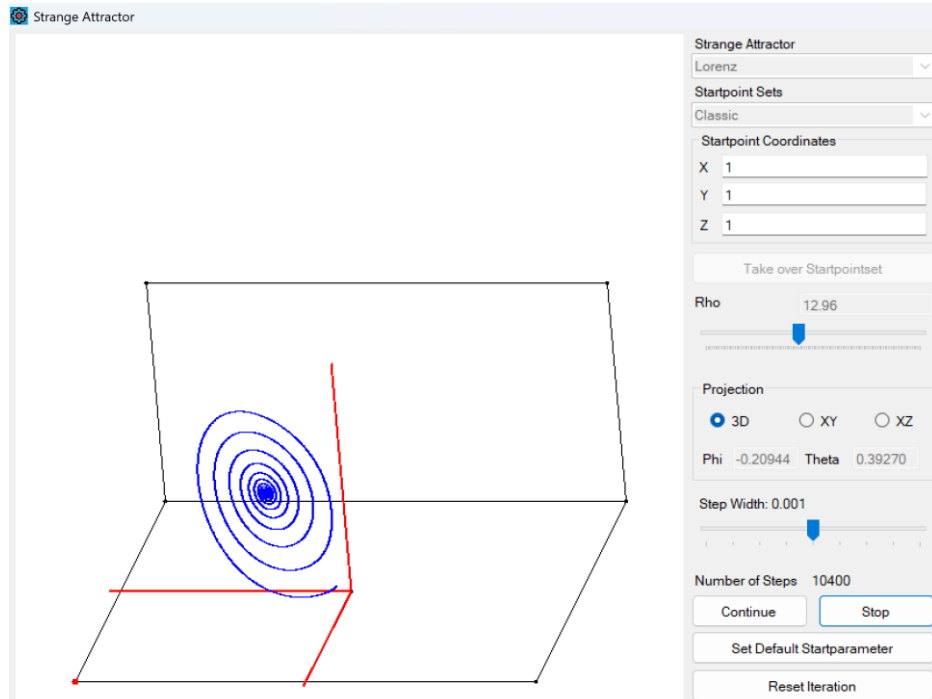
For a small $h \in \mathbb{R}$. Then the mapping equation reads:

$$\dot{\vec{x}} = A\vec{x} = A\vec{c}^+ + hA\vec{e}_1 = \vec{0} + h\lambda_1\vec{e}_1$$

And we have the solution: $\vec{x}(t) = hCe^{\lambda_1 t}, C \in \mathbb{R}$. For $\lambda_1 < 0$ and growing t the starting point converges to the equilibrium position C^+ .

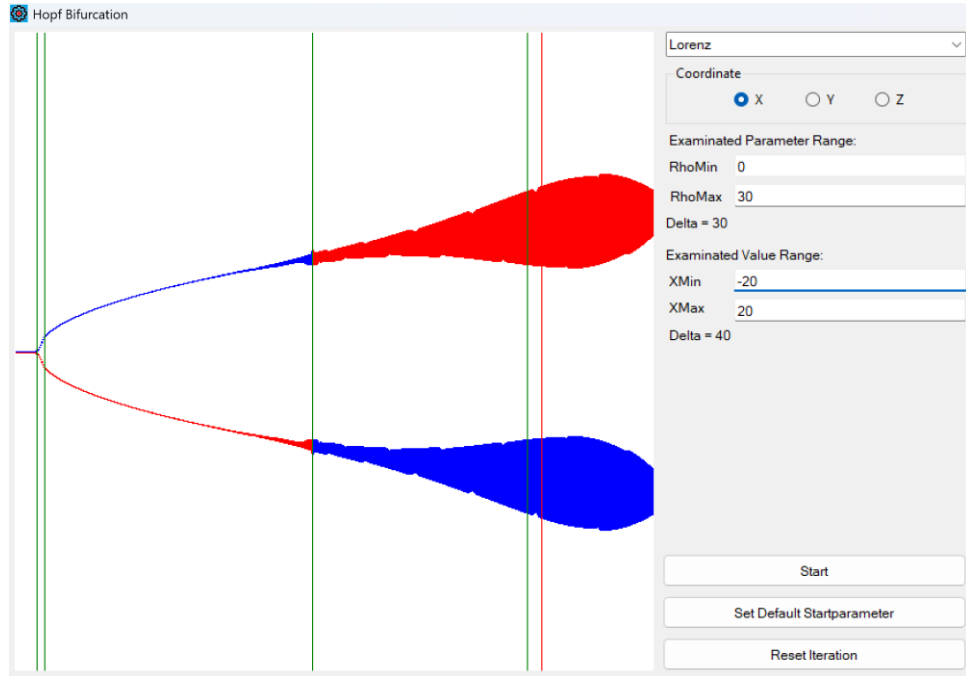
The same applies to a complex zero $\lambda_{2,3} = \alpha \pm i\beta$ with a negative real part $\alpha < 0$. Then $\vec{x}(t) = hCe^{\lambda_{2,3}t} = hCe^{\alpha t}(\cos(\beta t) \pm i\sin(\beta t))$.

This means that the mapping is contracting in the direction of the associated eigenvector. There is always such a direction, as there is always at least one negative real eigenvalue, and this explains why the orbits are "flattened" into a plane perpendicular to the corresponding eigenvector.



"Flattened" orbit that levels out into a plane

At the point $\varrho = 1$, a so-called *pitchfork* bifurcation takes place as ϱ grows. As with the Feigenbaum diagram, the previous attractive fixed point zero becomes repulsive. However, it does not split into an attractive 2-cycle, but into the two (separately) attractive points C^\pm . You can see this in the "Simulator" if you generate the corresponding diagram in the window for the Hopf bifurcation.



Horizontal: ϱ varies. Vertical: The values of the x parameter are plotted.

In the diagram, you can choose which parameter to plot vertically when ϱ grows along the horizontal axis. The vertical lines mark interesting values of ϱ . The first line shows $\varrho = 1$, where the zero point becomes unstable and splits into the stable equilibrium positions C^\pm .

To further analyse and simplify the polynomial, we apply a standard transformation $\mu := \lambda + \frac{a}{3}$. The polynomial then reads:

$$\left(\mu - \frac{a}{3}\right)^3 + a\left(\mu - \frac{a}{3}\right)^2 + b\left(\mu - \frac{a}{3}\right) + c = \mu^3 + p\mu + q$$

With

$$\begin{cases} p = b - \frac{a^2}{3} = \frac{8}{3}\varrho - \frac{961}{27} \approx \frac{8}{3}\varrho - 35.5926 \\ q = \frac{2a^3}{27} - \frac{ab}{3} + c = \frac{1112}{27}\varrho + \frac{10402}{27^2} \approx 41.1852\varrho + 14.2689 \end{cases}$$

As a simple recalculation shows.

And it applies:

$$p_\lambda(\lambda) = \lambda^3 + a\lambda^2 + b\lambda + c = 0 \Leftrightarrow p_\mu(\mu) = \mu^3 + p\mu + q = 0$$

The formulae of Gerolamo Cardano (1501 - 1576) exist for the zeros of the transformed polynomial. We do not want to calculate these explicitly, but merely analyse their character. The Cardano formulae are used to determine the so-called determinant:

$$D = \left(\frac{q}{2}\right)^2 + \left(\frac{p}{3}\right)^3 \approx 0.7023\varrho^3 + 395.9327\varrho^2 + 669.1938\varrho - 1619.0954$$

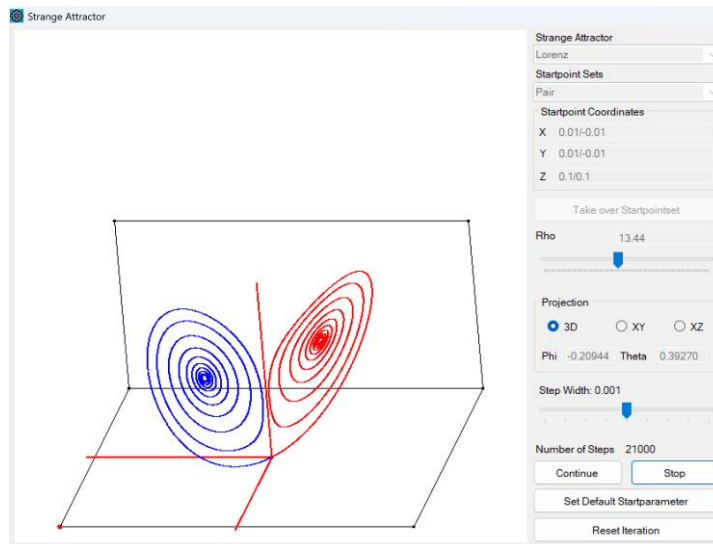
The following case distinction now applies:

$$\begin{cases} D > 0: \text{There is a real and two conjugate complex solutions} \\ D = 0 \text{ and } p = 0: \text{We don't have this case here} \\ D = 0 \text{ and } p \neq 0: \text{There are two real solutions} \\ D < 0: \text{There are three real solutions} \end{cases}$$

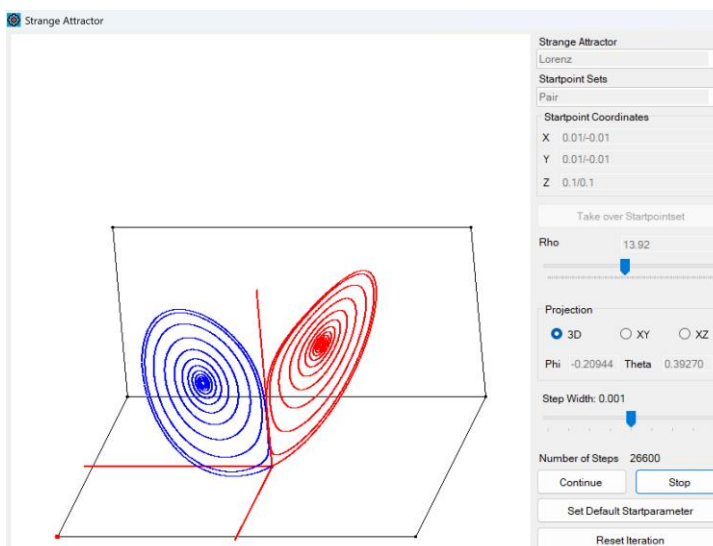
For $\varrho = 1$ is $D < 0$. $D(\varrho)$ is monotonically increasing. As you can check, $D = 0$ for $\varrho = 1.346 \dots$. This means that there are three different real zeros or eigenvalues in the interval $\varrho \in [1, 1.346 \dots]$, all of which are negative. Thus, C^\pm are attractive equilibrium positions for ϱ in this range. However, these are so close to zero that they are not visible in the "simulator".

We will not investigate the case $D = 0$ and $p \neq 0$ any further. We then have two real zeros and one of them is a double zero.

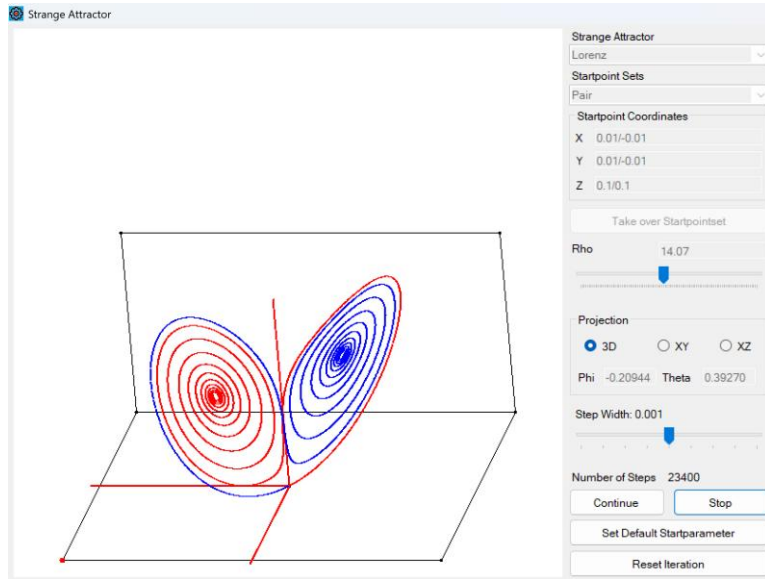
If ϱ continues to grow, $D > 0$. Then there is a real zero of p_μ , let's call it μ_1 . This is not necessarily negative, because only the corresponding $\lambda_1 = \mu_1 + a/3$ is necessarily negative. Furthermore, there are two conjugate complex zeros for $D > 0$.



Stable equilibrium positions for $\varrho = 13.44$



When ϱ approaches the value 13.926, the orbits almost touch each other



For $\varrho > 13.926$ the same starting points run to the respective other fixed point

Now we will analyse the case $D > 0$ further and define it:

$$\begin{cases} u := \sqrt[3]{-\frac{q}{2} + \sqrt{D}} \\ v := \sqrt[3]{-\frac{q}{2} - \sqrt{D}} \end{cases}$$

In this case, Cardano's formulae for the required zeros $\mu_{1,2,3}$ are as follows:

$$\begin{cases} \mu_1 = u + v \\ \mu_{2,3} = -\frac{1}{2}(u + v) \pm i \frac{\sqrt{3}}{2}(u - v) \end{cases}$$

Example $\varrho = 20$

You get:

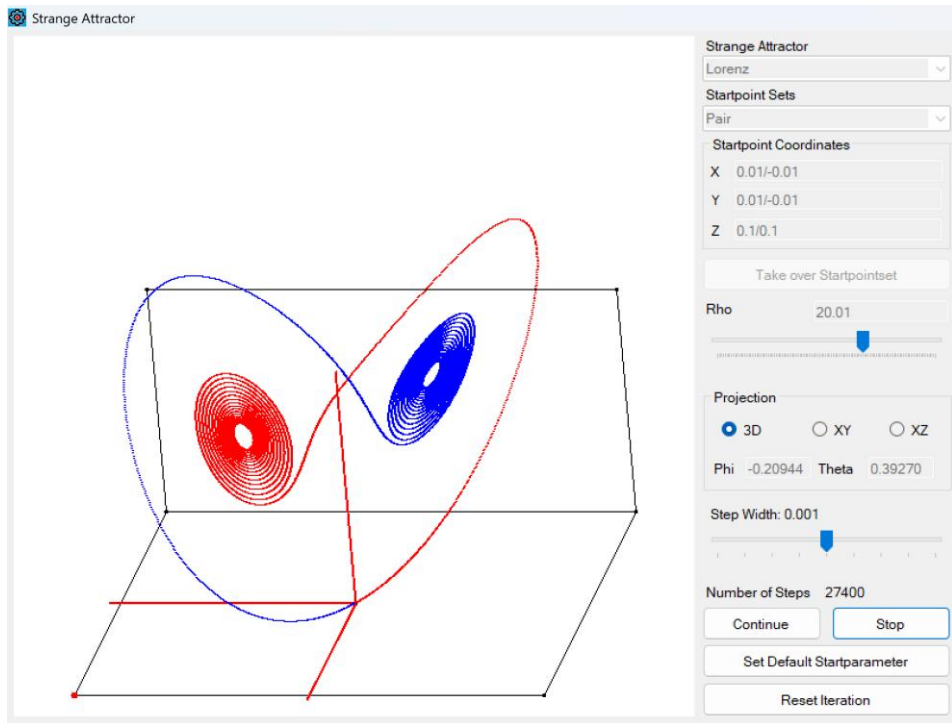
$$q(20) = 837.9729, D(20) = 175705.3602, \sqrt{D(20)} = 419.1722, u = 0.5705, v = -9.4285$$

$$\begin{cases} \mu_1 = -8.8580 \\ \mu_{2,3} = 4.4290 \pm 8.6594i \end{cases}$$

After the reverse transformation we get:

$$\begin{cases} \lambda_1 = -13.4136 \\ \lambda_{2,3} = -0.1266 \pm 8.6594i \end{cases}$$

This means that the equilibrium positions C^\pm are stable. The mapping is contracting in the direction of the eigenvectors.



$$\varrho = 20.01: C^\pm \text{ are attractive}$$

Example $\varrho = 28$

You get:

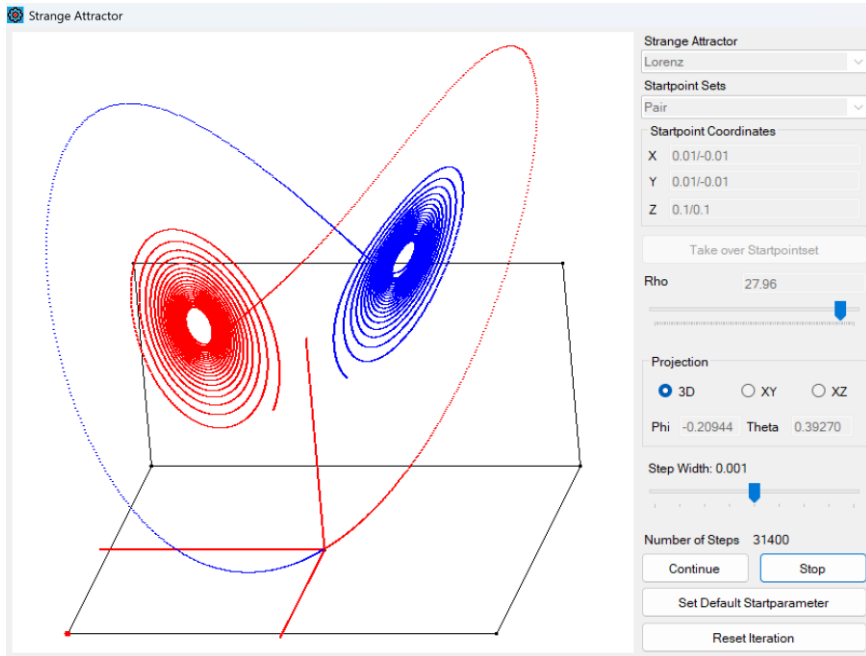
$$q(28) = 1167.4545, D(28) = 342946.4574, \sqrt{D(28)} = 585.6163, u = 1.2362, v = -10.5353$$

$$\begin{cases} \mu_1 = -9.2991 \\ \mu_{2,3} = 4.6496 \pm 10.1944i \end{cases}$$

After the reverse transformation we get:

$$\begin{cases} \lambda_1 = -13.8546 \\ \lambda_{2,3} = 0.0940 \pm 10.1944i \end{cases}$$

This means that the equilibrium positions C^\pm are unstable. The mapping is contracting in the direction of the first eigenvector, but dilating in the direction of the other two.



$$\varrho = 27.96: \text{The orbits move away from } C^\pm$$

The question now is, where is this "tipping point" for which C^\pm becomes unstable? This is at the transition when the real part of the complex zero changes from negative to positive. At the critical point, the real part is zero, i.e. the complex zeros are purely imaginary.

We would therefore have to solve the following equation for ϱ :

$$Re(\lambda_2) = -\frac{1}{2}(u + v) + \frac{a}{3} = 0$$

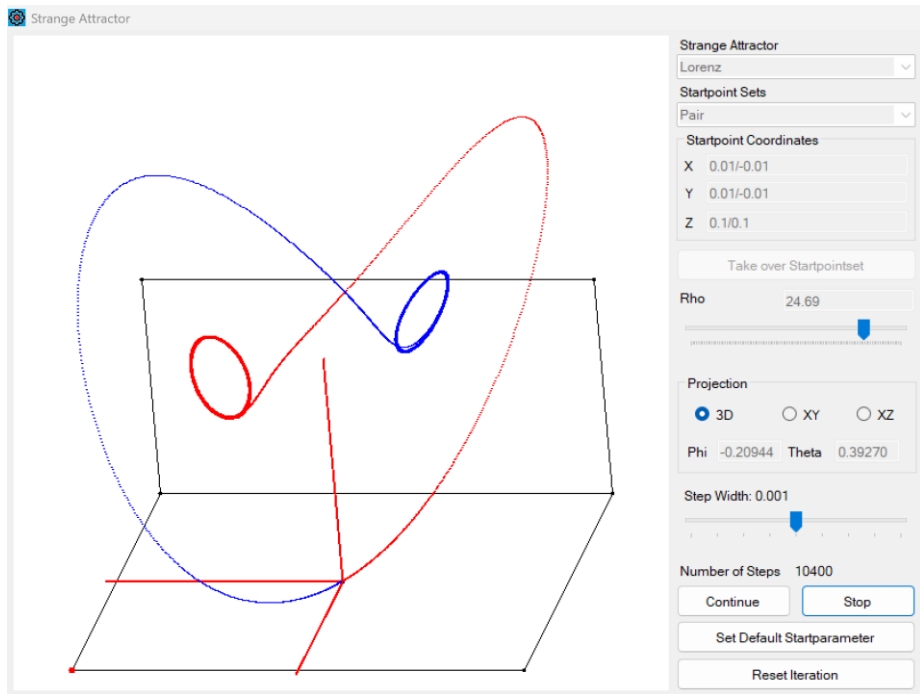
This seems complicated, as this expression contains cubic and quadratic roots and the variable ϱ is in the determinant D in the form of a third degree polynomial. We prefer to try an approach $\lambda_2 = i\eta$ and compare the coefficients. It is:

$$p_\lambda(\lambda) = \lambda^3 + a\lambda^2 + b\lambda + c = 0$$

So

$$\begin{aligned} p_\lambda(\lambda_2) &= -i\eta^3 - a\eta^2 + bi\eta + c = 0 \\ \Rightarrow i\eta(-\eta^2 + b) &= 0 \text{ and } -a\eta^2 + c = 0 \\ \Rightarrow \eta^2 &= b \text{ and } \eta^2 = \frac{c}{a} \\ \Rightarrow ab &= c \\ \Rightarrow \frac{41}{3} \cdot \frac{8}{3}(\varrho + 10) &= \frac{160}{3}(\varrho - 1) \end{aligned}$$

This provides the solution $\varrho \approx 24.7368$



$\varrho = 24.69$: The orbits each remain almost on a stable circle around C^\pm

At this point, the equilibrium positions C^\pm become indifferent in the plane perpendicular to the eigenvector, which belongs to the (negative) real eigenvalue. The iteration moves in a circle around the respective equilibrium position. If ϱ continues to grow, the equilibrium positions in this plane become repulsive. However, no other new attractive equilibrium positions arise, but the orbits approach a complicated-looking quantity, the Lorenz attractor, which is called a *strange attractor*. The behaviour of the dynamics at the equilibrium positions C^\pm during the transition from $\varrho < 24.7368$ to $\varrho > 24.7368$ is called a *Hopf bifurcation* after the mathematician Eberhard Hopf (1903 - 1983).

2.6 Projection of the Lorenz attractor

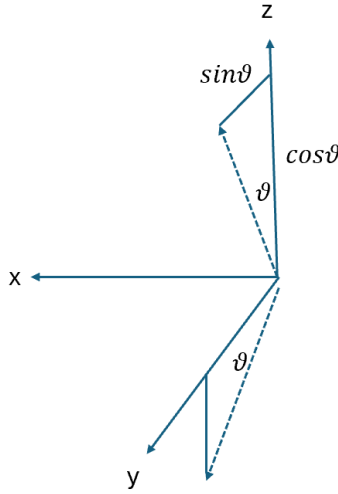
In the "Simulator" we have a two-dimensional representation of the Lorenz attractor. To obtain different views of the attractor, you can use the mouse to rotate the three-dimensional coordinate system.

If the mouse is moved vertically, this causes the coordinate system to rotate around the x-axis and an angle ϑ , which increases or decreases in proportion to the mouse position, but always remains within the range $[0.01, 1]$ (in radians).

If the mouse is moved horizontally, this causes a rotation around the z-axis and an angle φ , which also increases or decreases proportionally to the mouse position, but always remains within the range $[-\frac{\pi}{2}, \frac{\pi}{2}]$.

If $\vec{r} = \begin{pmatrix} x \\ y \\ z \end{pmatrix}$ is any point in space, this point must also be rotated. To do this, we need to find the corresponding linear mapping. In the section on linear mappings, we saw that this is defined by the images of the basis vectors. These are in the columns of the mapping matrix.

Let's first look at the rotation around the x-axis:



Rotation around the x-axis and the angle ϑ

The first base vector (in the x-axis direction) remains invariant. The second base vector (in the y-axis direction) changes to $\begin{pmatrix} 0 \\ \cos\vartheta \\ -\sin\vartheta \end{pmatrix}$ and the third base vector changes to $\begin{pmatrix} 0 \\ \sin\vartheta \\ \cos\vartheta \end{pmatrix}$. The rotation around the x-axis thus has the matrix:

$$D_x(\vartheta) = \begin{bmatrix} 1 & 0 & 0 \\ 0 & \cos\vartheta & \sin\vartheta \\ 0 & -\sin\vartheta & \cos\vartheta \end{bmatrix}$$

Using an analogue sketch, you can show that a rotation around the z-axis and the angle φ has the matrix:

$$D_z(\varphi) = \begin{bmatrix} \cos\varphi & -\sin\varphi & 0 \\ \sin\varphi & \cos\varphi & 0 \\ 0 & 0 & 1 \end{bmatrix}$$

If we perform both rotations in succession, we get:

$$D_z(\varphi) \circ D_x(\vartheta) = \begin{bmatrix} \cos\varphi & -\sin\varphi \cos\vartheta & -\sin\varphi \sin\vartheta \\ \sin\varphi & \cos\varphi \cos\vartheta & \cos\varphi \sin\vartheta \\ 0 & -\sin\vartheta & \cos\vartheta \end{bmatrix}$$

If the "3D projection" option is selected in the "Simulator",



3D projection

The three-dimensional coordinate system can be adjusted using the mouse. The angles φ and ϑ are then displayed. If the orbit of a starting point is now calculated, each point on the orbit is rotated after the calculation using the above matrix.

The point is then projected onto the plane $y = 1$.

```
'Projection to plane y = 1, and the x-direction is inverted
Dim PlanePoint = New ClsMathpoint With {
    .X = -RotatedPoint.X,
    .Y = RotatedPoint.Z
}
```

In the diagram, the y-axis points upwards, i.e. takes on the role of the three-dimensional z-axis.

Alternatively, the projection of an orbit in the xy-plane or xz-plane is available in the "Simulator". In this case, there is no previous rotation. To ensure that the (strange) attractor is optimally visible, a correction can be defined for each dynamic system, which shifts the y-coordinate vertically.

2.7 Strange attractors

A comment on the concept of the strange attractor is appropriate here. The Lorenz attractor is also called a "strange" attractor. We have found that in simple systems such as logistic growth we had either fixed points or cycles as attractors. In the Lorenz system, however, a set of points in phase space appears to be attractive. This set of points appears as the final state of the Lorenz system: any starting point within the defined area of the phase space gradually fills up the entire set of points of the attractor with its orbit, if the behaviour is chaotic, that is if $\rho > 24.7368$.

The definition of an attractor from the one-dimensional case must therefore be generalised here. A precise mathematical definition of a strange attractor can be found in [3]. Here we want to sketch the idea of the definition using the example of the Lorenz attractor.

Firstly, the set of points belonging to the attractor must be invariant. This means that once points have landed in this set, they should no longer move out of the set. Then sets of points that lie in the neighbourhood of the attractor should be "attracted" by it. We can therefore express the definition of an attractive set of points as follows:

Definition

Let (X, f) be a discrete dynamic system, and A a closed subset of X that is invariant under f .

Thus: $f(A) \subseteq A$. A is called *attractive* if an environment U of A exists with the property: For every environment V of A (no matter how small) the following applies: $f^n(U) \subset V$ for sufficiently large $n \in \mathbb{N}$. \square

All points from U therefore come arbitrarily close to the set A in the course of the iteration.

Now this does not mean that an attractive set of points has chaotic behaviour or something like sensitivity and transitivity. For transitivity, the points in the neighbourhood of A or A itself should be arbitrarily "intermixed". We therefore define:

Definition

Let (X, f) be a discrete dynamical system, and let A be an *f-invariant* subset of X . f is called *topologically transitive* on A if for every pair of open sets $\emptyset \neq U, V \subset A$ there is an $n \in \mathbb{N}$ with $f^n(U) \cap V \neq \emptyset$. \square

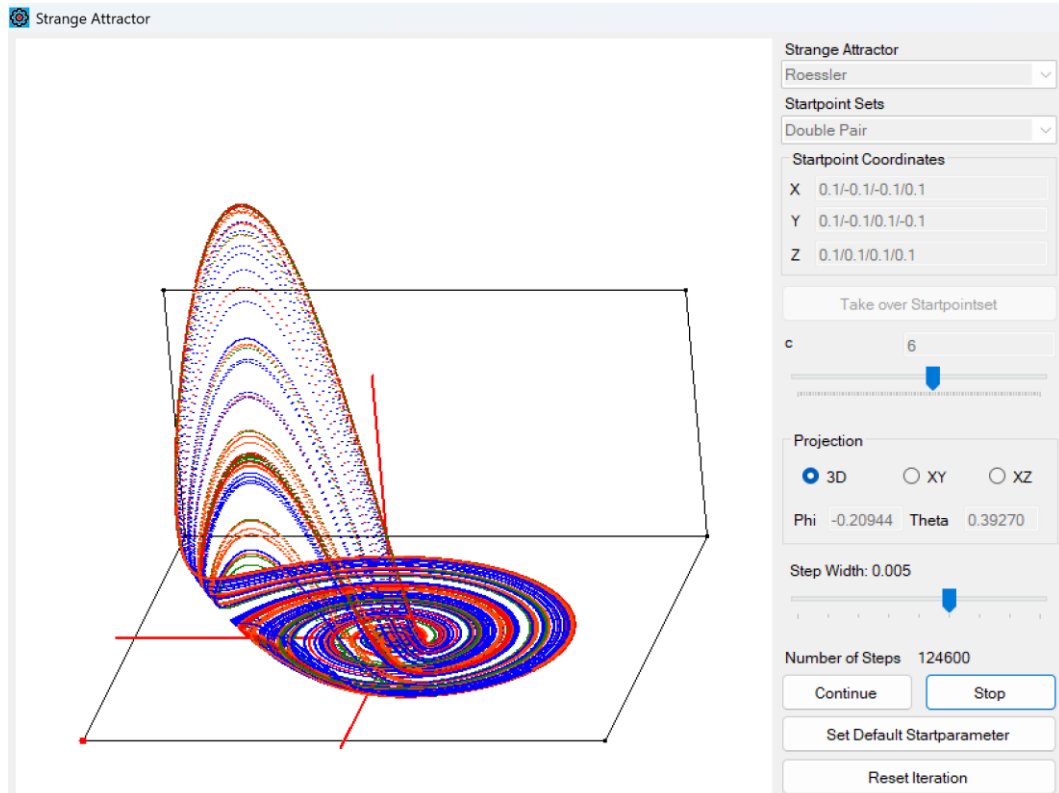
In the one-dimensional case, we have required for transitivity that you move from the neighbourhood of any starting point to the neighbourhood of any destination point in the course of the iteration. Here U replaces the role of the starting point and V the role of the destination point. So if I choose U arbitrarily and iterate long enough, then $f^n(U)$ will intersect with any given target set V .

If an f -invariant subset $A \subset X$ is attractive and at the same time topologically transitive, then it is also sensitive to initial conditions. In this case, A is called a *strange attractor*.

In addition to the Lorenz attractor, two other strange attractors are implemented in the "Simulator". The first is the so-called *Roessler attractor*, named after the biochemist and chaos researcher Otto Rössler (1940 -). The Roessler system is defined by the differential equation system:

$$\begin{cases} \dot{x} = -(y + z) \\ \dot{y} = x + ay \\ \dot{z} = b + xz - cz \end{cases}$$

Whereby $a = b = 0.2$ is selected and $c \in [1,10]$. For $c > 2$ you have chaotic behaviour.

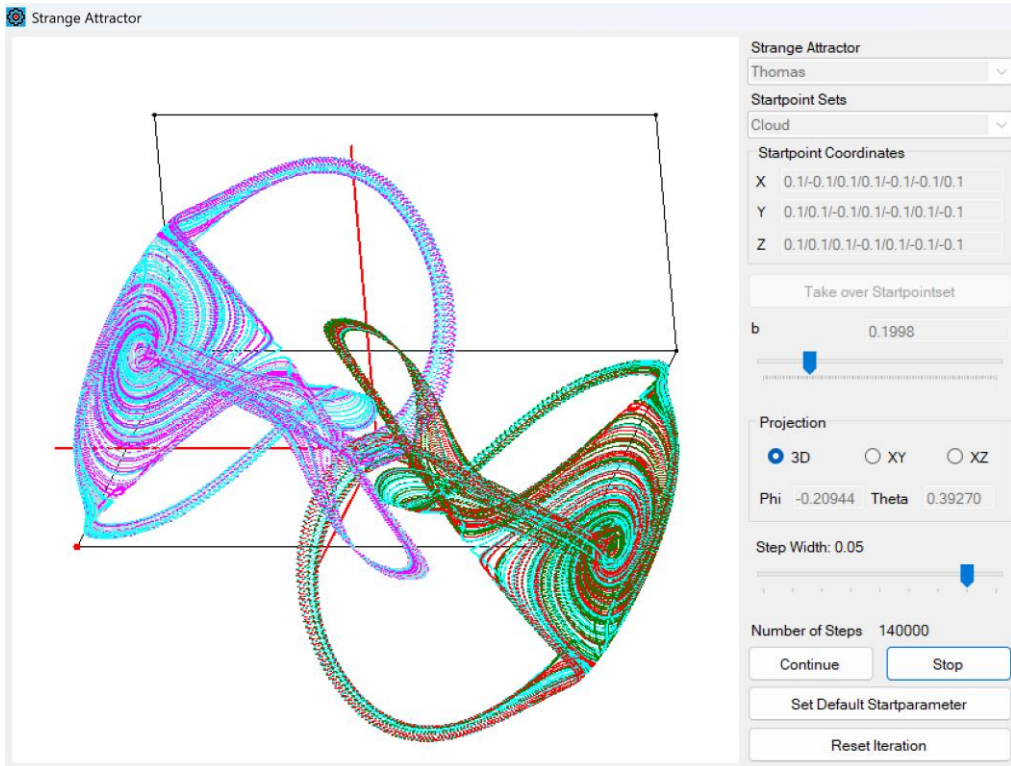


The Roessler attractor for $c = 6$

Another implemented attractor is the *Thomas attractor*. It is named after the French mathematician and physicist René Thomas (1928 - 2017). The system was proposed by him for modelling feedback mechanisms in biological networks. The system is defined by the differential equation system:

$$\begin{cases} \dot{x} = \sin y - bx \\ \dot{y} = \sin z - by \\ \dot{z} = \sin x - bz \end{cases}$$

The parameter $b \in]0,1]$ shows chaotic behaviour for $b < 0.215$.



The Thomas attractor for $b = 0.1998$

2.8 Numerical solution with the Runge Kutta method

The linear mapping $\mathbb{R}^3 \rightarrow \mathbb{R}^3$, the Lorenz system, the Roessler and the Thomas attractor are implemented in the "Simulator". The linear mapping can be used directly for each iteration step. With the other attractors, however, a system of differential equations must be approximated using a Runge-Kutta method.

We introduce the parameters (u, v, w) for the Runge Kutta method. In all cases for the Lorenz system, the Roessler attractor and the Thomas attractor, we can write

$$\begin{cases} \dot{u} = F(u, v, w) \\ \dot{v} = G(u, v, w) \\ \dot{w} = H(u, v, w) \end{cases}$$

The corresponding four-stage Runge Kutta process then starts with:

$$\begin{cases} k_1 = F(u, v, w) \\ l_1 = G(u, v, w) \\ m_1 = H(u, v, w) \end{cases}$$

$$\begin{cases} k_2 = F\left(u + \frac{h}{2}k_1, v + \frac{h}{2}l_1, w + \frac{h}{2}m_1\right) \\ l_2 = G\left(u + \frac{h}{2}k_1, v + \frac{h}{2}l_1, w + \frac{h}{2}m_1\right) \\ m_2 = H\left(u + \frac{h}{2}k_1, v + \frac{h}{2}l_1, w + \frac{h}{2}m_1\right) \end{cases}$$

Where h is the increment of the method. We then continue:

$$\begin{cases} k_3 = F(u + \frac{h}{2}k_2, v + \frac{h}{2}l_2, w + \frac{h}{2}m_2) \\ l_3 = G(u + \frac{h}{2}k_2, v + \frac{h}{2}l_2, w + \frac{h}{2}m_2) \\ m_3 = H(u + \frac{h}{2}k_2, v + \frac{h}{2}l_2, w + \frac{h}{2}m_2) \end{cases}$$

And

$$\begin{cases} k_4 = F(u + hk_3, v + hl_3, w + hm_3) \\ l_4 = G(u + hk_3, v + hl_3, w + hm_3) \\ m_4 = H(u + hk_3, v + hl_3, w + hm_3) \end{cases}$$

As a result of this iteration step, the next value for the parameters is set to: (u, v, w)

$$\begin{cases} u = h(k_1 + 2k_2 + 2k_3 + k_4)/6 \\ v = h(l_1 + 2l_2 + 2l_3 + l_4)/6 \\ w = h(m_1 + 2m_2 + 2m_3 + m_4)/6 \end{cases}$$

2.9 Exercise examples

1. A point reflection at the origin is given in the space \mathbb{R}^3 . Show that this mapping is linear and determine the corresponding mapping matrix.
2. A rotation around the z-axis and the angle φ is given in the space \mathbb{R}^3 . Show that this mapping is linear and determine the corresponding mapping matrix.
3. Determine the centre of the mapping $A = \begin{bmatrix} 1 & -2 & -1 \\ -1 & 1 & 0 \\ 2 & -1 & 1 \end{bmatrix}$
4. Determine $\lambda \in \mathbb{R}$ so that the *Kern A* with $A = \begin{bmatrix} 1-\lambda & -1 & 2 \\ -1 & 2-\lambda & 0 \\ 2 & 0 & 3 \end{bmatrix}$ is different from $\vec{0}$.
5. Let $A: \mathbb{R}^3 \rightarrow \mathbb{R}^3$ be a linear mapping. Prove: Then the kernel of A is either the origin, a straight line through the origin, a plane through the origin or the whole space.
6. The mapping $A = \begin{bmatrix} 2 & -1/2 & 1/2 \\ -1 & 3/2 & -1/2 \\ 1 & 1/2 & 5/2 \end{bmatrix}$ is given. Determine its eigenvalues and eigenvectors.

Discuss the behaviour of the mapping near the zero point.

7. Consider the Lorenz system with the zero point as a fixed point. Investigate different paths to the zero point and under which conditions the zero point is attractive.
8. Given is the mapping

$$A = \begin{bmatrix} -\sigma & \sigma & 0 \\ 1 & -1 & \mp\sqrt{\beta(\varrho-1)} \\ \pm\sqrt{\beta(\varrho-1)} & \pm\sqrt{\beta(\varrho-1)} & -\beta \end{bmatrix}$$

at the location of the equilibrium positions C^\pm for the Lorenz system. We are looking for eigenvalues λ and eigenvectors \vec{e} such that: $A\vec{e} = \lambda\vec{e}$. Show that the condition for their

existence is given by: $p(\lambda) = \lambda^3 + (\sigma + \beta + 1)\lambda^2 + \beta(\sigma + \varrho)\lambda + 2\sigma\beta(\varrho - 1) = 0$.

9. Investigate the zeros of the transformed characteristic polynomial of the Lorenz system $p(\mu) = \mu^3 + p\mu + q$ for $\varrho > 1$ using Cardano's formulae. Create an Excel table for the calculations of the zeros when different values of ϱ are entered. Then calculate the original eigenvalues $\lambda = \mu + a/3$ and discuss the stability.
10. Check that in the Lorenz system for $\varrho = 24.7368$ the real part of the complex zero of $p_\lambda(\lambda)$, i.e. the expression $-\frac{1}{2}(u + v) + \frac{a}{3} \approx 0$.
11. Examine the Roessler attractor regarding fixed points and their properties.
12. Examine the Thomas attractor regarding fixed points and their properties.
13. Proof: If you rotate the room so that the zero point remains fixed, there is always an axis through the zero point that also remains fixed.

3. Fractal Sets

3.1 Lindenmayer Systems

Lindenmayer systems (or L-systems) are named after the Hungarian biologist Aristid Lindenmayer (1925 - 1989), who developed them for an axiomatic theory of biological systems. We will not give an abstract definition of these systems here but describe them as they are used in the "simulator".

An *L-system* consists of:

- a) An *alphabet* \mathcal{A} . This is a finite set of characters. In the case of the "Simulator" is:
$$\mathcal{A} = \{A, B, C, D, E, F, G, \dots, X, Y, Z, f, g, +, -, (,), [], 0, 1, 2, 3, 4, 5, 6, 7, 8, 9\}$$
- b) An *axiom* $\omega\omega$ is either a single element of \mathcal{A} or a character string (usually consisting of a few characters) that is formed with elements from \mathcal{A} .
- c) A list of replacement rules. These are mappings that assign a character string (the target) to an element from \mathcal{A} (the source), which is formed from elements from \mathcal{A} .
- d) In an iteration step, the source is then replaced by the target. This results in an increasingly longer string through continuous iteration. (We also use "string" as a synonym for "character string").

In the following, \mathcal{A} is always the above alphabet, which is used in the "Simulator".

Example

\mathcal{A} as above. $\omega = F$. Replacement rule: $F \rightarrow F - F + +F - F$

With the help of the replacement rules, an increasingly longer string is now formed recursively, starting with the axiom. In the example, this leads iteratively to the following strings in the first three steps:

F

$F - F + +F - F$

$F - F + +F - F - F - F + +F - F + +F - F + +F - F - F - F + +F - F$

The following comments on the replacement rules are also important:

1. The application of the replacement rules is *not "distributive"*. For example, if it is $X \rightarrow F + F$ with the axiom FX , then the first string is $FF + F$ and not $F(F + F) = FF + FF$
2. The replacement of symbols takes place simultaneously and not one after the other.

Example: Axiom YFX with replacement rules: $X \rightarrow FX + Y, Y \rightarrow X + FY$. Then the first string generated is :

$X + FYFFX + Y$ and not in two steps (first replace all X and then all Y)

$$YFX \rightarrow YFFX + Y \rightarrow X + FYFFX + X + FY$$

This has to do with the much simpler serial processing of a string. For a specific L-system, the rules must be formulated in such a way that the desired result is still achieved.

3. If the replacement rules are applied simultaneously, their order is irrelevant. When traversing the string to be replaced, the rule that is currently required for the corresponding symbol is simply accessed each time.

The turtle

The idea is that this string controls a turtle that records its path. The characters in the alphabet should fulfil certain tasks or pass certain commands to the turtle.

State of the turtle

After each step, the turtle is in a state that consists of the following parameters:

- Position in (x,y) coordinates
- Angle relative to the x-axis. Anticlockwise is the positive direction of rotation
- current character colour
- Step length. This must be continuously shortened the longer the controlling string is so that the path of the turtle still has room in the diagram. For curves without branching, it makes sense to reduce the step length by a constant factor for each iteration step, i.e. "per iteration". With a tree structure, on the other hand, it makes sense to reduce the step length by a constant factor when a new branch is drawn, i.e. "per branch". After returning to its root, the original step length is used again. The reduction factor is entered globally for the L system and determined either by calculation or experimentally.

Start position

The coordinates of the start position are entered for the L-system. At the start, the turtle is always aligned parallel to the x-axis, i.e. the start angle is zero.

Instructions to the turtle

"F", "G": Take a step forward and record your path. (There are two characters available here to make the replacement rules more flexible).

"f", "g": Take a step forward without recording your path.

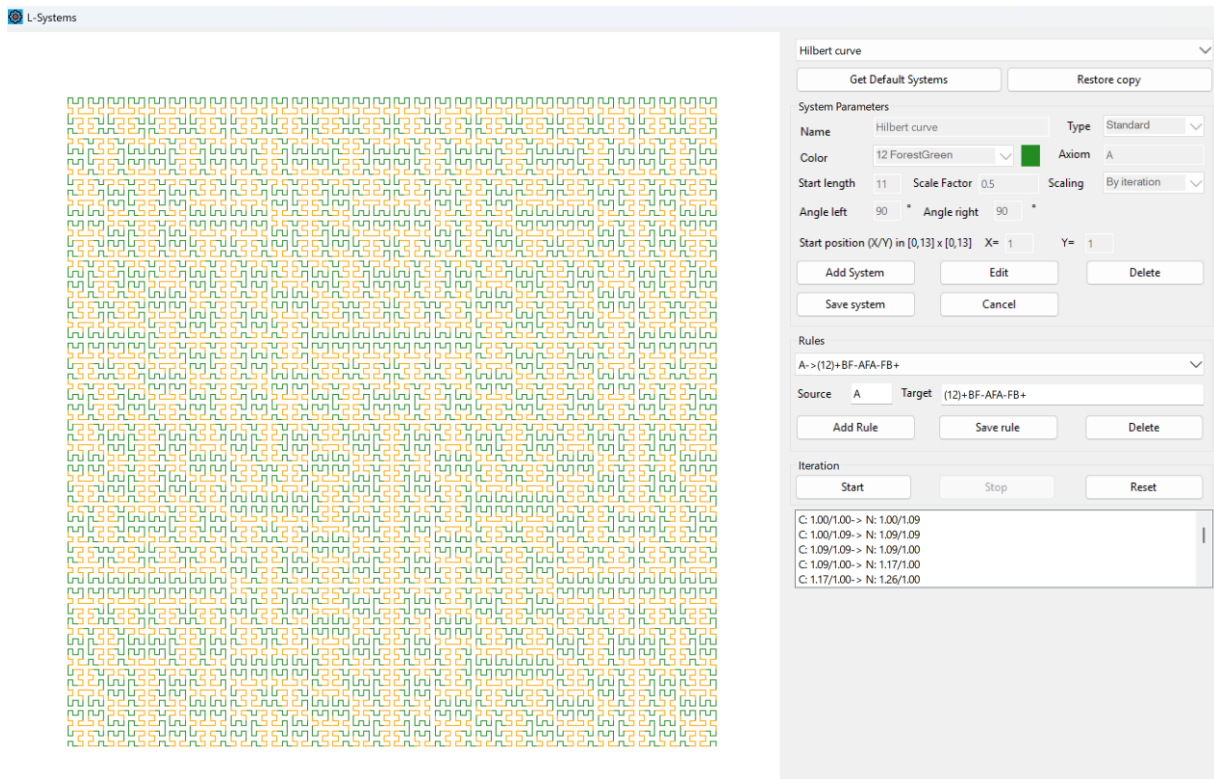
"+": Turn anticlockwise by a fixed angle α .

"-": Turn clockwise by a fixed angle β . The angles α and β are defined globally for each L-system and remain fixed.

(12): The colour codes in which the path is to be drawn are indicated in round brackets. If the turtle encounters such a code, it draws all subsequent steps in this colour. This also means that only natural numbers in the range 0 to 25 may be placed between round brackets.

These are the colours offered in the "Simulator". If no such brackets occur, the turtle uses a globally defined colour for each L-system. Conversely, numbers may only be used in this context. No numbers occur without round brackets.

- "[]" Square brackets mark a branch in a tree structure. [is used to mark the root. At this point, the turtle saves its state and stores it in a stack. The end of the branch is marked with]. The turtle then retrieves the last saved state from the stack and continues working there. As the stack is a FILO (=First in last out) memory, nested structures are also possible.
- {A, ..Z} All other capital letters except "F, G" have no effect on the control of the turtle. They are used to summarise larger structures and a replacement rule for this letter is used to break down the structure.



Example: Hilbert curve

In the top right-hand area of the user window, you can see the entries for the global parameters such as start length, scaling factor, rotation angle and start position. Further down you can see a replacement rule for axiom "A".

For the use of the above window, please refer to the user manual.

Many examples and beautiful animations including the replacement rules can be found in [5].

3.2 Historical Excursus: From descriptive to abstract thinking

The L-systems described in this section are more than just decorative fractals - they exemplify a profound change in the history of mathematics. In the 19th century, mathematics began to develop from purely descriptive geometry and informal analysis into a strictly axiomatically based science. During this time, numerous fundamental questions were raised that radically challenged the intuitive understanding of space, function and dimension.

For example, the question arose as to whether there could be functions that were continuous everywhere but not differentiable anywhere - a contradiction to the perception of "smooth" curves at the time. Karl Weierstrass answered this question in 1872 with the explicit construction of such a function.

Shortly afterwards, curves were discovered that completely filled a finite surface, although they were generated by a continuous mapping of a one-dimensional line - so-called space-filling curves, for example by Peano (1890) or Hilbert (1891). These objects contradicted the classical understanding of dimension and led to a re-evaluation of fundamental concepts such as "length", "area" or "continuity".

New questions were also formulated in analysis: Can discontinuous functions be integrable everywhere? How do infinite series behave with non-"smooth" functions? What types of convergence need to be differentiated? And how do we deal with "pathological" objects such as so-called "monster curves", which seem to contradict all conventional ideas, but are nevertheless mathematically correctly defined? Examples include curves that intersect themselves infinitely often or functions that have any number of extrema in any interval.

The emergence of these so-called **pathological examples** led to the development of new concepts: various notions of convergence, measure theory, set theory, and finally to the idea of fractal geometry - a term that was only coined in the 20th century by Benoît Mandelbrot, but whose roots can be traced back deep into 19th century mathematics.

L-systems are to be understood in this context: They generate geometric objects that often have a **non-integer fractal dimension**, as we will see in a later section. They thus stand between the classical dimensions. Their recursive, formal definition is typical of modern mathematics, whose objects no longer must be descriptive, but logically consistent and precisely defined.

The L-systems thus build a bridge between historical questions and modern mathematical practice. They vividly demonstrate how simple rules can lead to complex structures - a central theme of mathematics since the 19th century.

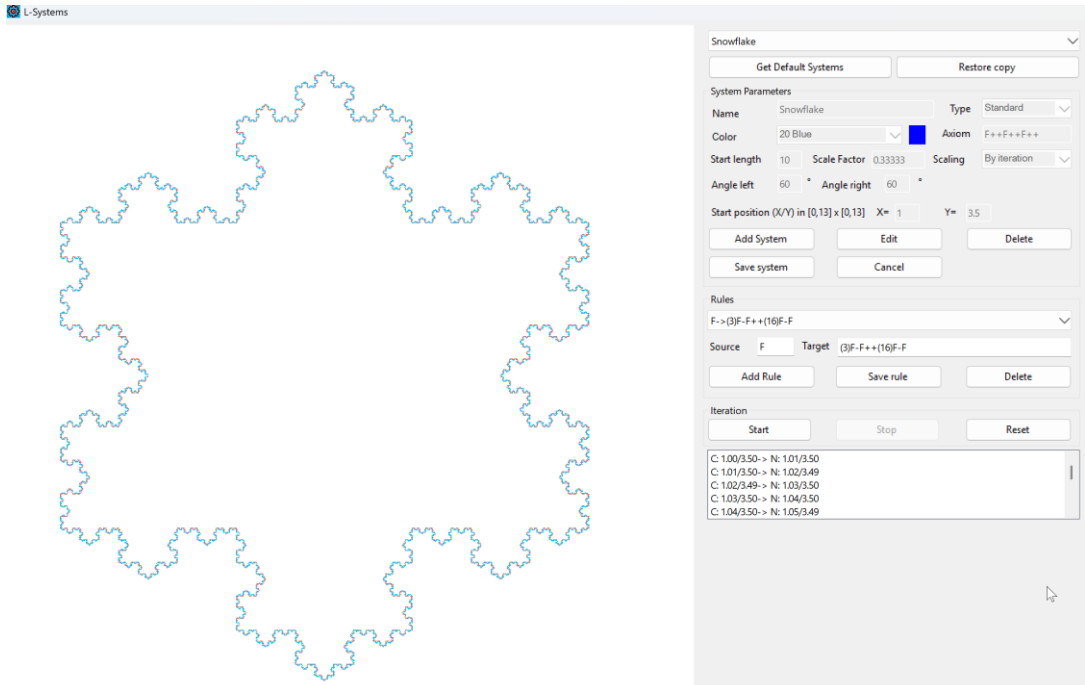
The implemented L-systems described in the following section should also be understood in this light.

3.3 The Koch curve (or snowflake curve)

One of the simplest L-systems is the so-called Koch curve, named after the Swedish mathematician Helge von Koch (1870 - 1924). It is an example of a curve that

- lies within a finite area, but whose length is infinite
- Which is continuous everywhere but not differentiable anywhere

It can be described as an L-system and there are different variants. The variant, that is implemented in the "Simulator" is the snowflake-curve.



Snowflake curve of the sixth generation

Note: The curve is often referred to as a *Koch curve* if only the base line of a triangle is taken as the axiom and this line is then iteratively replaced. The curve obtained is then only the lowest part of the above figure. If you choose an equilateral triangle as the initial set, this is called the *snowflake curve*.

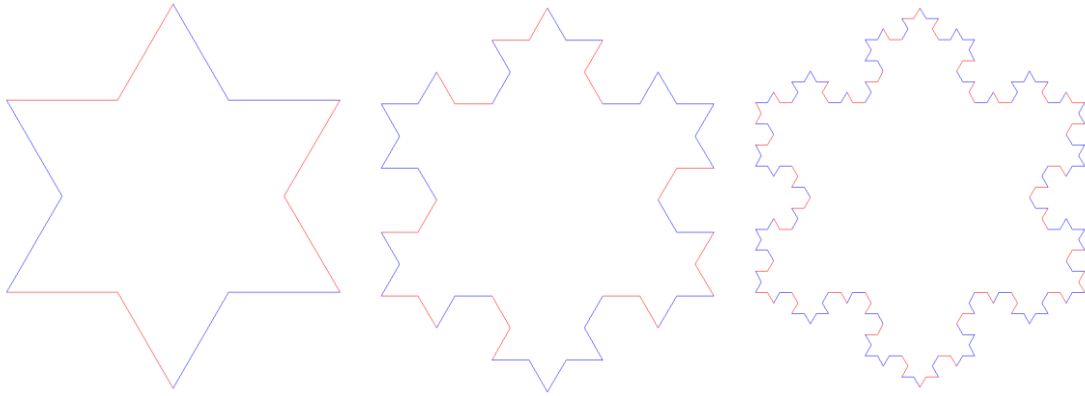
The global parameters can be taken from the right-hand area of the user window above.

Axiom: $F + +F + +F + +$ (for the Koch curve, the axiom is F)

With this axiom, you have a triangle as the initial set. Often only a straight line is taken as the initial set. In this case, the axiom is simply F .

Replacement rule (without colour control): $F \rightarrow F - F + +F - F$

This leads to the following strings in the first three generations:



Snowflake curve of the first three generations

In the "Simulator", the length of the first step is ten. With each iteration step, the step length is reduced by a third. If the initial triangle has the lower two corners A and B , the distance between A and B remains constant for each iteration step. This means that the Snowflake curve lies within the perimeter of the initial triangle, i.e. within a limited area.

The number of steps increases by a factor of four with each iteration step, but the step length only decreases by a factor of three. This means that the length of the curve increases by a factor of $4/3$ with each iteration step and tends towards infinity.

The curve is also continuous, as the replacement rule replaces each straight curve segment "F" with a continuous curve segment "F-F++F-F". If the number of iterations is allowed to approach infinity, there is a "kink" in every small neighbourhood of a curve point, at which point the curve is not differentiable.

Further properties of the Snowflake curve are demonstrated in the form of an exercise:

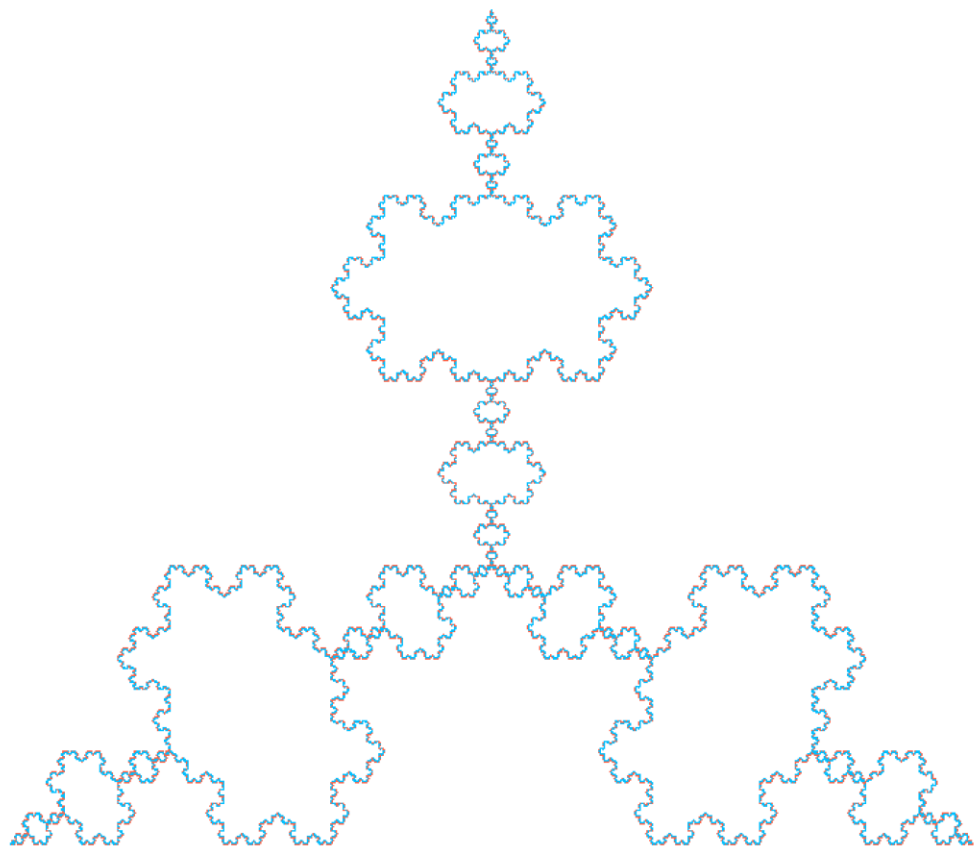
- Three consecutive points on the Snowflake curve always form an equilateral triangle with base angles of either 30° or 60° .
- The Snowflake curve lies entirely within the hexagon spanned by the Snowflake curve of the first generation.
- The Snowflake curve has 6 axes of mirror symmetry
- The Snowflake curve is rotationally symmetrical with a rotation angle of 60°
- The area of the Snowflake curve in the "Simulator" version is $\frac{2\sqrt{3}}{5}$

The inverse Snowflake curve

If you let the newly added triangles in the Snowflake curve "jump in" instead of "jump out", you get the "inverse Snowflake curve". The replacement rule is then:

$$F \rightarrow F + F - -F + F$$

While the other parameters remain unchanged.



Snowflake Koch curve of the seventh generation

3.4 The Dragon curve

The Dragon curve was discovered in 1966 by the NASA physicist John Heighway (biographical data does not appear to be available).

Dragon curve

System Parameters

- Name: Dragon curve
- Type: Dragon
- Color: 19 Navy
- Axiom: FX
- Start length: 3
- Scale Factor: 0.74
- Scaling: By iteration
- Angle left: 90°
- Angle right: 90°
- Start position (X/Y) in [0,13] x [0,13]: X= 7 Y= 7

Rules

X->(ZX+YF+

Iteration

C: 7.00/7.00-> N: 7.03/7.00
C: 7.03/7.00-> N: 7.03/7.03
C: 7.03/7.03-> N: 7.00/7.03
C: 7.00/7.03-> N: 7.00/7.07
C: 7.00/7.07-> N: 6.97/7.07

The fifteenth-generation Dragon curve

The global parameters are shown on the right of the user window. The scaling factor is $\frac{1}{\sqrt{2}}$.

Axiom: FX

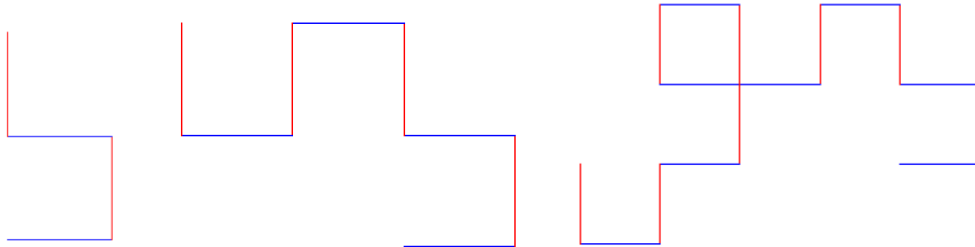
Replacement rules (without colour codes):

$$X \rightarrow X + YF +$$

$$Y \rightarrow -FX - Y$$

The generated strings are shown in the following list (+- cancel each other out and are not noted):

Generation	Character string	Relevant for the turtle
Axiom	FX	F
1	$FX+YF+$	$F+F+$
2	$FX+YF+FX-YF+$	$F+F+F-F+$
3	$FX+YF FX-YF+FX+YF-FX-YF+$	$F+F+F-F+F+F-F-F$
4	$FX+YF+FX-YF+FX+YF-FX-YF+FX+YF-FX-YF-FX-YF$	$F+F+F-F+F+F-F-F-$ $F+F+F+F-F-F+F-F-F$

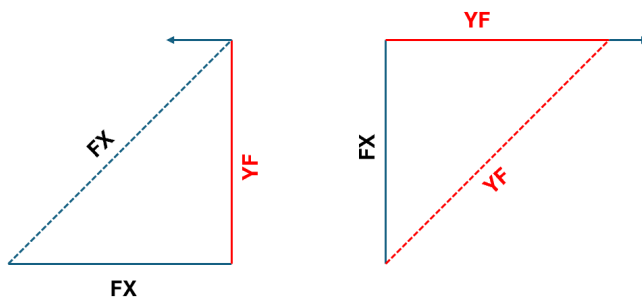


The Dragon curve of generation two, three and four

The starting point is always the point on the right or at the bottom. The colour changes with each segment.

We now want to understand in more detail what role the placeholder's "X" and "Y" play in this construction. "X" is used to mark a line segment, which will be replaced in the next generation by new segments to the right of it (in the direction of the turtle's movement). "Y" marks a segment that will be replaced by segments to its left.

If we consider a segment "FX" and then the corresponding specimen of the next generation, this is "FX+YF+". A segment "YF" is replaced by "-FX-YF". The corresponding images are:

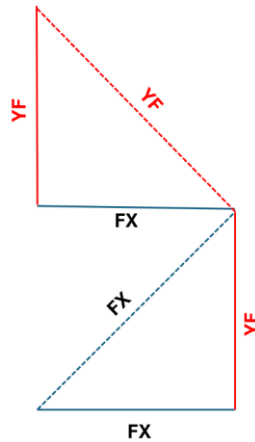


$$FX \rightarrow FX + YF +$$

$$YF \rightarrow -FX - YF$$

In the drawing, the turtle direction for the replacement segments is rotated by 45° for better understanding. The turtle always starts in the direction of the original segment.

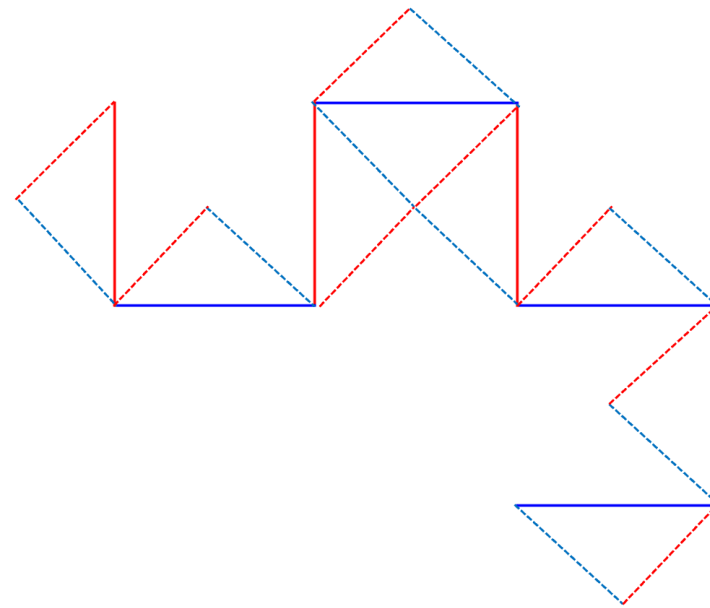
Let's look at how the assembled segment is replaced:



$$FX + YF + \rightarrow FY + YF + FX - YF +$$

You can also see from this sketch why the scaling factor $\frac{1}{\sqrt{2}}$ was chosen. The step length of the next generation is then adjusted so that the length of the replaced section remains constant.

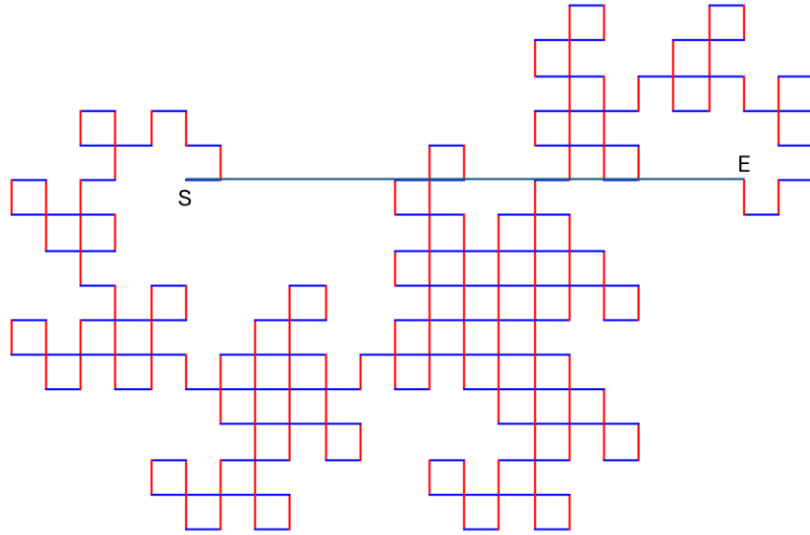
If the turtle replaces each segment in each curve of a certain generation, then this follows the above scheme. The turtle replaces each segment with two smaller segments, which form an isosceles and rectangular triangle on the replaced segment. The turtle "wobbles" and the new segments lie alternately to the right or left of the replaced segment (in the direction of movement).



Transition from the third to the fourth (dashed) generation through segment replacement

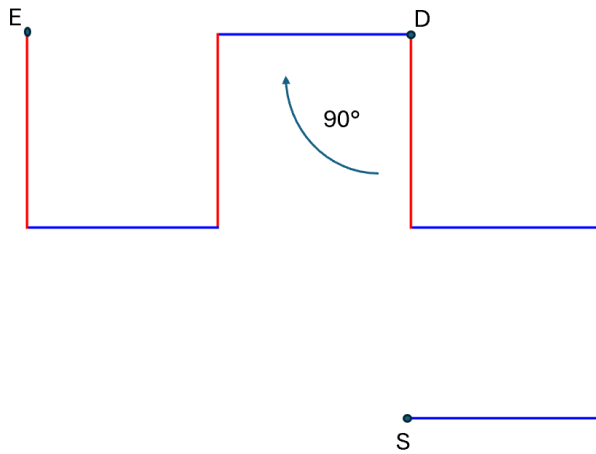
The segments are replaced without moving their start and end points. This means that the distance between the start point, and end point of the entire turtle path is constant for each iteration and corresponds to the first step length.

This means that the end point of each iteration lies on a circle around the starting point with the radius of the first step length. This also means that the entire curve lies in a limited plane area, for example in a circle with a radius of 1.5 times the first step length.



The starting point and end point of the eighth generation are also the starting point and end point of the axiom

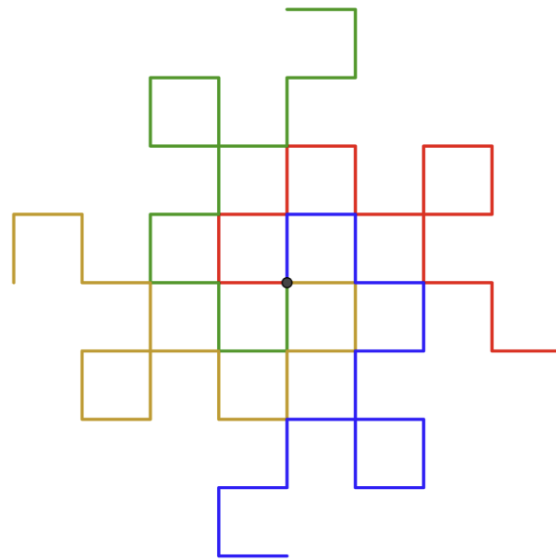
If the curve of the n^{th} generation is rotated clockwise by 90° around its end point and the original curve is also left standing, the curve of the $(n+1)^{\text{th}}$ generation is obtained.



Transition from the second to the third generation

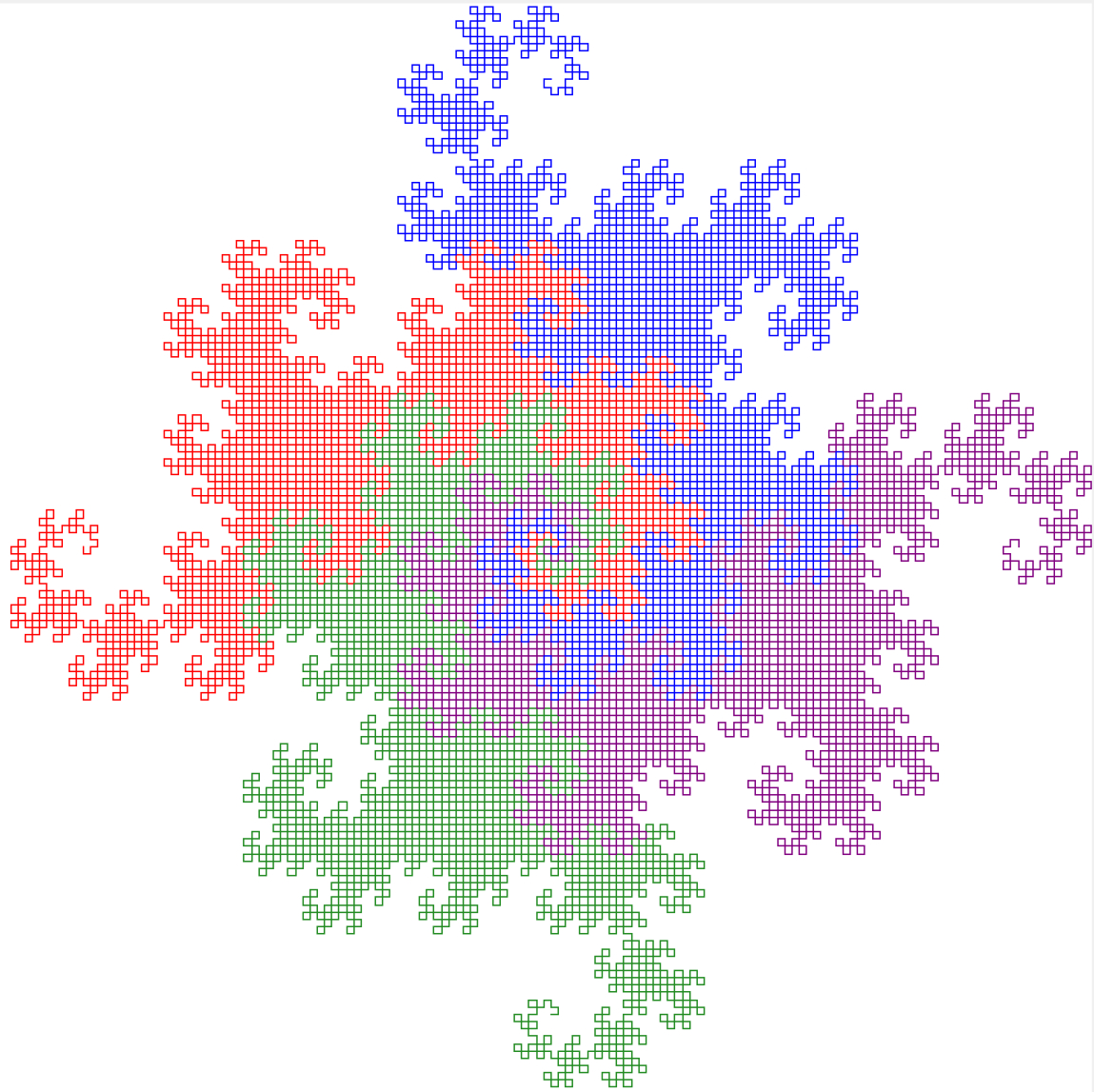
This can be proven by complete induction. The assertion is correct for the first, the second or, as you can see above, the third generation. The number of turtle steps is always even. This means that there is always a point D which is reached after exactly half the number of steps. Let us now assume that in the n^{th} generation, the second part of the turtle path (between D and E) is a 90° rotated copy of the first part of the turtle path (between S and D). In the next generation, each segment of the first part and the 90° rotated copy is replaced in exactly the same way, because an "FX" segment starts in D again. Thus, in the $(n+1)^{\text{th}}$ generation, the second part of the turtle path (between D and E) is also a copy of the first part (between S and D) rotated by 90° .

It is interesting to note, without proving it here, that part of the plane around the starting point can be parqueted with the Dragon curve. To do this, take four copies of the Dragon curve with the same starting point, but with the starting angle of the turtle rotated by 90° in each case. This image is then obtained for the fourth generation of the Dragon curve:



Four copies of the Dragon curve of the fourth generation, each rotated by 90°

In the "Simulator" you can activate the "extended" option for the Dragon curve. Four turtles are then sent on their journey, each with a starting angle rotated by 90° .

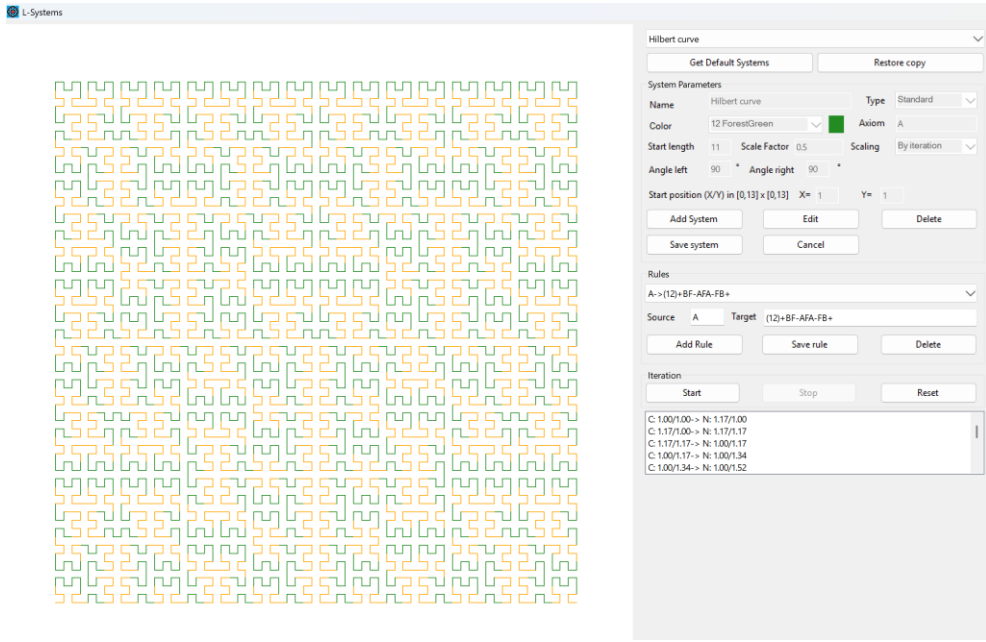


Four copies of the 12th generation Dragon curve, each rotated by 90°

3.5 The Hilbert and Peano curves

One question that occupied mathematicians in the 19th century was whether it is possible to find a mapping between a finite interval $I \subset \mathbb{R}$ and a square $J \times J \subset \mathbb{R}^2$ so that this mapping is continuous and its image "fills up" the square as densely as desired. This means that in any arbitrarily small neighbourhood of any square point there is a point that is an image of the mapping.

David Hilbert (1862 - 1943) found such a curve, which is named after him.



Hilbert curve of the fifth generation

The Hilbert curve is defined as an L-system as follows:

Axiom *A*

Replacement rules (without colour control)

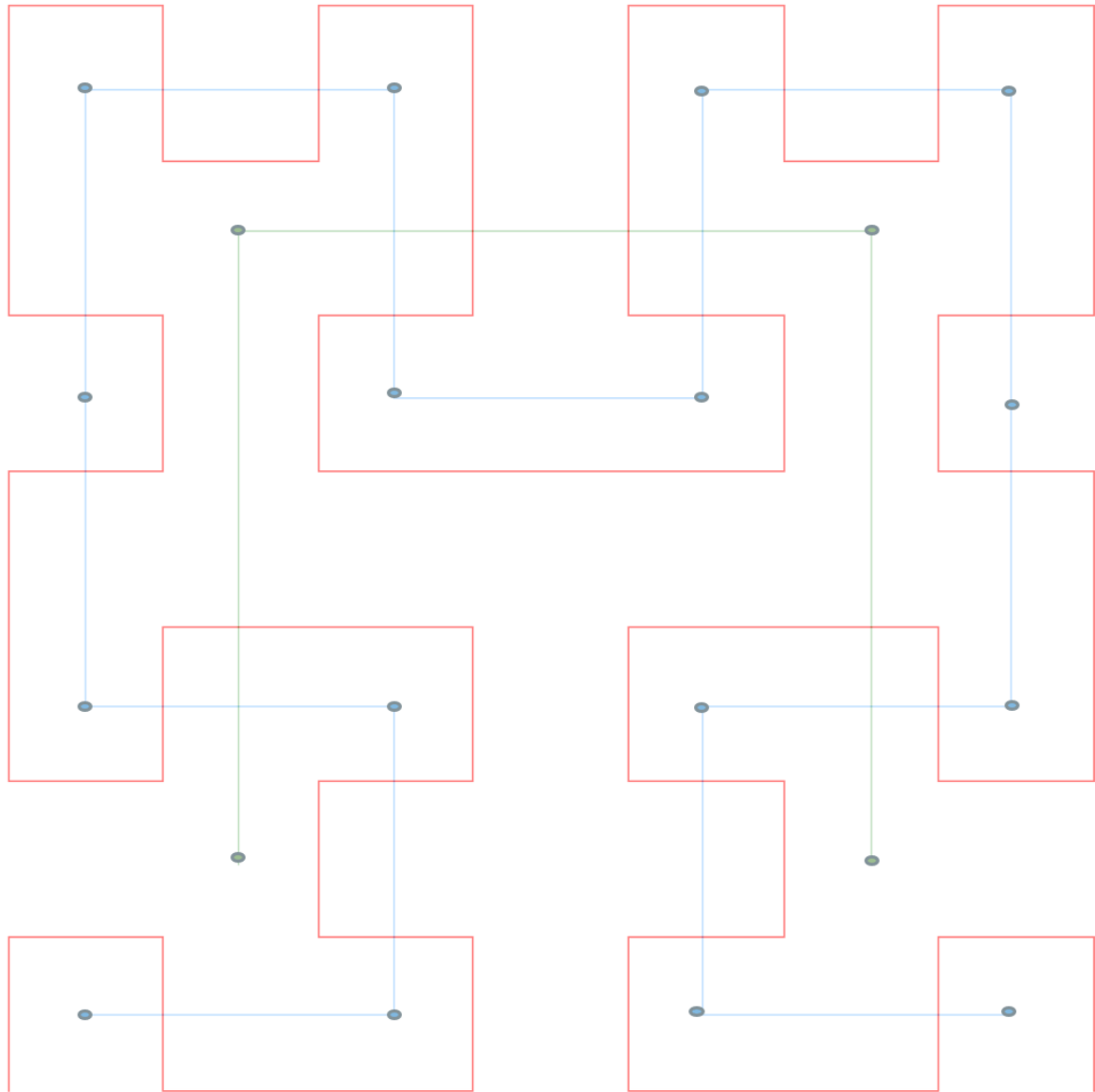
$$A \rightarrow +BF - AFA - FB +$$

$$B \rightarrow -AF + BFB + FA -$$

The first two generations are

Generation	Character string	Relevant for the turtle
Axiom	A	-
1	+BF-AFA-FB+	+F-F-F+
2	AF+BFB+FA-FBF-AFA-FB+F+BF-AFA-FBF-AF+BFB+FA	F+F+F-FF-F-F+F+F-F-F-FF-F+ F+F

The following diagram shows the design principle of the Hilbert curve:



Construction principle of the Hilbert curve

The axiom is shown in green. Its corner points are also green.

First generation: Now draw a blue square around each green corner point, but only the first three sides. Then move on to the next green corner point. The resulting blue line is the first generation of the Hilbert curve. The corresponding vertices of the blue squares are also marked in blue.

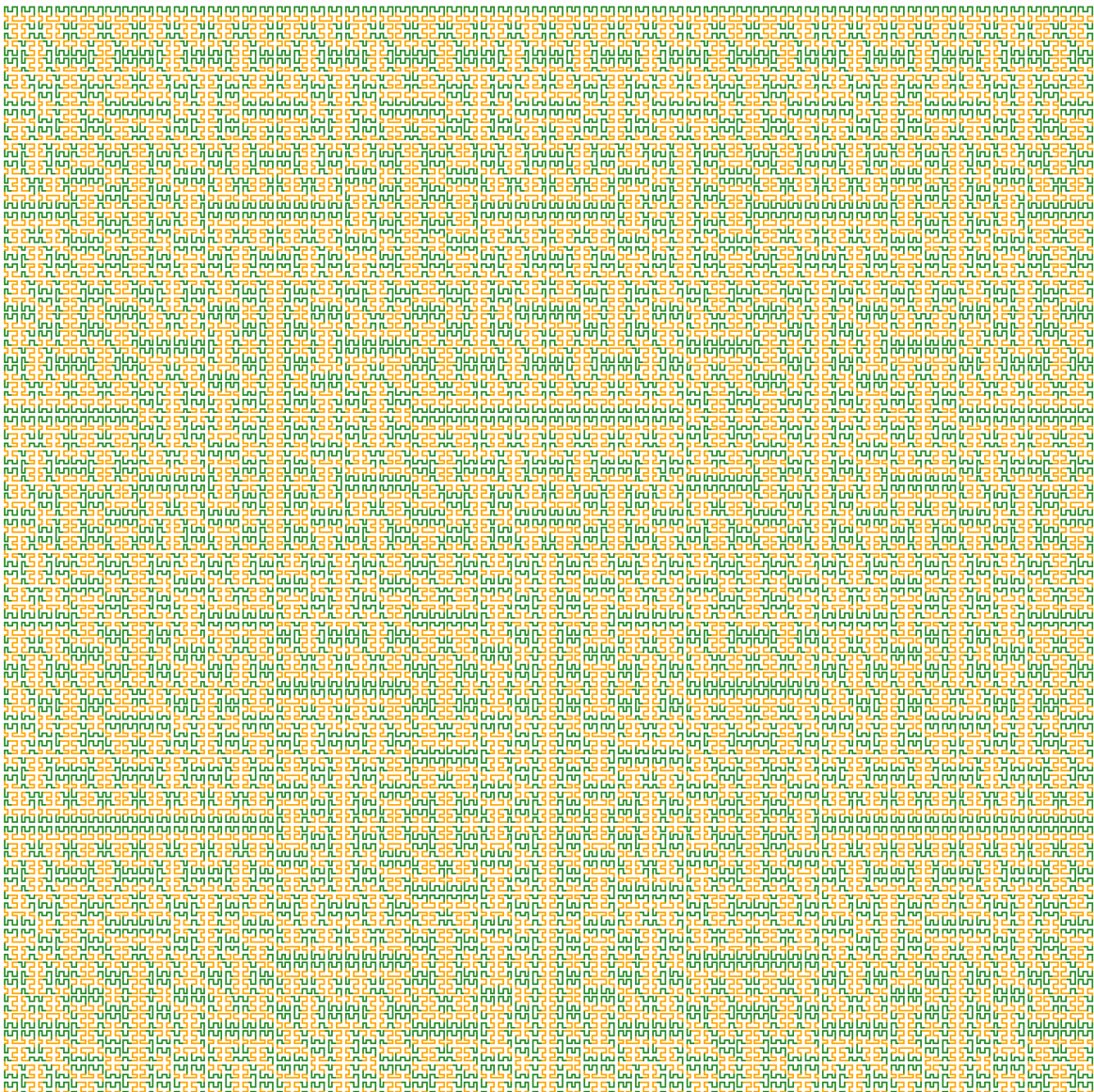
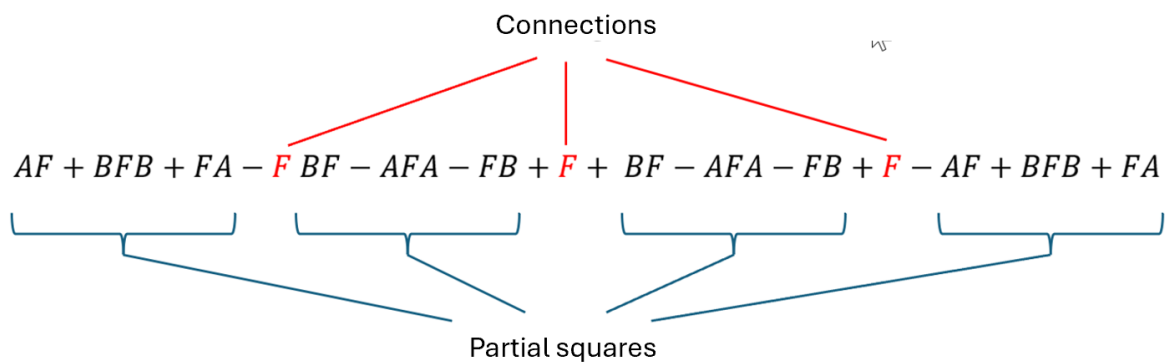
Second generation: Now repeat the procedure. Draw a red square around each blue corner point, but only the first three sides. Then move on to the next blue corner point. The resulting red line is the Hilbert curve of the second generation.

In the replacement rules, the chain $+BF - AFA - FB +$ stands for a partial square that opens downwards and the chain $-AF + BFB + FA -$ for a partial square that opens outwards. The "F" in these chains mark the subsquares of the current generation and at the same time establish the connection between the later replacement squares.

Example: Transition from the first to the second generation

First generation: $+BF-AFA-FB+$

Second generation:



Hilbert curve of the seventh generation

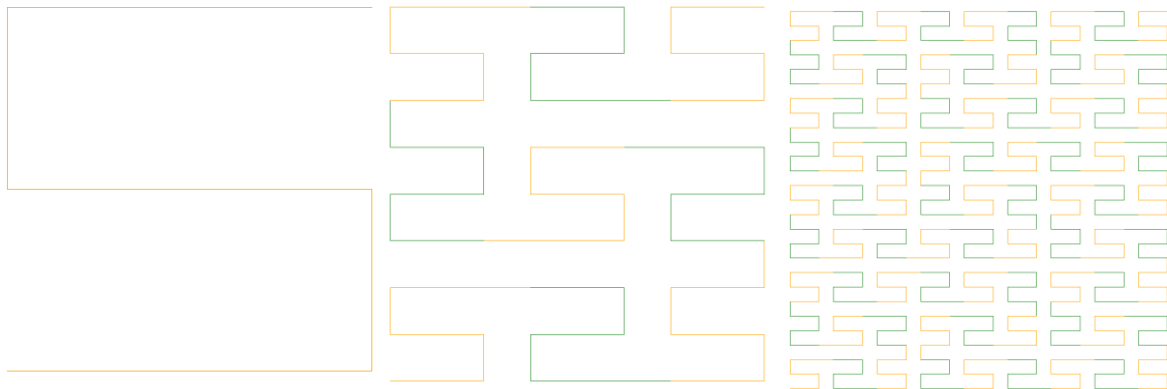
Another example of a continuous square-filling curve is the Peano curve, named after Giuseppe Peano (1858 - 1932), probably best known for the Peano axioms for the natural numbers. As an L-system, the Peano curve is defined by:

Axiom: X

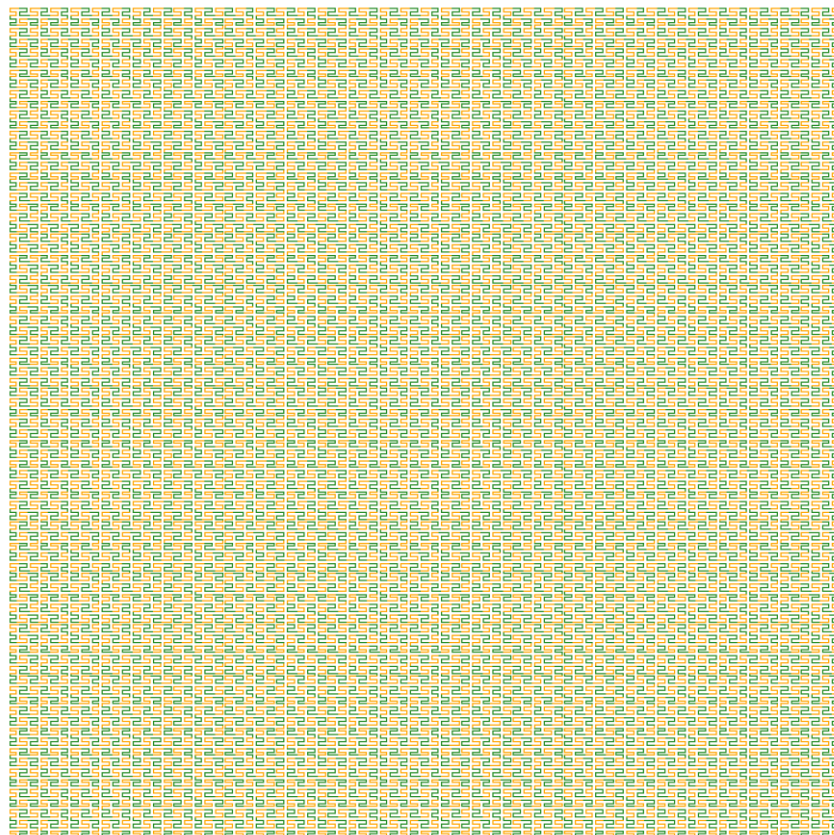
Substitution rules:

$$X \rightarrow XFYFX + F + YFXFY - F - XFYFX$$

$$Y \rightarrow YFXFY - F - XFYFX + F + YFXFY$$

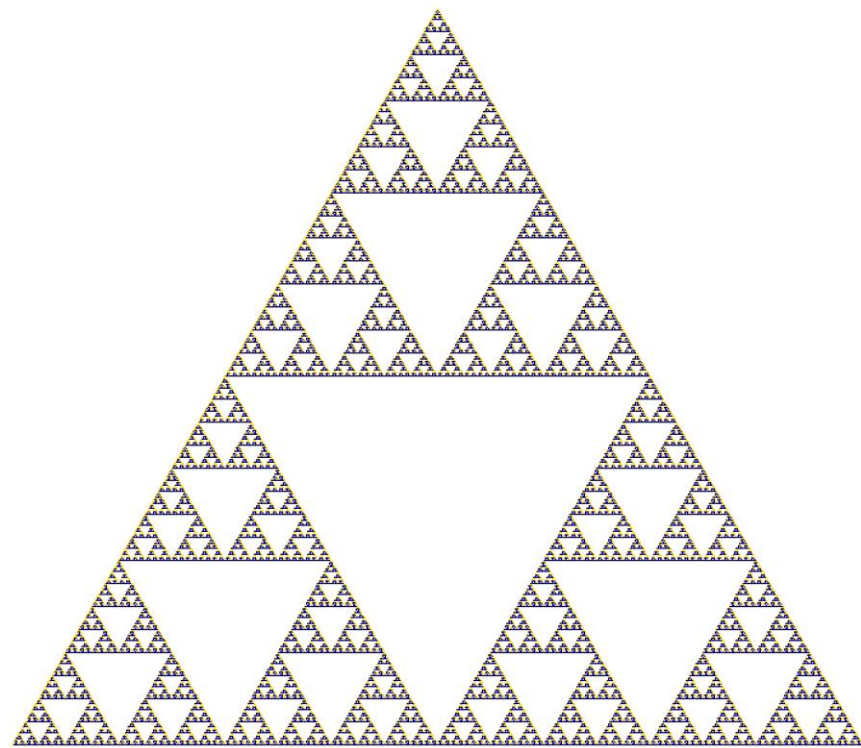


Peano curve: Axiom. First and second generation

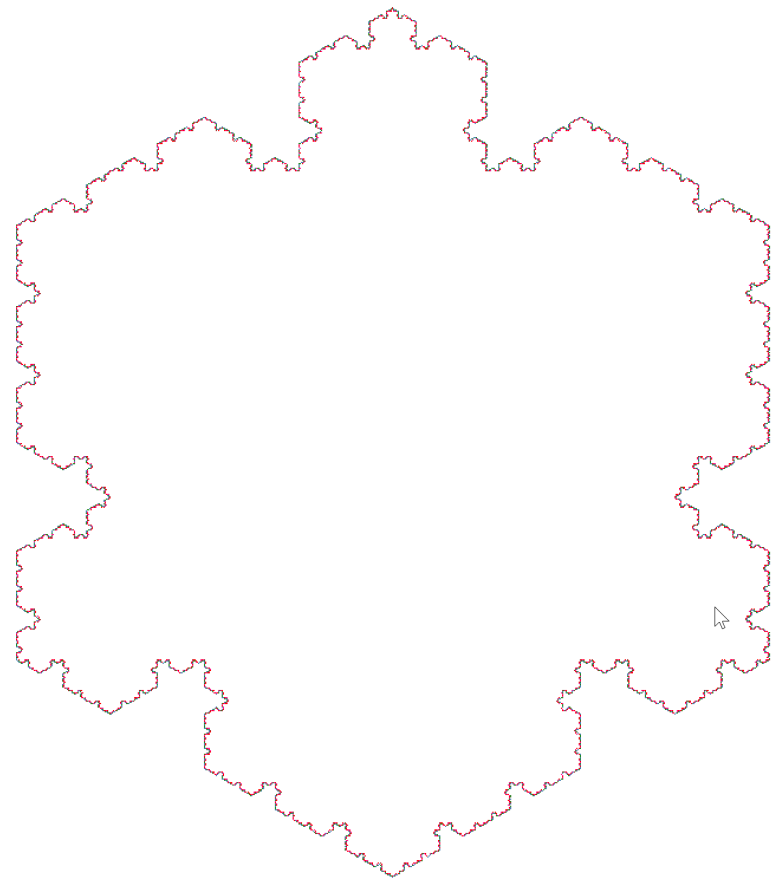


Peano curve of generation four

We leave further analysis to the reader as well as the analysis of the Sierpinski curve and the Sierpinski triangle (Waclaw Sierpinski 1882 - 1962).



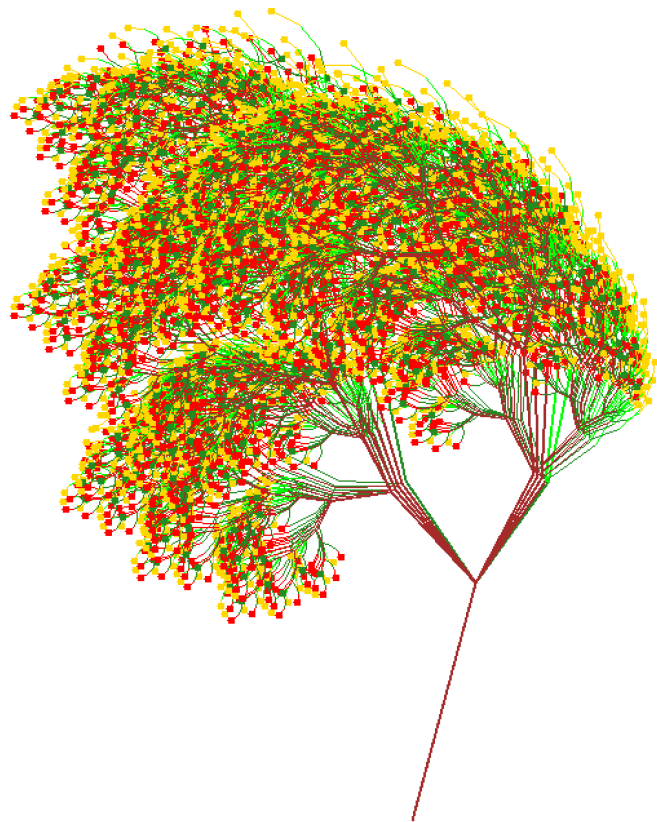
Eighth generation of the Sierpinski triangle



Sierpinski curve of generation five

3.6 Tree structures

So far, we have learnt about curves without branches. With L-systems, however, branches can also be modelled using the brackets [and]. The bracket [means that the turtle should memorise its status (position, angle relative to the x-axis, current step length). The turtle then continues to walk along the string until it reaches a] bracket. It then returns to the saved position and adopts the status there. In the simulator, a] bracket, a bud is drawn if this option is activated. This only makes sense for "tree" type L-systems.



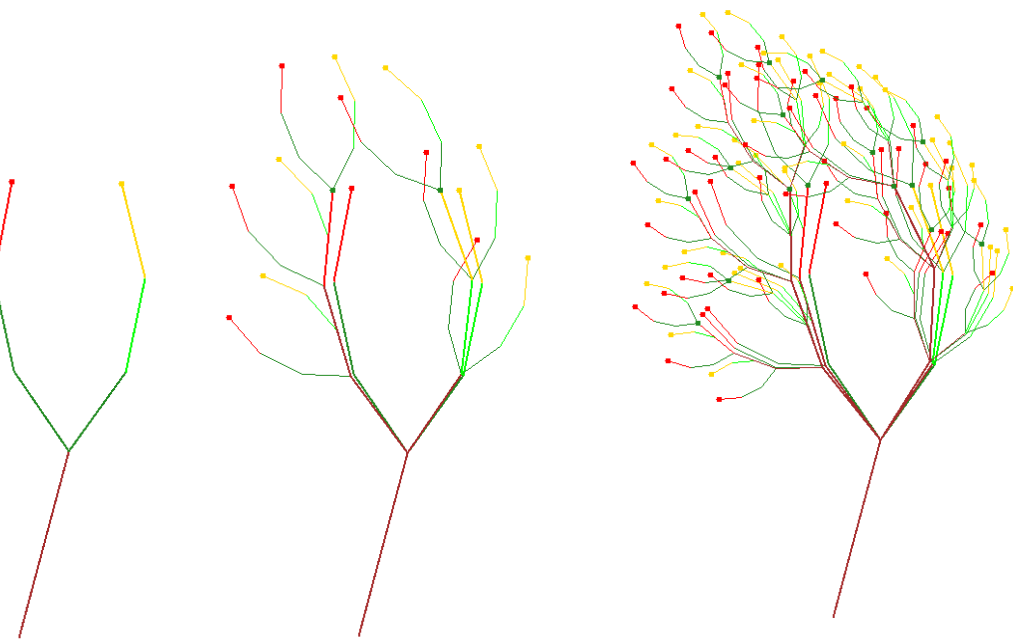
Tree structure with buds

The above tree is defined as an L-system by:

Axiom: + + +F

Replacement rule: $F \rightarrow F + [+F - F - F] - [-F + F + F]$

At each step, one element "F" of the tree structure remains, but is extended by two three-part "branches". The angle "+" to the right (25°) is slightly larger than the angle belonging to "-" (23°). This explains why the tree is hanging to the left.



The first three generations of the tree.

A plant formed according to the rules:

Axiom: $++ +F$

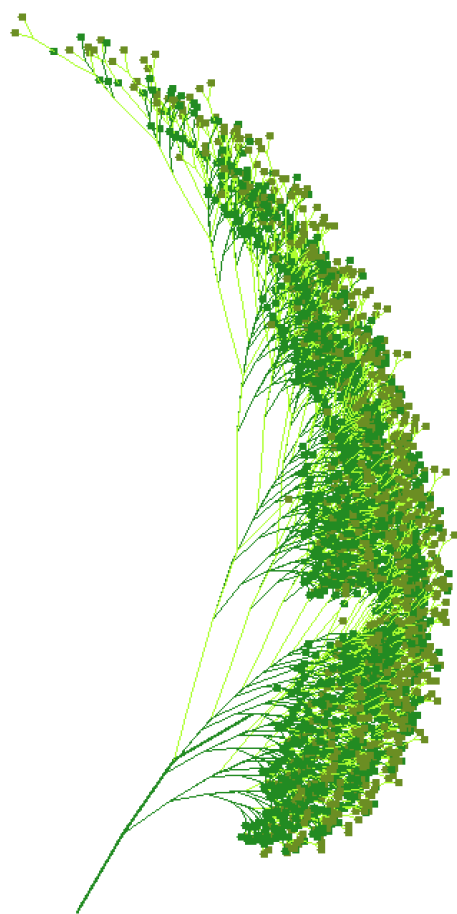
Replacement rule: $F \rightarrow F[--F+F+F][+F-F-F]$

Is the following:

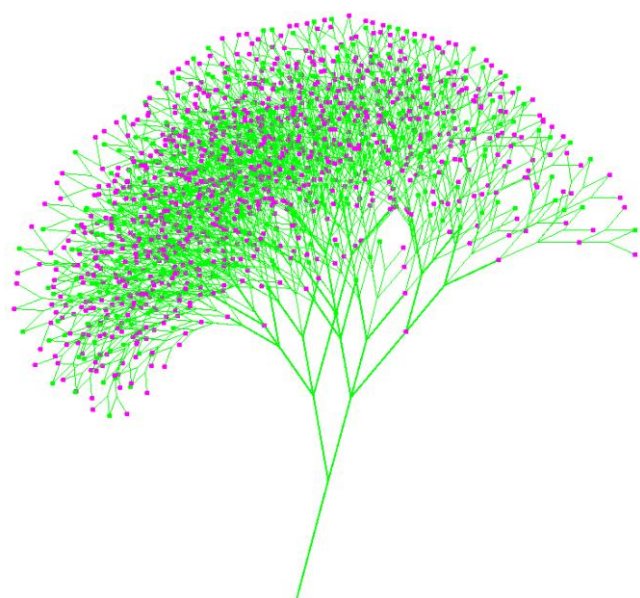


The fifth generation of the plant

Other examples that are implemented:



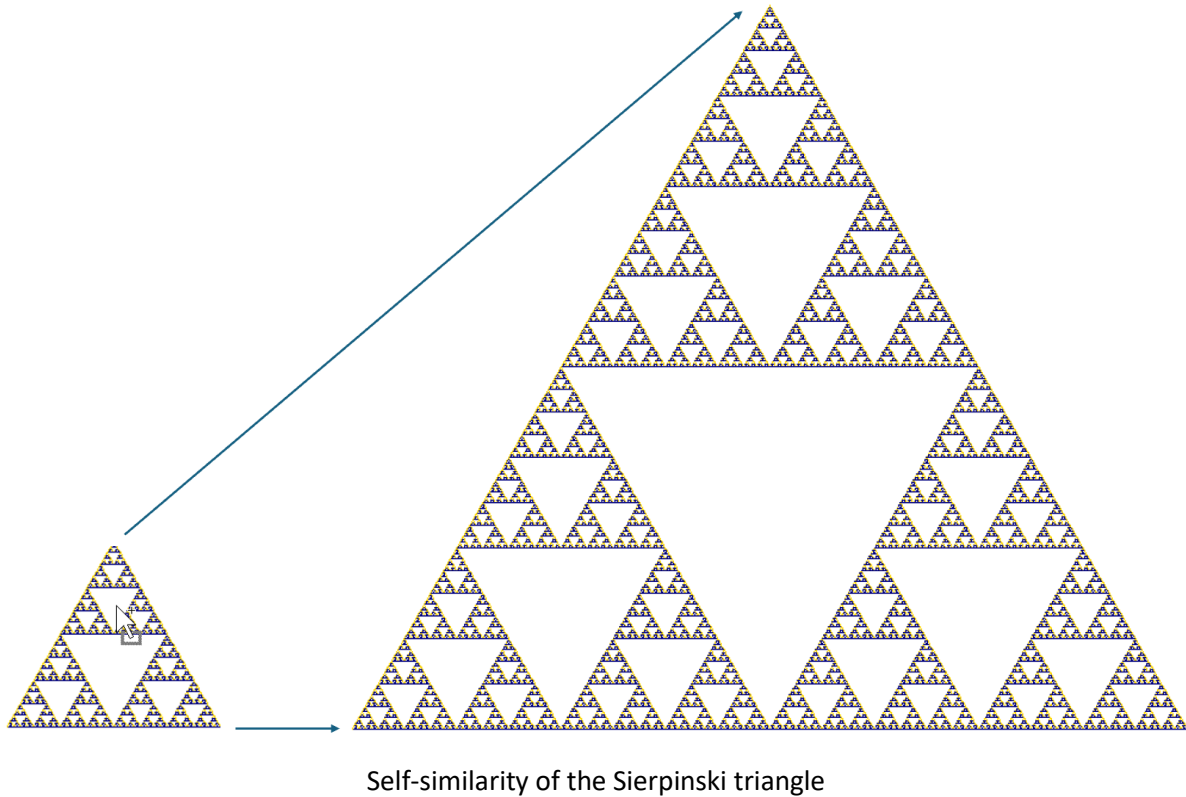
The "fern"



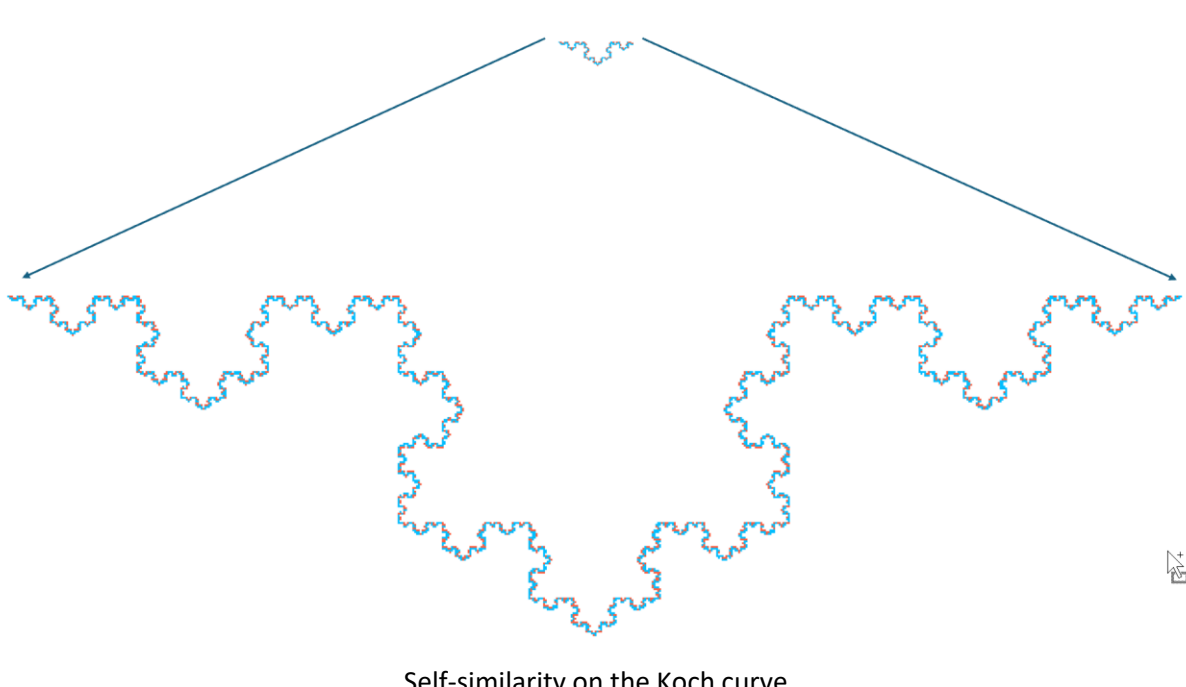
The "bunch"

3.7 Self-similarity

If we look at the Sierpinski triangle, we realise that we get back the original whole triangle if, for example, we enlarge a sub-triangle at the bottom left accordingly.



We also see the same phenomenon with sections of the Koch curve:

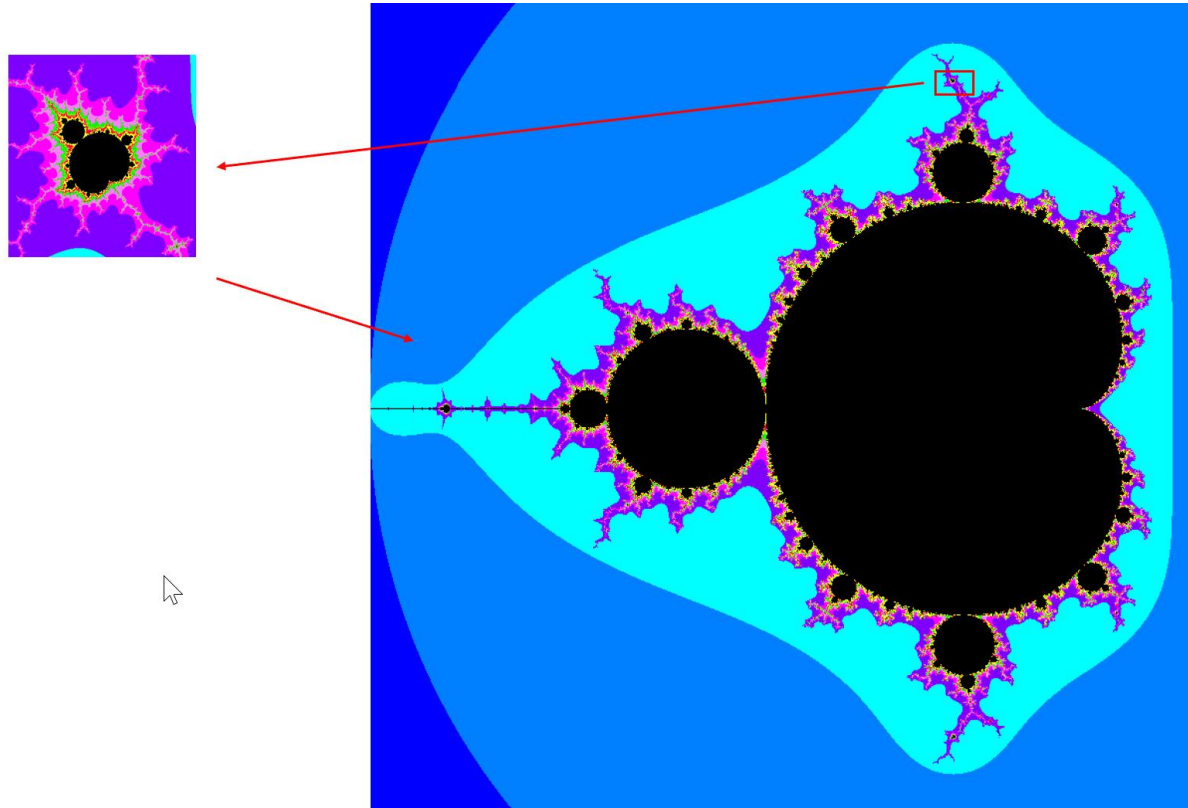


We also find that the other implemented L-systems are either strictly self-similar (like the Sierpinski triangle) or at least partially self-similar (like the Snowflake curve). This is less obvious in the case of

tree structures, because strict self-similarity only applies everywhere when the number of the generation approaches infinity.

We have encountered self-similar objects before, namely in iteration in the complex plane. There, for example, it is the basins of the n^{th} roots of unity and the Newton method, or the Julia and Mandelbrot sets.

We call an object *self-similar* if the same structure appears again and again when iteratively enlarged to infinity. This can be expressed in more abstract and precise mathematical terms, but the essential point is made here.



Self-similarity of the Mandelbrot set

Self-similar objects are also called *fractals*.

Self-similarity plays an important role in the next section, which deals with the fractal dimension.

3.8 Fractal Dimension

If you believe that you live in a Euclidean space, then the concept of dimension is unproblematic. The dimension is then equal to the number of basis vectors that span the associated linear space. Our space then has the dimension three and to specify the position of a point in a spatial coordinate system, you need three coordinates (length, width, height).

This is also referred to as the *dimension of a vector space* or the *Euclidean dimension*.

If you consider the complex plane, then this has the dimension two as a Euclidean plane. However, if you consider it as a space above the complex numbers, then it "only" has the dimension one, because "one coordinate", namely *one* complex number, is sufficient to determine the position of a point in the complex plane.

$$\dim_{\mathbb{R}} \mathbb{C} = 2, \quad \dim_{\mathbb{C}} \mathbb{C} = 1$$

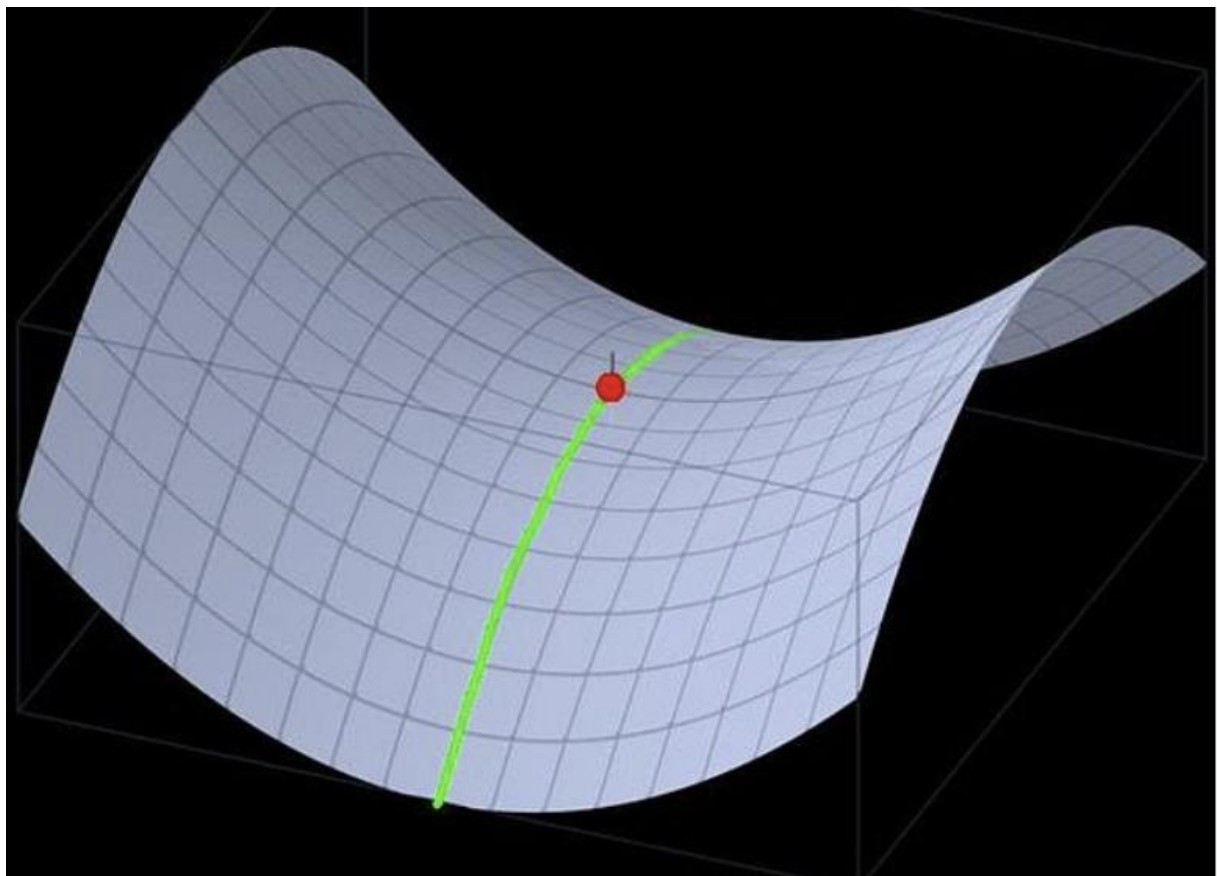
Here you can see a first complication: When we talk about the dimension of a vector space, it matters *over which field this vector space is considered*.

In the real world, however, we are usually *not* in a Euclidean space. The surface of a sphere and therefore our living environment on the globe is *not Euclidean*. The shortest connection between two points on the sphere is not a straight line, but a great circle. Nevertheless, we don't feel any of this when we go for a walk. Because we only see a very small section of the globe in our immediate surroundings, we can understand this as a Euclidean plane, and this is completely sufficient for our everyday lives.

We can say that the *surface of the sphere is locally Euclidean*. This means that it behaves like a Euclidean space if only the section of the spherical surface is small enough compared to the entire spherical surface. The dimension of the surface of the sphere is then equal to the dimension of the locally Euclidean section, namely two.

A set which is locally Euclidean everywhere and has the same locally Euclidean dimension at every point is also called a *manifold*. This locally Euclidean dimension is then the *dimension of the manifold*.

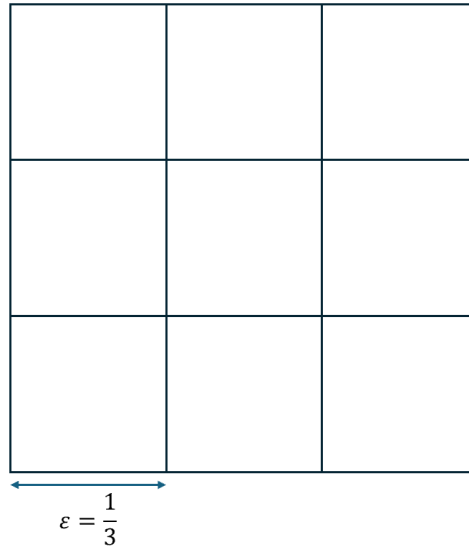
For example, a saddle surface is a manifold of dimension two.



Saddle surface (source: anthrowiki.at)

If you consider any point sets or other abstractly defined objects, then the idea of a dimension quickly becomes complicated and it becomes difficult to generalise the concept accordingly, if this is possible at all. In the case of plane point sets, for example, you could assign a grid to the plane, with the grid width being ε . Then you count the number of boxes containing points from the set under consideration: $N(\varepsilon)$. Then let ε approach zero and see how $N(\varepsilon)$ develops.

As an example, let's take a square (which in our world has the dimension two) with a side length of one and the entire interior of the square as the set of points.



If $\varepsilon = \frac{1}{3}$ is, then obviously $N(\varepsilon) = 9$. This means that 9 boxes of side length ε contain points from the total set. For $\varepsilon = \frac{1}{4}$ is $N(\varepsilon) = 16$. In general, you can see that applies:

$$N(\varepsilon) = \left(\frac{1}{\varepsilon}\right)^2$$

Where the exponent 2 is the dimension.

For a cube, an analogous consideration shows that the following applies:

$$N(\varepsilon) = \left(\frac{1}{\varepsilon}\right)^3$$

If you generalise this, you get:

$$N(\varepsilon) = \left(\frac{1}{\varepsilon}\right)^D$$

Where D is the dimension. You can then also write:

$$D = \frac{\log N(\varepsilon)}{\log (1/\varepsilon)}$$

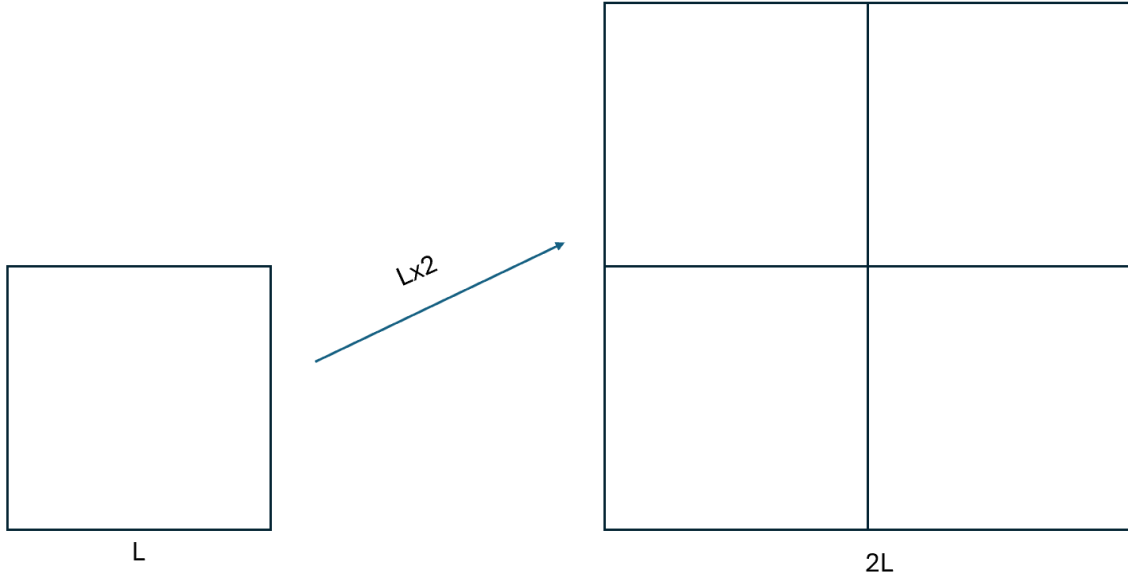
Now for the square and the cube, D was independent of the size of ε . If this is not the case and you allow ε to approach zero, you can define the dimension as a limit (if this exists):

$$D = \lim_{\varepsilon \rightarrow 0} \frac{\log N(\varepsilon)}{\log (1/\varepsilon)}$$

This is precisely the definition of the so-called *box dimension*.

A similar approach is used for the concept of *fractal dimension* (sometimes also called *similarity dimension*). This is based on self-similarity and the fact that when a section of a fractal is enlarged, the entire fractal is obtained again.

Let's start again with the Euclidean concept of dimension. A square is a flat object and has the Euclidean dimension of two.



If the side length is doubled, the area increases fourfold

If we increase the side length of the square by a factor of λ , its area increases by a factor of λ^2 . This means that we need λ^2 copies of the original square to fill the larger square.

If we look at the cube and increase its side length by a factor of λ , its volume increases by a factor of λ^3 . We need λ^3 original cubes to fill the new cube. The dimension of the cube is three.

In both cases:

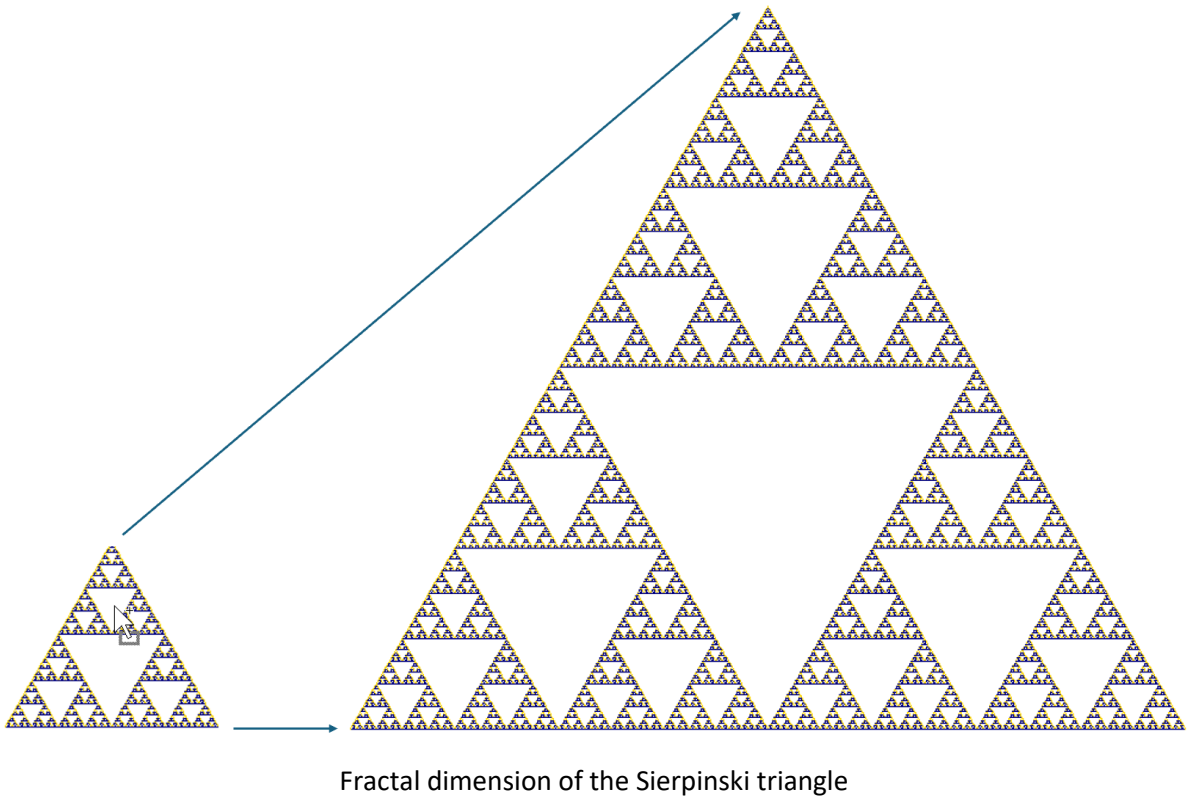
$$\lambda^D = N(\lambda)$$

Where λ is the stretch factor and $N(\lambda)$ is the number of cut-outs needed to fill the new object. D is then the dimension. Thus, the *fractal dimension* of a fractal set can be defined as:

$$D = \frac{\log N(\lambda)}{\log \lambda}$$

If for suitable sections of the set, which are stretched by the factor λ to coincide with the entire set, the value D is always consistently the same.

If we take the Sierpinski triangle and a section of it as shown in the picture:



Then we see: If we stretch the section by a factor of 4, then we need 9 copies of the section to fill the new larger Sierpinski triangle. The fractal dimension of the Sierpinski triangle is therefore

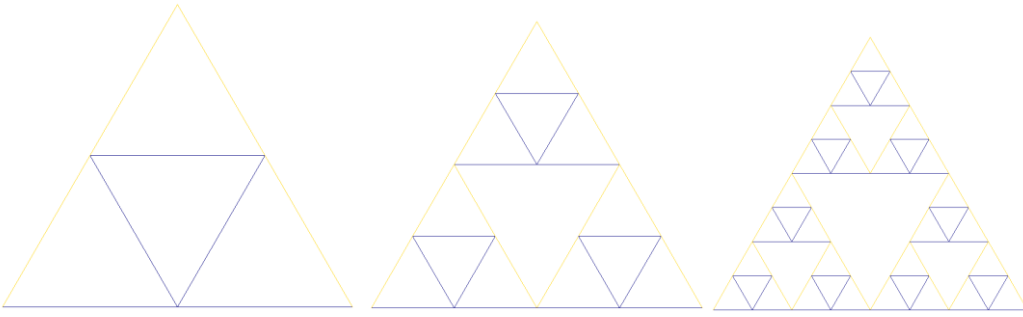
$$D = \frac{\log 9}{\log 4} \approx 1.58496 \dots$$

If we had taken a different section, e.g. the first large sub-triangle at the bottom left as the section, then stretching it by a factor of two would result in the original Sierpinski triangle again and, on the other hand, we would need three copies of the section to cover it. We would then have again:

$$D = \frac{\log 3}{\log 2} \approx 1.58496 \dots$$

We can consider that this applies to any suitable section that is stretched to form the original Sierpinski triangle, so its dimension is equal to 1.58496, i.e. a fractional number. This is where the term *fractal* comes from.

If we measure the Euclidean length of the Sierpinski triangle (i.e. the sum of the lengths of all line segments in the dimension one), then we assume a unit, e.g. that the base line of the original triangle (i.e. the axiom of the L-system) has the length one. The initial triangle (the axiom) then has the length 3. In the first step, an inner triangle with the perimeter $\frac{3}{2}$ is added.



The first three generations of the Sierpinski triangle

In the second generation, three triangles with the perimeter $\frac{3}{4}$ are added. In the third, 9 triangles with perimeter $\frac{3}{8}$. In each further step, the number of triangles is tripled and the perimeter of a single triangle is halved. In the end, this gives the total length of all the lines:

$$L = 1 \cdot 3 + \frac{3}{2} + 3 \cdot \frac{3}{4} + 9 \cdot \frac{3}{8} + 27 \cdot \frac{3}{16} + \dots = \sum_{n \geq 0} \frac{3^n}{2^n} = \infty$$

If we calculate the area of the Sierpinski triangle, then the axiom, i.e. the initial triangle, has the area $\frac{\sqrt{3}}{4}$. Then, in the first step, an inner triangle is cut out, which has the area $\frac{\sqrt{3}}{4} \cdot \frac{1}{2^2}$. In the second step, three triangles are cut out, each with an area of $\frac{\sqrt{3}}{4} \cdot \frac{1}{4^2}$. In each step, the number of triangles cut out is tripled. Their side lengths are halved and therefore their area is $\frac{\sqrt{3}}{4} \cdot \frac{1}{s^2}$. This gives the sum of the area of the Sierpinski triangle:

$$F = \frac{\sqrt{3}}{4} \cdot \left(1 - \frac{1}{2^2} - \frac{3}{4^2} - \frac{9}{8^2} - \dots \right) = \frac{\sqrt{3}}{4} \left(1 - \frac{1}{3} \sum_{n \geq 1} \frac{3^n}{4^n} \right) = \frac{\sqrt{3}}{4} \left(1 - \frac{1}{3} \cdot \frac{3}{4} \sum_{n \geq 0} \left(\frac{3}{4}\right)^n \right)$$

The sum is a geometric series and therefore is:

$$F = \frac{\sqrt{3}}{4} \left(1 - \frac{1}{4} \cdot \frac{1}{1 - \frac{3}{4}} \right) = \frac{\sqrt{3}}{4} (1 - 1) = 0$$

The Sierpinski triangle therefore has an infinite length in Euclidean dimension 1 (if the sum of all segments is calculated). In Euclidean dimension 2, the area is 0.

As a further example, we will analyse the fractal dimension of the Dragon curve.

We have chosen $\frac{1}{\sqrt{2}}$ as the scaling factor when creating the Dragon curve. The distance between the starting point and the end point of the curve then remains constant. At the same time, we have seen that the Dragon curve is also generated by reducing the curve by this factor $\frac{1}{\sqrt{2}}$ in an iteration step and then adding a copy of the curve at a right angle.

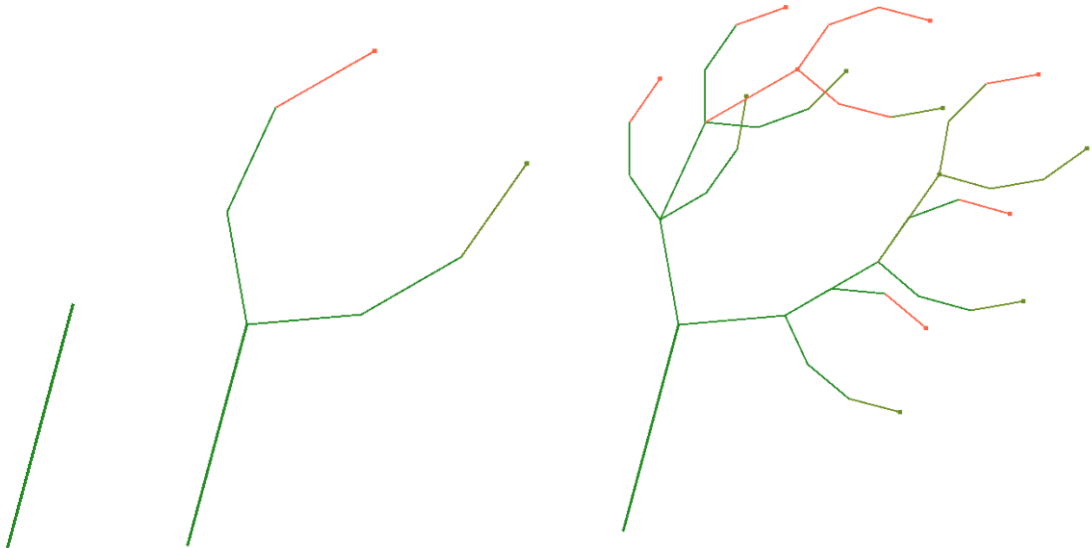
Conversely, stretching the curve by the factor $\frac{1}{\sqrt{2}}$ means that you get the same curve as if you had joined 2 copies of it together. This is the fractal dimension of the Dragon curve:

$$D = \frac{\log 2}{\log \sqrt{2}} = 2$$

This also means that the Dragon curve completely fills parts of the plane.

The number of lines doubles with each iteration step, whereby their length is reduced by a factor of $\frac{1}{\sqrt{2}}$. The total length of all segments therefore increases by a factor of $\sqrt{2}$ at each iteration step and approaches infinity.

We are still looking at the "plant" in the "simulator".



Axiom and the first two generations of the plant

As you can see from the replacement rule $F \rightarrow F[--F+F+F][+F-F-F]$, the initial element remains stationary during iteration. However, a further six elements "grow", but these are only half the length. This means that the total length of all sections increases by 3 at each iteration step and grows towards infinity over the course of the iteration.

With this construction, the plant is not strictly self-similar. However, as an approximation, we can venture that - if we take a version of the plant that is reduced by a factor of 2 - we need 6 of these elements to fill out the original plant (apart from the stem). Thus, this plant has the dimension as an approximation:

$$D = \frac{\log 6}{\log 2} \approx 2.58496$$

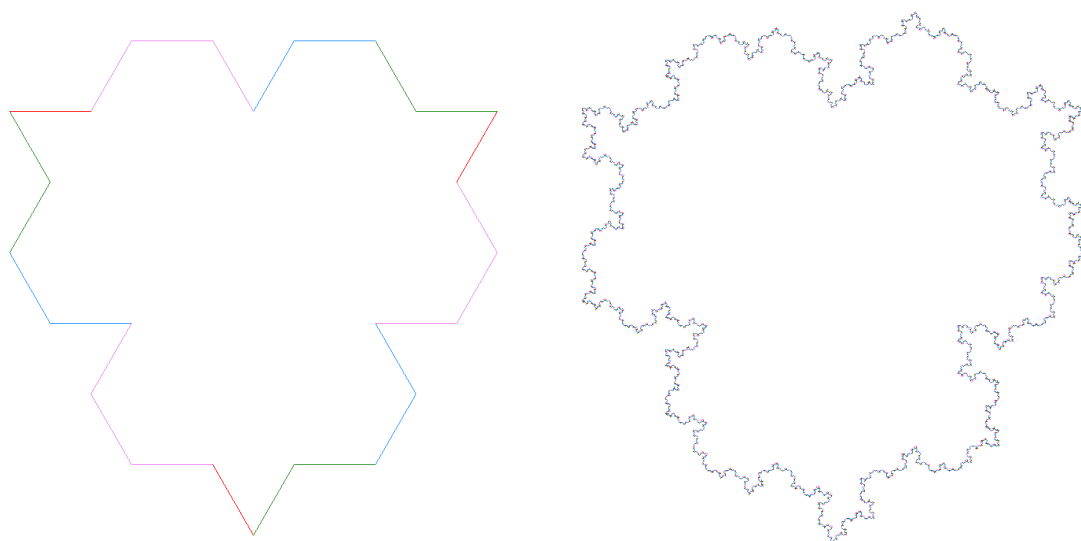
Further examples can be found in [6].

3.9 Exercise examples

1. Proofs for the Snowflake curve:

- a) Three consecutive points on the Snowflake curve always form an isosceles triangle with base angles of either 30° or 60° (with complete induction).
- b) The Snowflake curve lies completely within the hexagon spanned by the Snowflake curve of the first generation.
- c) The Snowflake curve has 6 axes of mirror symmetry
- d) The Snowflake curve is rotationally symmetrical with a rotation angle of 60°
- e) The area of the Snowflake curve in the "Simulator" version is $\frac{2\sqrt{3}}{5}$

2. Examine the inverse Snowflake curve regarding length, area, symmetry axes and types of triangles occurring. Create the strings for the first few iterations. Also prove that two segments of the inverse Snowflake curve do not intersect in the interior.
3. Create an L-system that is a combination of the Snowflake curve and the inverse Snowflake curve. The axiom consists of a hexagon. Then replace each side as for the Snowflake curve, but the first one is a protrusion as for the Snowflake curve and the next one is a re-entrant as for the inverse Snowflake curve. For the replacement rules, use the same technique as for the Dragon curve with placeholders "X" and "Y" to differentiate between lines that are replaced in the next generation by lines that jump out or jump in. The following image shows what this should look like (generation one and five).



4. Analyse the Sierpinski triangle and the Sierpinski curve.
5. Experiment with your own curves defined by L-systems.
6. Analyse the "Fern" and "Strauss" tree structures.
7. Experiment with your own tree structures.
8. Analyse the fractal sets implemented in the "Simulator" for self-similarity.
9. Determine the fractal dimension of the Koch curve and the Sierpinski curve. Also determine their Euclidean length.
10. Determine the fractal dimension of the Hilbert curve and the Peano curve.
11. Determine the fractal dimension of other tree structures in the "simulator".

Further reading

- [1] Orbital Motion, Archie E. Roy, Taylor & Francis Group, 2005
- [2] Celestial Mechanics, John M.A. Danby, Willmann-Bell Inc., 1992
- [3] The Lorenz System, Seminar on Ordinary Differential Equations, University of Hamburg, Uwe Jönck and Florian Prill, February 2003
- [4] Deterministic Nonperiodic Flow, Edward N. Lorenz, Journal of the Atmospheric Sciences, MIT, 1963
- [5] Classic Iterated Function Systems, Larry Riddle, Agnes Scott College, Website:
<https://www.larryriddle.agnesscott.org/ifs/ifs.htm>
- [6] Fraktale Geometrie und ihre Anwendungen, Florian Daikeler, Seminar im WS 2006/2007